uOttawa

L'Université canadienne
Canada's university

The Characterization of Bimodal Droplet Size Distributions in the Ultrafiltration of Highly Concentrated Emulsions Applied to the Production of Biodiesel

By:

Hamid Falahati

A thesis submitted to the
Faculty of Graduate and Postdoctoral Studies
In partial fulfillment of the requirements for the degree of

Master of Applied Science in Chemical Engineering

Department of Chemical & Biological Engineering
Faculty of Engineering
University of Ottawa

STATEMENT OF CONTRIBUTIONS OF COLLABORATORS

I hereby declare that I am the sole author of this Masters' thesis. All articles in this thesis are co-authored with my research supervisor Dr. André Y. Tremblay. All the experimental and analytical work related to these articles was performed by myself under the supervision and training received from professor Tremblay.

My supervisor, Dr. Tremblay, provided me with an excellent collaboration throughout this work with laboratory training, day-to-day supervision, discussions, supports and editorial comments for all of my written work. As a result the quality of this thesis has been tremendously improved through his guidance.

Signature:

Date: July 21, 2010

Hamid Falahati

To my grandma

ABSTRACT

The traditional source of energy, i.e. fossil fuel, will not sufficiently supply our increasing energy demands. This is due to industrialization, population increase and oil price fluctuations. Therefore there is a need to produce renewable energies which not only supply the energy demand that the world is facing but also they are more environmentally friendly in terms of reducing green house gases (GHG) and volatile organic compounds (VOC) emissions.

Biodiesel produced from lipid sources is a clean-burning, biodegradable, nontoxic fuel that does not contain sulphur, aromatic hydrocarbons, metals or crude oil residues. Current biodiesel production processes are tedious and involve two to three reaction steps each followed by a separation stage. Process intensification of reaction and separation in a membrane reactor offers several advantages over conventional reactors e.g. using ultralow catalyst concentration, typically 10 to 33 times less than is currently used commercially. This integration leads to the reduction of the environmental footprint of the process while maintaining the quality of the biodiesel produced.

However, limiting conditions of operation in such a reactor are not known. These are expected to be dependent on the type of feedstock processed and the operating conditions existing in the reactor. The limiting conditions will affect the quality of the biodiesel produced which might not be in accordance with ASTM and EN standards. This work is aimed at determining the limiting conditions such as the critical flux, based on pressure and composition, and residence time of the transesterification process, for a variety of feedstocks.

A non-reactive model system comprising a highly concentrated and unstable oil-in-water emulsion was used to investigate the retention of oil by the membrane in producing biodiesel with a membrane reactor. Critical flux was identified using the relationship between the permeate flux and transmembrane pressure along with the separation efficiency of the membrane. It was shown that separation efficiencies above 99.5% could

be obtained at all operating conditions up to the critical flux. The critical flux obtained in the model oil-water system ranged between 30 and 40 L/m^2/h for a cross flow velocity of 0.8 m/s. According to ASTM D6751 and EN 14214, the unreacted oil concentration in the biodiesel should not exceed 0.2 wt% (2000 ppm). It was observed that the concentration of oil in all collected permeate samples using the oil-water system was below 0.2 wt% (2000 ppm) when operating at a flux below the critical flux.

Studies to date have been limited to the characterization of low concentrated emulsions below 15 vol.%. The average oil droplet size in highly concentrated emulsions was measured as 3200 nm employing direct light scattering (DLS) measurement methods. Cake layer thickness was calculated based on a droplet size of 3200 nm for the various oil concentrations. It was observed that the estimated cake layer thickness of 20 to 80 mm, was larger than external diameter of the membrane tube i.e. 6 mm. Settling of the concentrated emulsion permitted the detection of a smaller particle size distribution (30-100 nm) within the larger particles averaging 3200 nm. It was identified that DLS methods could not efficiently give the droplet size distribution of the oil in the emulsion since large particles interfered with the detection of smaller particles. The content of the smaller particles represented 1% of the total weight of oil at 30°C and 5% at 70°C. This was too low to be detected using DLS measurements but was sufficient to affect ultrafiltration.

In order to study the critical flux in the presence of transesterification reaction and the effect of cross flow velocity on separation, various oils were transesterified in another membrane reactor providing higher cross flow velocity of 1.8 m/s. The oils tested were canola, corn, sunflower and unrefined soy oils (Free Fatty Acids (FFA< 1%)), and waste cooking oil (FFA= 9%). The quality of all biodiesel samples was studied in terms of glycerine, mono-glyceride (MG), di-glyceride (DG) and tri-glyceride (TG) concentrations. The composition of all biodiesel samples were in the range required by ASTM D6751 and EN 14214 standards. Therefore the critical flux, based on composition was determined to be above 70 L/m^2/h for a cross flow velocity of 1.8 m/s. For canola oil, higher cross flow velocity provides better separation by reducing materials deposition on the surface of the membrane due to higher shearing. A critical flux based on operating pressure in the reactor was reached for waste cooking and pre-treated corn oils. This flux ranged from 30 to 40

$L/m^2/h$. This is in a pretty good agreement with the non-reactive model system employed in this study.

It was identified that the reaction residence time in the reactor was an extremely important design parameter affecting the operating pressure in the reactor. Lower residence times increased the amount of unreacted oil inside the reactor which caused an increase in pressure within the reactor.

All FAME samples were water washed only once to remove free glycerine and residues. The glycerine concentration for these samples was very low after this single wash. In conventional reactors a number of water washing stages are required to remove all finely suspended hydrophilic materials from the biodiesel and reduce the glycerine content to below 0.02 wt% (200 ppm) as required by ASTM and EN standards. Since the membrane reactor integrates reaction and separation simultaneously, the permeate was ultrafiltered and free of hydrophilic colloidal matters e.g. cell debris. Previous work showed that the membrane reactor requires less catalyst than conventional reactors. The amount of catalyst required for the treatment of waste oil was optimized. This results in a neutral pH of the FAME phase (pH=7). The lower catalyst requirement combined with the decreased need for wash waters leads to a more environmentally friendly process.

RÉSUMÉ

Les sources d'énergie traditionnelles sont insuffisantes pour fournir nos demandes énergétiques croissantes. Ceci est dû à l'industrialisation, l'augmentation de la population et aux fluctuations de prix du pétrole. Par conséquent il y a un besoin grandissant de produire des énergies renouvelables qui fournissent non seulement nos demandes énergétiques favorables à l'environnement en termes de réduction des gaz à effet de serre (GHG) et les émissions volatiles des composés organiques (VOC).

Le biodiesel produit à partir de lipides est un combustible propre, biodégradable et non-toxique qui ne contient pas de soufre, d'hydrocarbures aromatiques, de métaux ou de résidus de pétrole brut. Les procédés de fabrication courants du biodiesel sont difficiles et impliquent deux à trois étapes de réaction suivies d'une étape de séparation. L'intensification de la réaction et de la séparation dans un réacteur à membrane offre plusieurs avantages par rapport aux réacteurs conventionnels, par exemple : concentration réduite de catalyseur, en général 10 à 33 fois moins que commercialement. Cette intégration mène à la réduction de l'empreinte environnementale du procédé tout en maintenant la qualité du biodiesel produit.

Cependant, les conditions limites reliées à l'opération d'un tel réacteur ne sont pas connues. On s'attend à ce que celles-ci dépendent de la matière première traitée et des conditions dans le réacteur. Les conditions limite affecteront la qualité du biodiesel produit qui ne pourrait pas être conforme aux normes d'ASTM et EN. Ce travail est orienté vers la détermination des conditions limites telles que le flux critique, basé sur la pression et la composition, et le temps de séjour du procédé de transestérification, pour une série de matières premières.

Une émulsion d'huile végétale et d'eau fortement concentrée et instable a été employée pour étudier la rétention d'huile par la membrane dans le réacteur à membrane. Le flux critique a été identifié utilisant le flux du perméat, la pression transmembranaire et la séparation de la membrane. On a démontré que des séparations au-dessus de 99.5%

pourraient être obtenues à toutes les conditions de fonctionnement jusqu'au flux critique. Le flux critique obtenu pour le système modèle était entre 30 et 40 L/m^2/h pour une vitesse d'écoulement transversal de 0.8 m/s. Selon les normes ASTM D6751 et en 14214, la concentration en huile non réagie dans le biodiesel ne devrait pas dépasser 0.2 % massique (2000 ppm). On a observé que la concentration d'huile dans tous les échantillons de perméat utilisant le système d'huile-eau était en-dessous de 0.2 % massique (2000 ppm) en fonctionnant à un flux au-dessous du flux critique.

Les études à date se sont limitées à la caractérisation d'émulsions de concentration inférieure à 15 % par volume. La taille moyenne de gouttelettes d'huile dans les émulsions fortement concentrées a été mesurée à 3200 nanomètres, utilisant des méthodes directes de mesure de dispersion de la lumière (DLS). L'épaisseur du gâteau à la surface de la membrane a été calculée basé sur une taille de gouttelette de 3200 nanomètres pour diverses concentrations d'huile. On a calculé que l'épaisseur du gâteau étais de 20 à 80 millimètres, ce qui est supérieur au diamètre interne du tube de la membrane c.-à-d. 6 millimètres. La sédimentation de l'émulsion concentrée a permis la détection d'une plus petite distribution de particules (30-100 nanomètre) parmi les particules de 3200 nanomètres. On a déterminé que les méthodes de DLS ne pouvaient pas efficacement évaluer la distribution de gouttelettes d'huile dans l'émulsion puisque les grandes particules nuisent à la détection des plus petites. La concentration des particules plus petites représente 1% de tout le poids d'huile à 30°C et 5% à 70°C. Ceci était trop bas pour être détecté par la technique de DLS mais suffisante pour influencer l'ultrafiltration.

Afin d'étudier le flux critique en présence de la réaction de transestérification et l'effet de la vitesse d'écoulement tangentiel sur la séparation, diverses huiles ont été transestérifiées dans un autre réacteur à membrane fournissant une vitesse plus élevée d'écoulement tangentielle de 1.8 m/s. Les huiles examinées étaient le canola, maïs, tournesol, une huile non raffinée de soja (acides gras libres (FFA< 1%)), et une huile de cuisson usée (FFA= 9%). La composition de tous les échantillons de biodiesel a été déterminée en terme de glycérine, monoglycéride (MG), diglycéride (DG) et en triglycéride (TG). La composition de tous les échantillons de biodiesel était dans la gamme exigée par les normes d'ASTM D6751 et EN 14214. Le flux critique, basé sur la composition est supérieur à 70 L/m^2/h

pour une vitesse d'écoulement transversal de 1.8 m/s. Pour l'huile de canola, une vitesse plus élevée d'écoulement tangentiel fournit une meilleure séparation en réduisant le dépôt de matériaux à la surface de la membrane. Un flux critique basé sur la pression de fonctionnement dans le réacteur a été atteint pour l'huile de cuisson usée et l'huile de maïs prétraitée. Ce flux est entre 30 et 40 $L/m^2/h$. Ces valeurs sont semblables à celles obtenues avec le modèle non-réactif utilisé dans cette étude.

On a identifié que le temps de séjour dans le réacteur était un paramètre de conception extrêmement important affectant la pression de fonctionnement du réacteur. Les temps de séjour inférieurs ont augmenté la quantité d'huile non réagie à l'intérieur du réacteur qui a causé une augmentation de pression dans le réacteur.

Tous les échantillons de FAME étaient lavés une seule fois à l'eau pour enlever la glycérine et les résidus. La concentration en glycérine pour ces échantillons était très basse après un seul lavage. Dans des réacteurs conventionnels un certain nombre d'étapes de lavage à l'eau sont nécessaires pour enlever tous les matériaux hydrophiles finement suspendus dans le biodiesel et pour ramener le contenu en glycérine à en-dessous de 0.02 % poids (200 ppm) selon les exigences des normes d'ASTM et EN. Puisque le réacteur de membrane intègre la réaction et la séparation simultanément, le produit était ultrafiltré et exempte de débris colloïdaux hydrophiles tels que des résidus de cellules de plantes. Les travaux précédents ont prouvé que le réacteur de membrane exige moins de catalyseur que les réacteurs conventionnels. La quantité de catalyseur exigée pour le traitement d'huile de cuisson usée a été optimisée. Les résultats étant que le pH de la phase de FAME était neutre (pH 7). La réduction de catalyseur combinée avec le besoin diminué en eaux de lavage offrent un processus qui est plus favorable à l'environnement.

ACKNOWLEDGMENTS

I wish to express my sincere appreciation and deep gratitude to my research supervisor, Dr. André Tremblay, for his guidance in the completion of this thesis. I enjoyed a great deal of freedom and learnt a lot through our lively and animated discussions! I've been fortunate to do my Masters under his supervision. I thank him for his endless support and assistance even in his busiest times. Undoubtedly, without his patience and endless help, this study would not be possible. I will always remember and appreciate his support which was far beyond the regular requirements for an academic supervisor.

I wish to thank the support staff within the department of chemical and biological engineering, Louis Tremblay, Gérard Nina and Franco Ziroldo, for their outstanding technical support.

Finally, I wish to thank my parents, Mehdi Falahati and Nooshfar Moeini, for their support, encouragement and understanding throughout this work.

NOMENCLATURE

a_p	radius of the solute particle (m)
A_c	cake layer area (m^2)
c_s	cake concentration (%)
C	constant
J	flux ($L/m^2/h$)
n	indication of cake compressibility
$P_{Critical}$	critical pressure (kPa)
Q	volumetric flow rate (L/h)
R_c	cake layer resistance (m^{-1})
$R_{f\ (reversible)}$	resistance due to reversible fouling (m^{-1})
$R_{f\ (irreversible)}$	resistance due to irreversible fouling (m^{-1})
R_m	membrane hydraulic resistance (m^{-1})
r_p	radius of the oil droplet (m)
r_{pore}	pore radius (m)
$r_{droplet}$	oil droplet radius (m)
R_{Total}	total resistance (m^{-1})
t_{ss}	steady state cake layer formation duration (s)
v	velocity (m/s)
V	volume fraction of the oil in the emulsion (vol.%)
We	Weber number (dimensionless number)

Greek symbols

α	specific cake layer resistance (m^{-1})
α'	exponential coefficient
α_0	specific cake layer resistance at unit pressure drop (m^{-1})
γ	interfacial tension (N/m)
γ_{MeOH}	interfacial tension of methanol (N/m)
γ_{Oil}	interfacial tension of oil (N/m)
$\gamma_{Oil/MeOH}$	interfacial tension between oil and methanol (N/m)
ΔP_L	transmembrane pressure (kPa & psi)
ρ	density (kg/m^3)
ϕ_b	solute volume fraction in the emulsion (%)
ϕ_{max}	maximum solute volume fraction in the cake layer (%)

ABBREVIATIONS

ASTM	American society for testing materials (Standard)
DAF	Dissolved air flotation
DG	Di-glyceride
DLS	Direct (dynamic) light scattering
DOTM	Direct observation through membrane
FAME	Fatty acid methyl ester
FFA	Free fatty acid
FID	Flame ionization detector
GC	Gas chromatography
GHG	Green house gases
kD	kilo Daltons (Unit)
MF	Microfiltration
MG	Mono-glyceride
MR	Membrane reactor
MWCO	Molecular weight cut-off
O/M	Oil-in-methanol
O/W	Oil-in-water
ppm	Parts per million (Unit)
RBD	Refined, bleached and degummed
RT	Residence time (min)
RTD	Resistance temperature detector
TG	Tri-glyceride
TMP	Transmembrane pressure (kPa & psi)
UF	Ultrafiltration
VOC	Volatile organic compounds
WCO	Waste cooking oil
W/O	Water-in-oil

TABLE OF CONTENTS

LIST OF TABLES

CHAPTER I

CHAPTER II

CHAPTER III

APPENDIX B

APPENDIX C

APPENDIX D

LIST OF FIGURES

CHAPTER I

CHAPTER II

CHAPTER III

APPENDIX A

APPENDIX C

CHAPTER I

Introduction

The combustion of fossil fuels is the main source of greenhouse gases (GHG) and volatile organic compound (VOC) emissions [Klass, 1998]. In addition, harmful gases including NOx and SOx, and particulate matter produced through the combustion of fossil fuels are the major air pollutants. Conventional sources of energy, i.e. fossil fuel, do not meet increasing energy demands. It has been reported that between 1990 and 2003, the total energy consumption in Canada increased by 23% from 8,549 to 10,477 petajoules. One petajoule is equal to the amount of energy required to operate the Montréal subway system for a year [Ménard, 2009].

The production of renewable energies including biodiesel, bioethanol, biogas, etc using cost-effective methods is of increasing interest. Interest in combusting vegetable oil and its derivatives as a fuel has officially begun since late 1970s [Knothe, 2001]. Even though biodiesel production date is back to the 1950s or even earlier, there has not been a clear evidence of advanced researches in this area until 1970s.

"In any case, they make it certain that motor-power can still be produced from the heat of the sun, which is always available for agricultural purposes, even when all our natural stores of solid and liquid fuels are exhausted"

Rudolf Diesel, the inventor of diesel engine, Paris exhibition, 1900

Biodiesel (fatty acid methyl ester - FAME in short) is a clean-burning, biodegradable, less toxic fuel [Haws, 1997] and does not contain sulphur, aromatic hydrocarbons, metals or crude oil residues [Knothe et al., 2005; Dubé at al., 2007] produced from renewable sources, i.e. biomass. Increasing demand in the biodiesel production resulted in more interest in this area of research, for instance, biodiesel sales increased from 1.89 million L

to 113 million L per year between 1999 and 2004 in the United States [Williams, 2005]. It was reported that the biodiesel production in the U.S. was increased to 700 million gallons in 2008[1].

In fact, one of the advantages associated to the use of biomass is that photosynthesis reaction takes place by absorbing sun light energy in the presence of carbon dioxide and water. Therefore the net amount of CO_2 in the atmosphere is not increased due to the fact that the carbon dioxide produced from burning the biodiesel is used to produce the feedstock again. In other words, burning biodiesel, as one of the forms of bioenergy, has zero contributions to the global warming [Van Gerpen, 2005]. Several advantages have been reported in using biodiesel including better lubrication properties [Graboski and McCormick, 1998] and higher flash point (>130 °C)[2].

Biodiesel is a promising alternative to petroleum based diesel (Diesel derived from mineral crude oil; petro-diesel in short) in terms of GHG and VOC emissions reduction. In fact, it can be directly burned in compression-ignition engines, i.e. B100 containing 100 vol.% biodiesel, or can be blended with petro-diesel, e.g. B20 containing 20 vol.% biodiesel and 80 vol.% petro-diesel. Although the engine requires no major modifications, minor engine modifications might be required to prevent the dissolution of the various seals and gaskets [Tremblay et al., 2008] in the case of using B100 biodiesel. This is due to the fact that the biodiesel is a strong solvent. However the production cost of biodiesel is much higher than that of petro-diesel. Plant size, feedstock cost, purification of biodiesel and the value of by-products are still main issues [Kulkarni and Dalai, 2006]. Among these, feedstock cost and biodiesel purification are the main factors that should be taken into account. It has been reported that the feedstock contribute 70% to the production cost when using edible oils [Haas et al., 2004]. To date, most biodiesel products have been produced from refined vegetable oils. Despite the use of vegetable oils as major sources for biodiesel production over the past years, various feedstocks including waste cooking oil, animal fats and soapstock can also be considered as much cheaper feedstocks. Using waste cooking oil as a feedstock reduces the production cost of biodiesel significantly [Zhang et al., 2003], even

[1]Production statistics derived from U.S. Census statistics collected on M311K survey.
[2]Generic biodiesel material safety data sheet (MSDS), Retrieved July 18, 2010.

though some technical challenges, due to the existence of free fatty acid, should be addressed beforehand.

Transesterification reaction

Vegetable oils have higher viscosities than diesel fuel. Their direct use in diesel engines can form deposits in fuel injection systems. The viscosity and boiling point of these oils must first be reduced in order to use them in compression engines. Even though many processes exist to reduce the viscosity of oils including thermal cracking, micro-emulsions and blending; the transesterification reaction of vegetable oils and animal fats is the most common method [Ma et al., 1999].

Several transesterification techniques have been employed to produce biodiesel including enzyme-catalyzed transesterification, catalyst-free transesterification, acid-based esterification and alkali-transesterification [Kulkarni and Dalai, 2006]. However, each of these methods have several design and operating difficulties, for instance non-catalytic (catalyst-free) transesterification requires high pressure (20MPa) and temperature (350°C) [Dasari et al., 2003] leading to higher capital investment and safety issues. Very long reaction residence times have been reported for acid-based esterification reactions.

The most common biodiesel production method is through the alkali-transesterification of various lipid feedstocks, even though soap is formed for the case of waste cooking oil feedstock. Waste cooking oil contains free fatty acid (FFA). FFA is neutralized in contact with base forming soap and water. Long reaction residence time of acid-catalyzed esterification is not desirable; in many cases reaction residence time ranged between 3 and 48 hours [Freedman et al., 1984]. It has been reported that alkali-transesterification can be 4000 times faster that acid-based esterification for the same catalyst concentration [Fukuda et al., 2001]. Acid-catalyzed esterification has also been used as a pre-treatment stage of high FFA content oils. Sodium hydroxide (NaOH), potassium hydroxide (KOH) and sodium methoxide (CH_3ONa) are common bases used in this reaction. It has been reported that 100 wt% biodiesel yield was obtained using sodium methoxide [Vicente et al., 2005]. Catalytic activity of sodium methoxide is much higher compared to other alkaline catalysts

in the presence of FFA and water in the feedstock. FFA content of the waste cooking oil is not a critical factor using sodium methoxide as a catalyst [Alcantara et al., 2000].

Transesterification reaction occurs on the surface of the oil droplets which are suspended in alcohol [Ataya et al., 2006]. Transesterification of oil (also referred to as alcoholysis of tri-glyceride) is shown in Fig.1. In this reaction, tri-glyceride (TG) reacts with an alcohol in the presence of a catalyst to form alkyl ester and glycerine. Intermediate products are di-glyceride (DG) and mono-glyceride (MG), which are converted to alkyl ester and glycerine during the course of the reaction [Freedman et al., 1984]. R_1, R_2 and R_3 shown in Fig.1 are fatty acid chains. This reaction reduces the viscosity of the oil by the factor of eight and increases the volatility of the fuel [Ma et al., 1999].

$$\text{tri-glyceride (TG)} + C_nH_{2n+1}OH \xleftrightarrow{\text{Catalyst}} \text{di-glyceride (DG)} + C_nH_{2n+1}COOR_1$$

$$\text{di-glyceride (DG)} + C_nH_{2n+1}OH \xleftrightarrow{\text{Catalyst}} \text{mono-glyceride (MG)} + C_nH_{2n+1}COOR_2$$

$$\text{mono-glyceride (MG)} + C_nH_{2n+1}OH \xleftrightarrow{\text{Catalyst}} \text{glycerine} + C_nH_{2n+1}COOR_3$$

Figure 1. Transesterification (Alcoholysis) reaction scheme.

This is an equilibrium reaction, thus 100% reaction yield can never be reached. However according to the strict guidelines in the purity of commercial biodiesel required by ASTM D6751 and EN 14214 standards; the maximum total glycerine in the biodiesel must not exceed 0.25%. This implies that the reaction completion must be about 99.7% to meet this specification [Cao at al., 2007]. In addition, the unreacted materials including mono-glyceride (MG), di-glyceride (DG) and tri-glyceride (TG) could be retained in the FAME mixture causing quality problems.

The most common lipids used in transesterification reactions are soybean, sunflower, canola, palm and corn oils. Among these feedstocks, canola oil has less content of saturated fat compared to other vegetable oils, i.e. (< 7 %), resulting in biodiesel products

that have an excellent cold-flow properties [Coleman, 2006]. Refined oils are expensive feedstocks, thus using waste cooking oil as the main feedstock could help the economics of the biodiesel production.

Biodiesel quality standards

Biodiesel products must comply with international standards. EN 14214 in Europe and ASTM D6571 in the United States are well-established standards in determining the quality of the biodiesel. According to these standards, the maximum concentration of free glycerine in the finished biodiesel should not exceed 0.02 wt%. Glycerine is insoluble in biodiesel so almost all glycerine can be easily removed by settling or centrifuging the biodiesel phase. The common method to remove the glycerine in the biodiesel is through multi-stage water washing since glycerine is soluble in water. Although distillation can be utilized to remove glycerine, this process is very energy intensive. The quality of the glycerine produced in the transesterification reaction depends on the catalyst concentration used. In certain circumstances it might not be sold for other applications e.g. cosmetics.

ASTM D6584 is the most common method employed to measure the glycerine content of biodiesel. A brief procedure of this method is given in Appendix C. The maximum MG, DG and TG concentrations can also be calculated using the chromatograms as shown in Appendix C. The concentrations of MG, DG and TG must not exceed 0.8, 0.2 and 0.2 wt% respectively according to ASTM D6571 and EN 14214 standards.

Transesterification in a membrane reactor

Conventional reactors including batch and stirred tank reactor have been extensively employed in the production of biodiesel through transesterifying various lipids. Since the reaction is reversible and 100% conversion cannot be achieved in most cases, some unreacted materials can be left in the biodiesel mixture. This causes quality problem with respect to international standards. Therefore, the biodiesel mixture needs to further reacted and purified in the post treatment stages leading to higher capital and operational cost.

Many factors may affect the reaction completion including molar ratio of alcohol to oil, catalyst concentration, reaction temperature and reactor type.

The integration of reaction and separation in a membrane reactor offers several advantages over conventional reactors currently employed. The membrane technology offers reduction in the number of equipment utilized in the production plant leading to a lower capital and operational cost [Hsieh, 1991]. There are still several challenges that should be addressed prior to scale up though. The idea of utilizing a membrane reactor is to retain the unreacted materials, mostly oil, inside the reactor while products, i.e. FAME, glycerine, catalyst and alcohol, penetrate through the membrane pores. This is due to the fact that oil droplet size exceeds that of the membrane pores [Cao et al., 2007]. This can significantly increase the quality of the biodiesel. Membrane reactor plays an important role in shifting the reaction towards completion by removing products from the reacting mixture resulting to higher reaction yields.

Although waste cooking oil should be filtered and dried prior to the reaction, some small particles and inert components remain in the oil affecting the properties of the biodiesel. This is not the case when using a membrane reactor. In fact, the biodiesel produced in a membrane reactor ultrafiltered while permeating.

In the present study, two laboratory scale membrane reactor apparatuses were employed. Details of the membrane reactors are given in Appendix A.

Membrane

The most common materials used in the production of membranes are polymers and ceramics. Although there are some advantages to use polymer membranes, ceramic membranes are well-known for their stability at high pressure, temperature [Cheryan et al., 1998]. They are not sensitive to pH changes as well. Ceramic membranes have a narrow pore size, high porosity, high flux and long lifetime [Siskens, 1996]. They can be backwashed and autoclaved easily [Kołtuniewicz et al., 1996]. In this study two multi-lumen tubular ceramic membranes were employed. Their characteristics are shown in Tables 1 and 2.

Since ceramic membranes are expensive, the surface area of the membrane should be minimized for a given production capacity. This is possible by increasing the flux through the membrane. Pore size selection is the key factor in design of membrane reactor systems where retention of a reactant inside the membrane is required. Therefore the best selection could be the highest permselectivity with lowest pressure drop using the actual feed to be treated.

Table 1. Membrane characteristics (First study).

Membrane materials type	Ceramic
Active layer materials	Titanium oxide
Ceramic support materials	Titanium oxide
Nominal Molecular Weight Cut-Off	300 kD
Length	400 mm
Number of channels	8
External diameter	25 mm
Channel diameter	6 mm
Surface area	0.047 m^2
Maximum temperature	150 °C
pH operating range	0-14
Bursting pressure	90 bars

Table 2. Membrane characteristics (Second study).

Brand name	Ultrafiltration inopore® Ultra
Materials	Titanium oxide
Mean Pore Size	30 nm
Open porosity	30% - 55%
Length	500 mm
Number of channels	1
External diameter	10 mm
Channel diameter	7 mm
Filtration area	0.011m^2
Inflow area per tube	38 mm^2

Problem definition

High-quality biodiesel production is maintained by separating lipid phase within the membrane reactor. However because of the limitation imposed by mass transport, this is not always achievable at certain operating fluxes and pressures because the concentration of oil is relatively high in the reactor. The existence of high pressure inside the reactor may significantly increase the oil penetration through the membrane pores. Operating above a certain flux, referred to as a critical flux, is not desirable because this causes oil penetration. Therefore flux, pressure, alcohol to oil ratio, catalyst concentration and temperature should be optimized in such a way that the final biodiesel meets the ASTM D6751 and EN 14214standards.

All biodiesel products should be water washed to remove free glycerine and residues. Typically a large quantity of waste water is produced during the water washing process. In some cases three to five water washes are employed. This is against the idea of using biodiesel as an environmentally friendly fuel.

Thesis and objectives

This research thesis is aimed at gaining knowledge on the behaviour of membrane reactor systems in separating unreacted materials, i.e. MG, DG and TG from products in the biodiesel production through alkali-transesterification reaction.

The objectives of this thesis can be divided into four sections:

1) Investigation of a highly concentrated and unstable oil-in-water emulsion as a model system for oil retention inside the membrane reactor. Determination of critical flux based on composition and pressure in the model system prior to the study of the reactive system to facilitate the data interpretation.

2) Multi-feedstock biodiesel production using a two phase membrane reactor. Determination of critical flux based on composition and pressure for the production of biodiesel through alkali-transesterification of low free fatty acid (FFA) content oils and high FFA content oil.

3) The possibility of performing one water washing stage. This will reduce the waste water production leading to a more sustainable process.

4) Studying the possibility of operating at a higher flux to minimize the membrane surface area. This reduces the capital investments significantly.

Organization of the thesis

Two papers have been prepared and submitted for publication. These papers are presented in chapters II and III.

The objective of paper 1 was to investigate a non-reactive model system containing a highly concentrated and unstable oil-in-water emulsion in order to study the separation and purification aspects of biodiesel production in a membrane reactor.

The objective of paper 2 was to study the critical flux based on pressure and composition in biodiesel production through alkali-transesterification of various lipids in a membrane reactor.

References

Alcantara, R.; Amores, J.; Canoira, L.; Fidalgo, E.; Franco, M. J.; Navarro, A. Catalytic Production of Biodiesel from Soybean Oil, Used Frying Oil and Tallow. Biomass Bioenergy 2000; 18:515-527.

Ataya F.; Dubé M.A.; Ternan M., Single-Phase and Two-Phase Base-Catalyzed Transesterification of Canola Oil to Fatty Acid Methyl Esters at Ambient Conditions, Ind. Eng. Chem. Res., 2006; 45:5411.

Cao P.; Tremblay A.Y.; Dubé M.A.; Morse K., "Effect of membrane pore size on the performance of a membrane reactor for biodiesel production", Ind. Eng. Chem. Res., 2007; 46-52.

Coleman B., Canola: An Excellent Feedstock for Biodiesel, Biodiesel Magazine, 2006; 1:50.

Cheryan M.; Rajagopalan N., Membrane processing of oily streams. Wastewater treatment and waste reduction, J.Membr.Sci., 1998; 151-13.

Dasari M.A.; Goff M.J.; Suppes G.J., Noncatalytic alcoholysis kinetics of soybean oil. JAOCS 2003;80:189-92.

Freedman, B.; Pryde, E. H.; Mounts, T. L. Variables Affecting the Yields of Fatty Esters From Transesterified Vegetable Oils. J. Am. Oil Chem. Soc. 1984, 61 (10), 1638-1643.

Fukuda, H.; Kondo, A.; Noda, H. Biodiesel Fuel Production by Transesterification of Oils. J. Biosci. Bioeng. 2001, 92 (5), 405-416.

Graboski M. S.; McCormick R.L., Combustion of Fat and Vegetable Oil Derived Fuels in Diesel Engines, Prog. Energy Comb. Set, 1998.

Haas M. J.; Scott K. M.; Manner W. N.; Foglia T.A., In situ Alkaline Transesterification: an Effective Method for the Production of Fatty Acid Esters from Vegetable Oils, J. Am. Oil Chem. Soc, 2004.

Haws R., Chemical Oxygen Demand, Biochemical Oxygen Demand and Toxicity of Biodiesel, Proceedings of the conference on commercialization of biodiesel: Environmental and health benefits, 1997.

Hsieh H.P., General Characteristics of Inorganic Membranes, Inorganic membrane characterization and application, Elsevier, Amsterdam, 1991.

Klass L.D., "Biomass for Renewable Energy", Fuels and Chemicals; Academic Press: New York, 1998; pp 1-2.

Knothe G., Historical perspectives on vegetable oil-based diesel fuels, vol. 12, inform, 2001, pp. 1103-1107.

Knothe G.; Krahl J.; Van Gerpen J., "The Biodiesel Handbook", AOCS Press: Champaign, IL, 2005, pp. 2-36.

Kołtuniewicz A.B., Field R.W., Process factors during removal of oil-in-water emulsions with cross-flow microfiltration, Desalination, 1996; 105-79.

Kulkarni M.G.; Dalai A.K., "Waste cooking oil-An economical source for biodiesel: A Review", Ind. Eng. Chem. Res. 2006, 45, 2901-2913.

Ma F.; Clements L. D.; Hanna M. A., Biodiesel Production: A Review, Biores. Tech., 1999; 70:1.

Ménard M., "a Big Energy Consumer: A Regional Perspective", Canada, 2009.

Tremblay A.Y.; Cao P.; Dubé M.A., "Biodiesel production using ultralow catalyst concentrations", Energy and Fuels, 2008; 22-2748.

Siskens C. A. M., Application of Ceramic Membrane in Liquid Filtration, Membrane science and technology series 4, Elsevier, Amsterdam, 1996.

Van Gerpen J., Biodiesel Processing and Production, Fuel Processing Technology, 2005; 86: 1097-1107.

Vicente G.; Mercedes M.; Jose A., Integrated Biodiesel Production: a Comparison of Different Homogeneous Catalysts Systems, Biores. Tech., 2005; 96:1425-1429.

Williams J., Presidential presence, Biodiesel Magazine, July, 7, 2005; 22-23.

Zhang Y.; Dubé, M. A.; Mclean D. D.; Kates M., Biodiesel Production from Waste Cooking Oil: 1. Process Design and Technology Assessment. Biores. Tech., 2003; 90:229.

CHAPTER II

The identification and effect of bimodal droplet size distributions in the ultrafiltration of highly concentrated and unstable oil-in-water emulsions.

H. Falahati, A.Y. Tremblay*

Department of Chemical and Biological Engineering, University of Ottawa
161 Louis Pasteur Street, Ottawa, ON, K1N 6N5, Canada

*Corresponding author:
André Y. Tremblay
Tel.: +1 613 562 5800x6108; Fax: +1 613 562 5172.
E-mail address: ay.tremblay@uottawa.ca

Article has been submitted for publication to the Journal of Membrane Science.

CHAPTER II (Paper 1)

The identification and effect of bimodal droplet size distributions in the ultrafiltration of highly concentrated and unstable oil-in-water emulsions.

H. Falahati, A.Y. Tremblay*
Department of Chemical and Biological Engineering, University of Ottawa
161 Louis Pasteur Street, Ottawa, ON, K1N 6N5, Canada

*Corresponding author. Tel.: +1 613 562 5800x6108; fax: +1 613 562 5172.
E-mail address: ay.tremblay@uottawa.ca (A.Y. Tremblay).

Abstract

Membrane technologies offer several advantages over conventional technologies for the separation of oil and water emulsions. However, studies to date have been limited to moderately concentrated emulsions below 15 vol.%. The current work is aimed at gaining knowledge on the behaviour of membrane systems in separating concentrated O/W emulsions up to their phase inversion point (55 vol.%). The average oil droplet size in these emulsions was measured as 3200 nm employing direct light scattering (DLS) measurement methods. Cake layer thickness was predicted based on a droplet size of 3200 nm for the various oil concentrations used in this study. It was observed that the estimated cake layer thickness of 20 to 80 mm, was larger than external diameter of the membrane tube i.e. 6 mm. Settling of the concentrated emulsion permitted the detection of a smaller particle size distribution (30-100 nm) within the larger particles averaging 3200 nm. It was identified that light scattering measurement methods could not efficiently give the droplet size distribution of the oil in the emulsion since large particles interfered with the detection of smaller particles. The content of the smaller particles represented 1% of the total weight of oil at 30°C and 5% at 70°C. This was too low to be detected using DLS measurements but was sufficient to affect ultrafiltration. The critical flux based on flow and oil penetration through the membrane for this system ranged between $1.1x10^{-5}$ and $0.8x10^{-5}$ m/s (30 and 40 L/m^2/h). The results indicate that ultrafiltration was dominated by the fine

particle size distribution present in the concentrated emulsion and that light scattering was not sufficient to predict particle size.

Keywords: Oil-in-water emulsion, Ultrafiltration, Direct light scattering measurement, Critical flux, Particle size distribution

1. Introduction

Oil-in-water emulsions are widely produced in various industrial applications including petrochemical, metallurgical, transportation, cosmetics, domestic sewage, textile etc. [1,2]. In general where immiscible organic compound is in contact with aqueous phases, emulsions of oil and water can be formed [3] therefore separation of oil-in-water (O/W) and water-in-oil (W/O) emulsions has been an area of considerable interest over the past years. The two common types of emulsions are defined as follows: 1) physical emulsions can be formed by mixing only, without the addition of emulsifiers or surfactants; 2) chemical emulsions are formed by adding emulsifiers or surfactants to a two phase system. Emulsion stability refers to the ability of an emulsion to resist changes in its properties over time. Surface active substances (surfactants) can increase the kinetic stability of the emulsion. Contrary to stable oil emulsions, unstable O/W emulsions will dephase and if dewatered, can revert to W/O emulsions. Although unstable emulsions have been widely formed in many industrial applications, there are only few articles regarding unstable highly concentrated emulsions and their treatment. Most of the works done to date are related to dilute O/W emulsion e.g. bilge water [4]. This study is aimed at studying highly concentrated oil-in-water emulsions and their separation constraints.

Ultrafiltration (UF) has been increasingly used over the past decades for the separation of O/W emulsions. A more uniform water quality in the permeate, no need to add chemicals, the possibility of recycling, lower energy costs and automation are some of the advantages associated with membrane technologies [5]. The most common materials used in the production of membranes are polymers and ceramics. Although there are some advantages to use polymer membranes, ceramic membranes are well-known for their stability at high pressure, temperature, pH [5]. Ceramic membranes can be backwashed and autoclaved

easily [6]. In many cases, polymer membranes cannot withstand high temperatures [5]. In general, membrane pore size influences effluent quality and flux. It was reported that UF membranes can remove “almost” all free and dispersed oil droplets from oil-in-water emulsions [7]. The pore size of UF membranes range from 0.001 to 0.1 μm and the regular driving force pressure is in the range of 10-100 psi [2]. It was reported that the smallest oil droplet in O/W emulsion is not expected to be less than 0.04 μm [8].

Conventional oil and water emulsions treatment approaches have included gravity separation and skimming, dissolved air flotation (DAF), de-emulsification, coalescence separation, hydrocyclones [9], pH adjustment and heat treatment. Emulsified oily waters should be pretreated chemically to destabilize the emulsion followed by gravity separation [10]. In some cases acidification will be employed as a pretreatment which could be corrosive. One of the problems reported in coalescence separation is the gradual adsorption of material on the coalescing media which can lead to loss of effectiveness [5].

Several disadvantages have been reported including high capital and operating cost, customization for each individual site, high susceptibility to changes, safety issues, contamination and degradation, mechanical parts aging, etc. [3,5]. For instance most of the conventional methods are not efficient at removing smaller oil droplets and emulsions.

Microfiltration (MF) and UF processes have been increasingly used over the past decades for the separation of oily waters. More uniform water quality in the permeate, no need to add chemicals, possibility of recycling, lower energy cost and automation are some of the advantages associated with membrane technology [5]. In separating oily waters, membrane pore size influences effluent quality and flux. Membrane fouling should be minimized as well. Although microfiltration membranes give higher flux, the risk of oil breaking through the selective layer of the membrane is higher due to their larger pore size [11].

The critical flux of highly concentrated O/W emulsions up to the phase reversal point was investigated by employing a controlled flux-pressure stepping observation and oil breakthrough analysis. Flux stepping (Flux-pressure profile), direct observation through

membrane (DOTM), mass balance and determination by fouling rate are different measurement methods that have been utilized for many years [12]. In the flux stepping method, the flux of permeate is increased incrementally and held constant for a fixed duration of time where a stable transmembrane pressure (TMP) is obtained. This method is more efficient than the TMP-stepping method because it provides much better control of permeate flow and material deposition on the membrane surface throughout the run. This is due to the fact that convective flow is constant during the run [13,14]. Basically critical flux can be defined as the flux below which a decline of flux with time does not occur; above it fouling is observed. This definition is more applicable for dead-end filtration. In the case of emulsion separation by membranes, critical flux was defined as the flux above which a significant amount of oil passes through the membrane pores [15].

Transesterification of oil with methanol to produce biodiesel by employing a membrane reactor is an example of the separation of a highly concentrated oil emulsion [16]. In this case oil and fatty acid esters/methanol are the dispersed and continuous phases respectively. Oil must be retained by the membrane and the reaction products; fatty acid esters and glycerine permeated through the membrane. However due to the limitation imposed by mass transport, this is not always achievable at certain fluxes. The concentration of oil is approximately 40 to 50 vol.% in the reactor which is a relatively high concentration [16]. According to ASTM D6751, the maximum oil concentration in the final biodiesel should not exceed 2000 ppm (0.2 wt%).

Membrane technologies offer several advantages over existing methods for the separation of oil and water emulsions. However, studies to date have been limited to moderately concentrated emulsions below 15 vol.%. The current work is aimed at gaining knowledge on the behaviour of membrane systems in separating concentrated emulsions up to their point of phase inversion.

2. Experimental

2.1 Emulsions

Refined bleached and degummed Canola oil (Spectra Canola, Canada) and distilled water were used in this study. The acid for neutralization was hydrochloric acid (Assay: 36.5-38%, Fisher Scientific, Canada).

2.2 Experimental set-up

In the present study, a UF membrane pilot scale apparatus was employed as shown in Fig.1. A membrane loop was utilized to perform all runs. It was equipped with a shell and tube heat exchanger to maintain the temperature of the fluid in the loop. A water bath was used to control the water temperature. A platinum resistance temperature detector (RTD) was used in the membrane loop to measure the temperature of the emulsion. Three pumps were used in the loop: two gear pumps were used to pump distilled water and oil separately to the loop and a canned motor pump (Laing, Model No. SM-1212-STW-26) was used to circulate the emulsion in the loop. The cross flow velocity of the flow inside the membrane loop was 0.8 m/s. The system was operated in a semi-continuous mode, where the desired amount of oil was loaded in the loop at the beginning of the run and only water was fed to the loop during the run. The water feed pump was also employed to backflush/backwash the membrane with distilled water between two subsequent runs to ensure that no fouling or oil deposition remained on the membrane surface and inside the pores. A valve in the system was utilized to change the direction of distilled water flow from retentate side to the permeate side in order to backflush the membrane. The process control software named Labview® (National Instruments), was employed to control the water feed pump and record the flux stepping, temperature, operational cycle and TMPs in all runs. Balances placed under the water, oil and permeate tanks were used to control and record flow rates. Recording TMPs during each run was achieved by a differential pressure gauge.

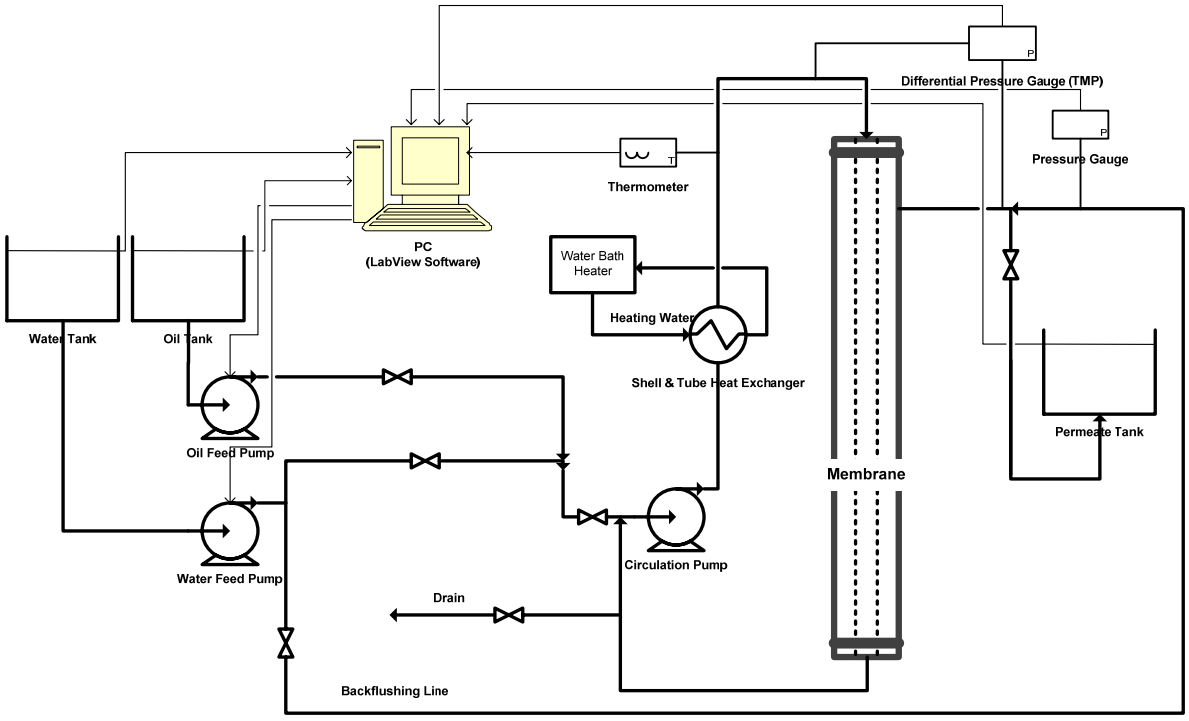

Figure 1. Process flow diagram of the experimental set-up.

2.3 Membrane

A tubular 8-channel ceramic membrane manufactured by TAMI Industries® having a 300 kD MWCO was employed in all experiments. The pore size of the membrane is in the range of 30 to 40 nm. The membrane characteristics are summarized in Table 1.

Table 1. Membrane characteristics.

Membrane materials type	Ceramic
Active layer materials	Titanium oxide
Ceramic support materials	Titanium oxide
Nominal Molecular Weight Cut-Off	300 kD
Length	400 mm
Number of channels	8
External diameter	25 mm
Channel diameter	6 mm
Surface area	0.047 m^2
Maximum temperature	150 °C
pH operating range	0-14
Bursting pressure	91 bars

2.4 Experimental Procedures and Analytical Method

A number of runs were performed and analyzed. The desired amount of oil needed to produce the emulsion was first fed to the loop and then water was added to fill the system. Hydrolysis can produce particles that result in fouling and pore plugging. The pH of the aqueous fraction of this mixture was adjusted to a value of 5.5 to 6. No hydrolysis was observed at this pH, since the membrane permeate was crystal clear and precipitates were not observed in the membrane loop.

The permeate valve was closed when filling the loop with water. The circulation pump was turned on once the loop was full. After circulating the emulsion for about 15 minutes, the permeate valve was opened and water only was pumped into the loop for the duration of the run. As oil was retained in the loop, this assured a constant oil concentration in the loop. Between two subsequent runs; the membrane was backwashed at a pressure greater than the operating pressure of the previous runs. Irreversible fouling was negligible because of the relatively short operating times. Pure water permeability runs were performed between runs to ensure that there was no irreversible fouling and the TMPs were recorded and compared with the initial pure water runs. The initial pure water runs for the membranes were performed prior to the runs. After backflushing for 15 min, the pure water flux had recovered to the initial measurement. Permeation was maintained for at

least one hour and half after steady state was reached and the permeate side of the membrane module was drained between each run.

Oil and water were mixed at different oil ratios; 10, 20, 30, 40, 45, 50 and 55 vol.%. The content of the loop was replaced before each run. The transmembrane pressure (TMP) was recorded at 10 second intervals during the run.

One litre of permeate was collected for each run and contacted with 100 mls of hexane in a separatory funnel. The organic phase was then transferred in a 250 ml flask and the hexane evaporated using boiling water for 2 hours. The amount of hexane extractable material (mostly tri-glycerides) was determined gravimetrically for each run. Temperature and oil concentration in the emulsion were studied and a mixed experimental design was employed to minimize the number of experiments as shown in Table 2. Runs were performed randomly to remove lurking factors [17].

Table 2. Mixed experimental design.

Run ID	Nominal fluxes (L/m^2/h)	Oil content (% oil (v/v))	Water content (% distilled water (v/v))	Temperature (°C)
		8 (Levels)	8 (Levels)	3 (Levels)
1 - 6	10 – 20 – 30 – 40 – 50 – 60	0	100	30
7 - 12	10 – 20 – 30 – 40 – 50 – 60	0	100	50
13 - 18	10 – 20 – 30 – 40 – 50 – 60	0	100	70
19 - 24	10 – 20 – 30 – 40 – 50 – 60	10	90	30
25 - 30	10 – 20 – 30 – 40 – 50 – 60	10	90	70
31 - 35	10 – 20 – 30 – 40 – 50	20	80	30
36 - 39	10 – 20 – 30 – 40	20	80	50
40 - 45	10 – 20 – 30 – 40 – 50 – 60	20	80	70
46 - 49	10 – 20 – 30 – 40	30	70	30
50 - 53	10 – 20 – 30 – 40	30	70	70
54 - 56	10 – 20 – 30	40	60	30
57	10	45	55	30
58 - 59	10 – 20	45	55	50
60	10	50	50	30
61	10	50	50	50
62	10	55	45	50
63	10	55	45	70

3. Results and discussion

3.1 Critical flux determination

In general, in constant pressure filtration: two types of critical fluxes are of great interest i.e. the strong and weak forms. The strong form of critical flux is the flux at which the transmembrane pressure begins to deviate from the pure water line which is linear. For the weak form, fouling occurs steadily during the unsteady state operation, on start-up of the operation, thus the flux-TMP relationship is below the pure water line. The critical flux (weak form) is the point on Flux-TMP plot at which this line deviates from a straight line [12,18].

Fig.2 depicts the relationship between flux and transmembrane pressure (TMP) for different oil ratios and temperatures. As a major trend, increasing the oil content in the emulsion can significantly increase the TMP at a given flux due to the thicker emulsion. As shown in Fig. 2, weak form of critical flux is the most common form of critical flux except for the concentration of 10 vol.% oil. The weak form of critical flux is obtained for most of the conditions studied due to the fact the concentration of oil on the boundary layer of the membrane is high enough to impose a non-linearity on flux-TMP relationship. Contrary to the strong critical flux, membrane resistance does not change until the critical flux is reached. In this study, the weak form of the critical flux was observed in most cases due to cake layer formation. Note that no pore plugging was observed.

Transmembrane pressure is lower at higher temperature due to the lower viscosity of the continuous phase. Since the critical flux can be affected by phase reversal, it is not always possible to have a high concentration of oil in contact with the membrane. In fact there is a maximum oil concentration above which phases will revert. Phase reversal at the surface of the membrane caused the TMP in the system to increase rapidly beyond the 691 kPa (100 psi) limit for our system. Phase inversions were observed at high oil concentrations; it was observed that phase inversion was a function of temperature. At higher temperatures, phases inverted at higher oil ratios. Since oil should remain the dispersed phase in water, oil concentration in the emulsion should not exceed 40 vol%, as this results in significantly high TMP even at a very low flux as shown in Fig.2.

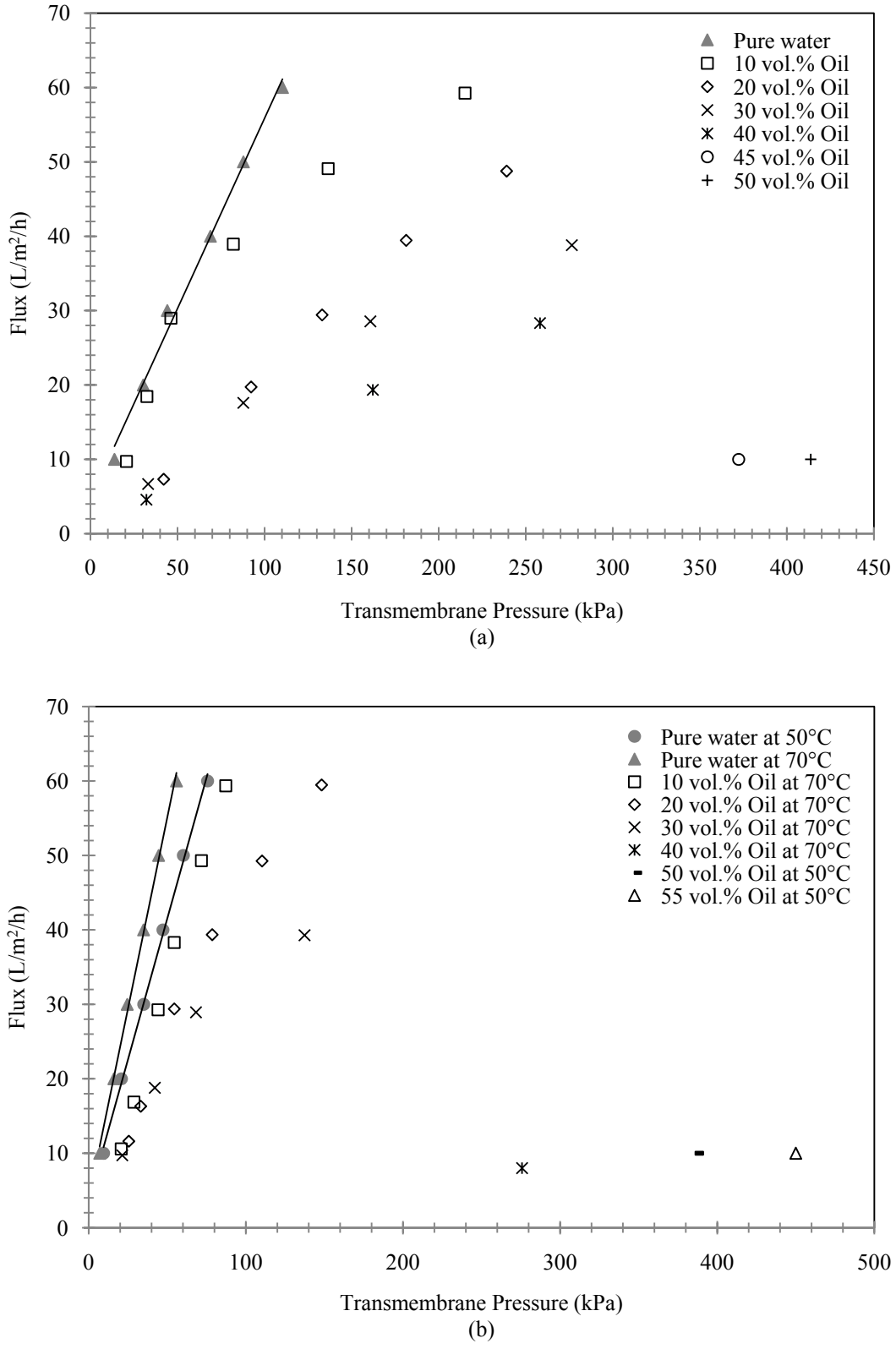

Figure 2. Flux vs. Transmembrane pressure for various operating conditions. (a) Flux-TMP relationship at 30 °C and (b) Flux-TMP relationship at 50 °C and 70 °C.

Steady state TMPs at various operating conditions, i.e. oil concentration and temperature, were obtained and the results are summarized in Table 3. In this table, cells marked in grey indicate operating fluxes lower than critical flux, cells containing infinity sign are fluxes either associated with the phase inversion point or critical flux due to the fact that the steady state TMP exceeded the limiting system pressure of 691 kPa (100 psi).

Table 3. Flux vs. TMP for different operating conditions.

Flux ($L/m^2/h$)	TMP (kPa) 10 vol% oil at 30°C	TMP (kPa) 10 vol% oil at 70°C	TMP (kPa) 20 vol% oil at 30°C	TMP (kPa) 20 vol% oil at 70°C	TMP (kPa) 30 vol% oil at 30°C	TMP (kPa) 30 vol% oil at 70°C	TMP (kPa) 40 vol% oil at 30°C	TMP (kPa) 45 vol% oil at 30°C	TMP (kPa) 45 vol% oil at 50°C	TMP (kPa) 50 vol% oil at 30°C	TMP (kPa) 50 vol% oil at 50°C	TMP (kPa) 55 vol% oil at 50°C	TMP (kPa) 55 vol% oil at 70°C
10	20	13.8	30.5	13.8	33.1	21.4	32.1	372	194	414	386	359	483
20	25	20.1	48.3	22.8	87.8	42.1	162	∞	331	∞	∞	∞	∞
30	52.4	35.9	*82.7*	44.8	*161*	*68.3*	258	∞	∞	∞	∞	∞	∞
40	*76.5*	*47.4*	175	*71*	276	137	∞	∞	∞	∞	∞	∞	∞
50	131	64.8	235	103	∞	∞	∞	∞	∞	∞	∞	∞	∞
60	213	81.9	∞	141	∞	∞	∞	∞	∞	∞	∞	∞	∞

Permeate was collected for each run and the amount of oil was measured by the gravimetric method mentioned above. The separation factor was calculated for the 30 and 70 °C runs by using Eq.1 [19] and plotted for various fluxes at different oil concentrations and temperature as shown in Fig.3. Separation factors were above 99.5 % at fluxes below the critical flux while these dropped to 96 % above the critical flux.

$$\text{Separation factor} = 1 - \frac{\text{oil concentration in permeate}}{\text{oil concentration in feed}} \quad (1)$$

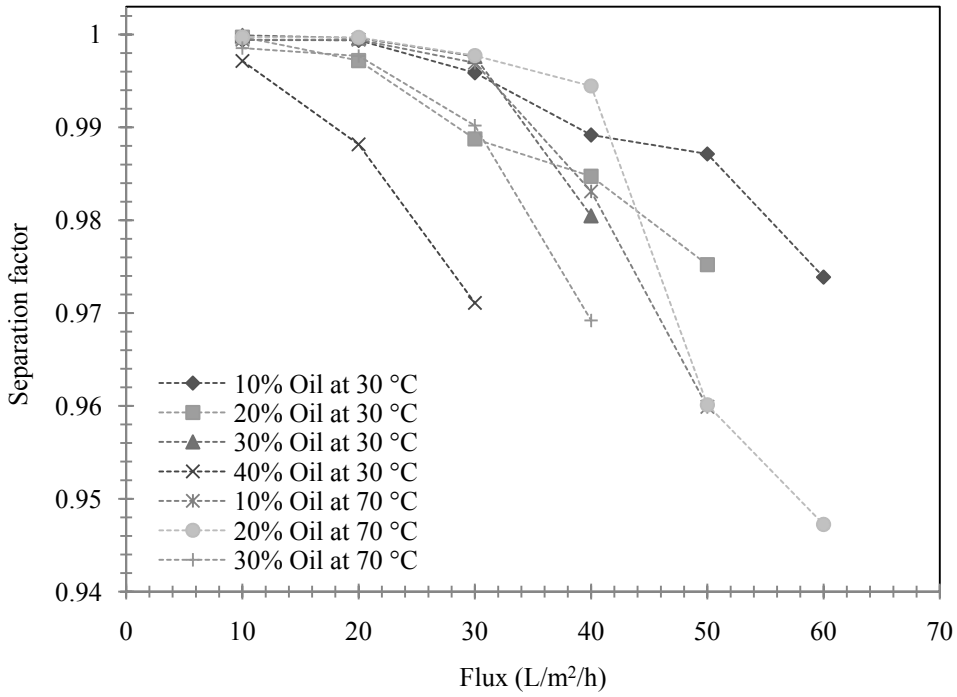

Figure 3. Separation factor at various fluxes for different operating conditions.

The maximum operating fluxes at different conditions, i.e. oil concentration and temperature, at which good separation efficiency has been obtained, are highlighted in Table 3. The maximum oil concentration in the permeate at these fluxes does not exceed 0.2 wt% which could be considered as a good separation. Critical fluxes were shown in italic in Table 3 below where less than 0.2 wt% oil was observed in the permeate. Operating at fluxes higher than critical flux can increase oil penetration resulting in poor quality permeate. In conclusion, the critical flux for this system was determined as 30 to 40 $L/m^2/h$. In the next section, we investigated the oil penetration mechanism.

3.2 Cake layer resistance

Cake layer is a mass transfer resistance that builds up when macromolecules and particulates deposit on the surface of the membrane [20] which results in higher TMPs. Cake layer formation is mainly a function of oil concentration in the emulsion and temperature, causing flow limitation leading to oil penetration.

The relationship between flux and TMP can be explained by Eq.2 [13,15]; it is clear that increasing the total resistance (R_{Total}) towards permeation results in higher TMP at a given flux.

$$J = \frac{\Delta P_L}{\mu \, . \, R_{Total}} \tag{2}$$

where: $R_{Total} = R_m + R_{f\,(reversible)} + R_{f\,(irreversible)} + R_c$ (2.a)

where J is the flux (which is held constant during a run), ΔP_L is the transmembrane pressure (TMP), μ is the viscosity of the mobile phase (distilled water in this study), R_m is the membrane hydraulic resistance, $R_{f\,(reversible)}$ is the resistance due to reversible fouling, $R_{f\,(irreversible)}$ is the resistance due to irreversible fouling and R_c is the cake layer resistance. It has been observed that negligible irreversible fouling occurred on the membrane; This was verified by performing pure water runs after several runs to see whether the membrane resistance increased compared to membrane hydraulic resistance; in addition, backflushing/backwashing was performed after each run to remove reversible fouling between runs. Thus fouling resistances can be neglected from Eq.2. This equation was employed to estimate the cake layer resistance using experimental data. Cake layer resistance at various fluxes for different conditions are shown in Fig.4. As a major trend, cake layer resistances increase as flux increases. Fig.4 indicates that higher oil concentration in the emulsion causes higher cake resistance except for the case of the 10 vol.% oil-in-water emulsion. As mentioned before, strong form of critical flux was

observed for the 10 vol.% oil-in-water emulsion; this implies that cake resistance does not change significantly as flux increases.

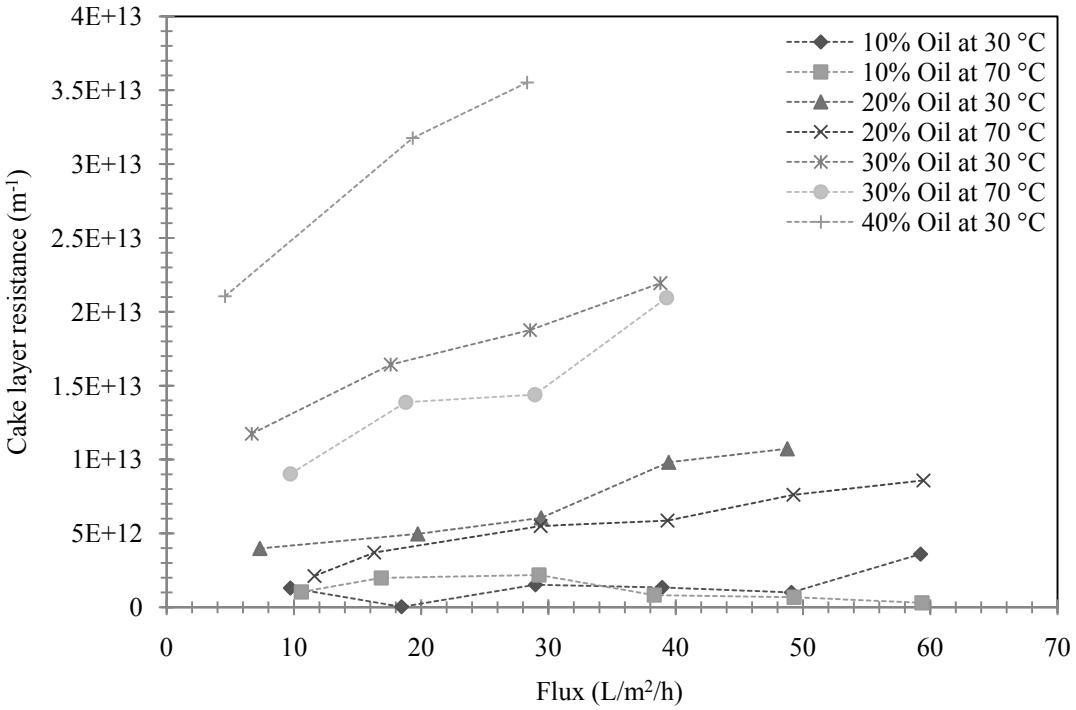

Figure 4. Cake layer resistance at different fluxes for various conditions.

3.3 Cake Compressibility

Cake layer compressibility has been studied at different oil concentration and temperature. Since the flux is constant during the run, Darcy's law can be used to derive an expression for the TMP rise [21]. This expression is explained by Eq.3.

$$\Delta P_L = \alpha \mu c_s \frac{Q^2}{A_c^2} t_{ss} + \mu R_m \frac{Q}{A_c} \quad (3)$$

where Q is the volumetric flow rate, A_c is the cake layer area, μ is the fluid viscosity, R_m is the membrane hydraulic resistance, α is the specific cake resistance, c_s is the concentration of oil in the cake layer, t_{ss} is the time to reach steady state and ΔP_L is the transmembrane

pressure. The relationship between specific cake resistance and transmembrane pressure for the compressible cake layer can be explained by Eq.4.

$$\alpha = \alpha_0 \, \Delta P_L^n \tag{4}$$

where α_0 is the specific cake layer resistance, n is an indication of the cake compressibility and ΔP_L is the transmembrane pressure. By substituting Eq.4 into Eq.3 the following equation can be obtained.

$$\Delta P_L{}^{1-n} = \alpha_0 \, (1-n) \, \mu \, c_s \, \frac{Q^2}{A_c^2} \, t_{ss} \tag{5}$$

where plot of log ΔP_L versus t_{ss} gives a straight line if the cake layer is compressible [21]. Plot of log ΔP_L versus t_{ss} at the flux of 20 ($L/m^2/h$) was obtained at different operating conditions as shown in Fig.5. This implies that this system is in conformity with this model therefore the cake layer is compressible.

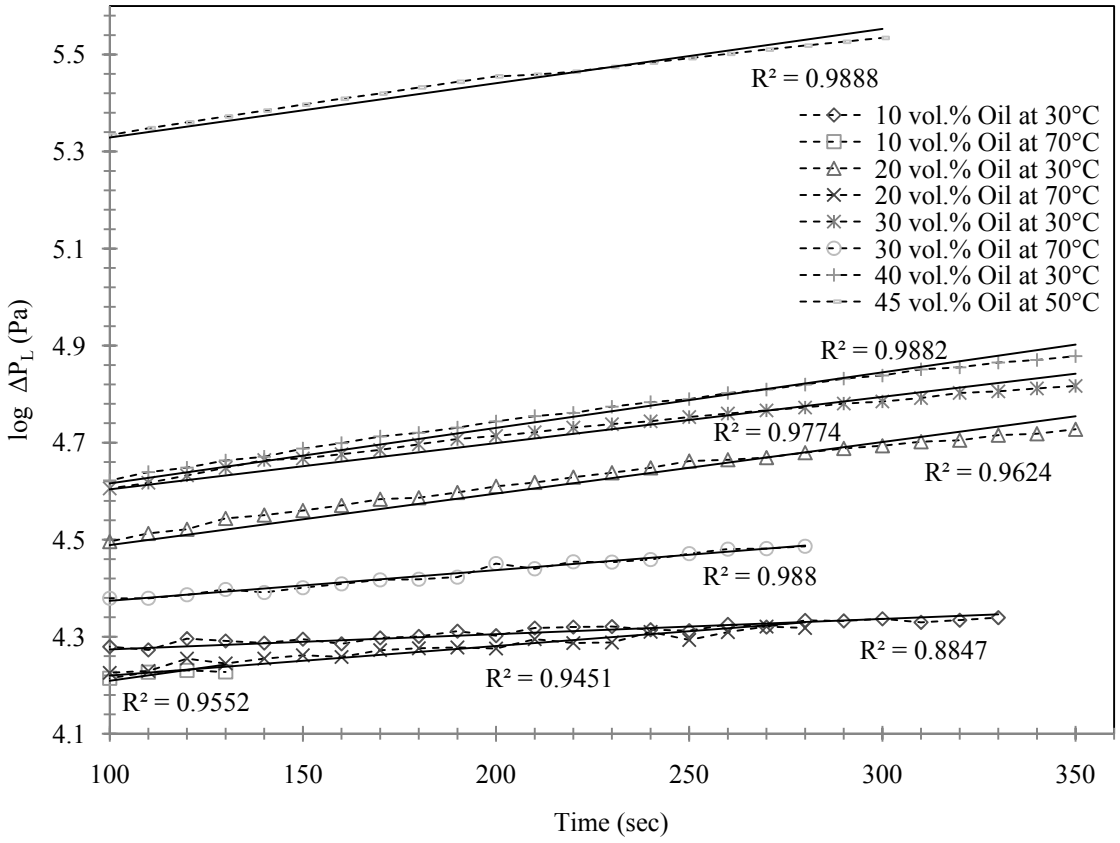

Figure 5. log ΔP_L vs. Time.

3.4 Prediction of Cake layer thickness

Particle size distributions were obtained by employing light scattering techniques. Malvern® Mastersizer™ 2000 and Malvern® Zetasizer™ instruments were used together. The results show that the majority of the particles do have larger diameter than that of membrane pores as shown in Fig.6. As a result, this pore size could be considered as a good candidate. Although much lower pore size can be utilized to avoid pore blinding by smaller particles, this leads to higher transmembrane pressures that can cause oil penetration in membrane pores leading to lower separation.

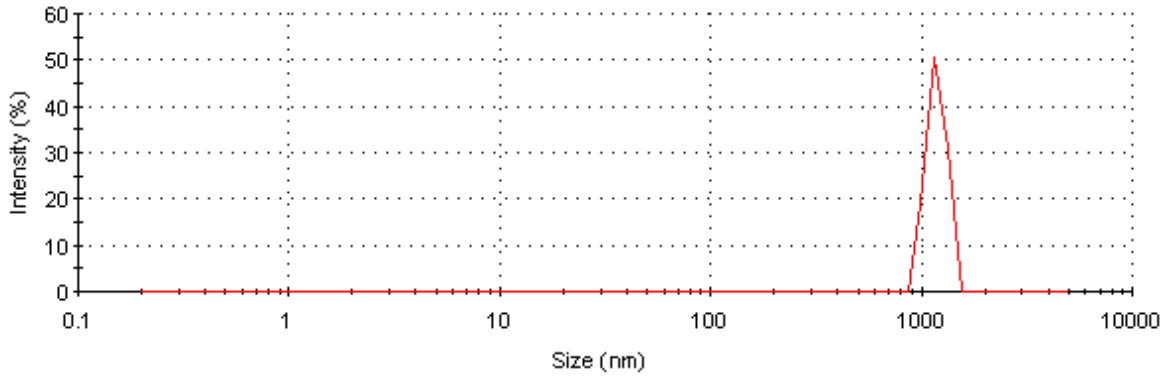

Figure 6. Oil droplet size distribution by intensity (Malvern® Zetasizer™ instrument).

The steady state cake layer thickness was then calculated based on a particle size of 1.2 microns as shown in Fig.6, using Eq.6 [22,23].

$$\delta_{ss} = \frac{\sqrt{(R_m^2 + 2\, C\, \alpha\, t_{ss})} - R_m}{\alpha} \tag{6}$$

where:

$$C = \frac{\Delta P_L\, \phi_b}{\mu\, (\phi_{max} - \phi_b)} \tag{6.a}$$

$$\alpha = \frac{37.5\, \phi_{max}^2}{a_p^2\, (1 - \phi_{max})^3} \tag{6.b}$$

where ΔP_L is the transmembrane pressure (TMP), ϕ_b is the solute volume fraction in the emulsion, ϕ_{max} is the maximum solute volume fraction in the cake layer, μ is the viscosity, α is the specific cake layer resistance, R_m is membrane hydraulic resistance, a_p is particle size and t_{ss} is the time required to reach steady state transmembrane pressure. The maximum solute volume fraction should not exceed 0.58 [24] and can be used when the cake layer is compressible. For a particle size of 1.2 microns and total oil concentration of

20 vol.%, the thickness was calculated and ranged from 2 to 8 cm. This is much greater than the lumen size of the membrane i.e. 6 mm.

The possibility of an inaccurate determination of particle size distribution in the concentrated emulsion was investigated as a possible cause of this discrepancy. The particle size of the concentrated emulsion was determined by two DLS measurement instruments (Malvern® Mastersizer™ 2000 and Malvern® Zetasizer™); both gave relatively the same results. It was hypothesized that the highly concentrated oil emulsion could have obstructed the light path through the sample and this prohibited the detection of a less concentrated distribution of smaller particles. These could have greatly influenced membrane permeability. In order to investigate this possibility, a method was devised where a 20 vol.% oil-in-water emulsion was prepared and circulated for 2 hours at a given temperature in the membrane loop to form a homogenous O/W emulsion. The loop was then quickly emptied and the emulsion allowed to dephase in a separatory funnel. Two samples containing 10 mls of emulsion were taken after 10 and 15 minutes of settling. Their droplet size was measured using DLS. The particle size distributions are shown in Fig.7. It can be observed from Fig.7, that the oil does have a bimodal droplet size distribution. It was reported that the smallest oil particle radius is not expected to be less than 0.04 μm [8]; this is in pretty good agreement with the results of this measurement. Peng and Tremblay [25] also reported that a fine particle size distribution was centered around 0.18 μm in synthetic bilge water; a mixture containing, 2000-mg/L oils, 500-mg/L detergents and surfactants, and a 50/50 mixture of fresh water + seawater (approximately 99.75%).

It was observed in this work that the smallest oil droplets are in the range of 30~100 nm while the larger particles range from 1.2 to 3.2 microns. This bimodal distribution and its effect on cake formation are illustrated in Fig.8. Small particles contribute more significantly to cake layer formation than large particles because the diffusivity of smaller particles is much higher than that of larger ones. In fact Brownian diffusivity is inversely proportional to particle size [24], shear diffusion is much higher for the larger micron sized particles and these will not be found in the cake. A minimum in diffusivity vs. particle size

is obtained at approx 100 nm. In addition, Van der Waals forces contribute to cake layer structure formation and these forces are significantly higher among small oil droplets [26]. The pore size of the 300 kD membrane was estimated at 30 nm [27]. This is at the lower end of the size of the droplets in the smaller distribution. Small oil droplets can deform and penetrate through the membrane pores. The proximity of size does not require a large driving force i.e. TMP. Regular light scattering methods were not an efficient method to find the small oil droplet distribution. The next experiments were used to determine the amount of small oil droplets, i.e. 30~100 nm, in the emulsion.

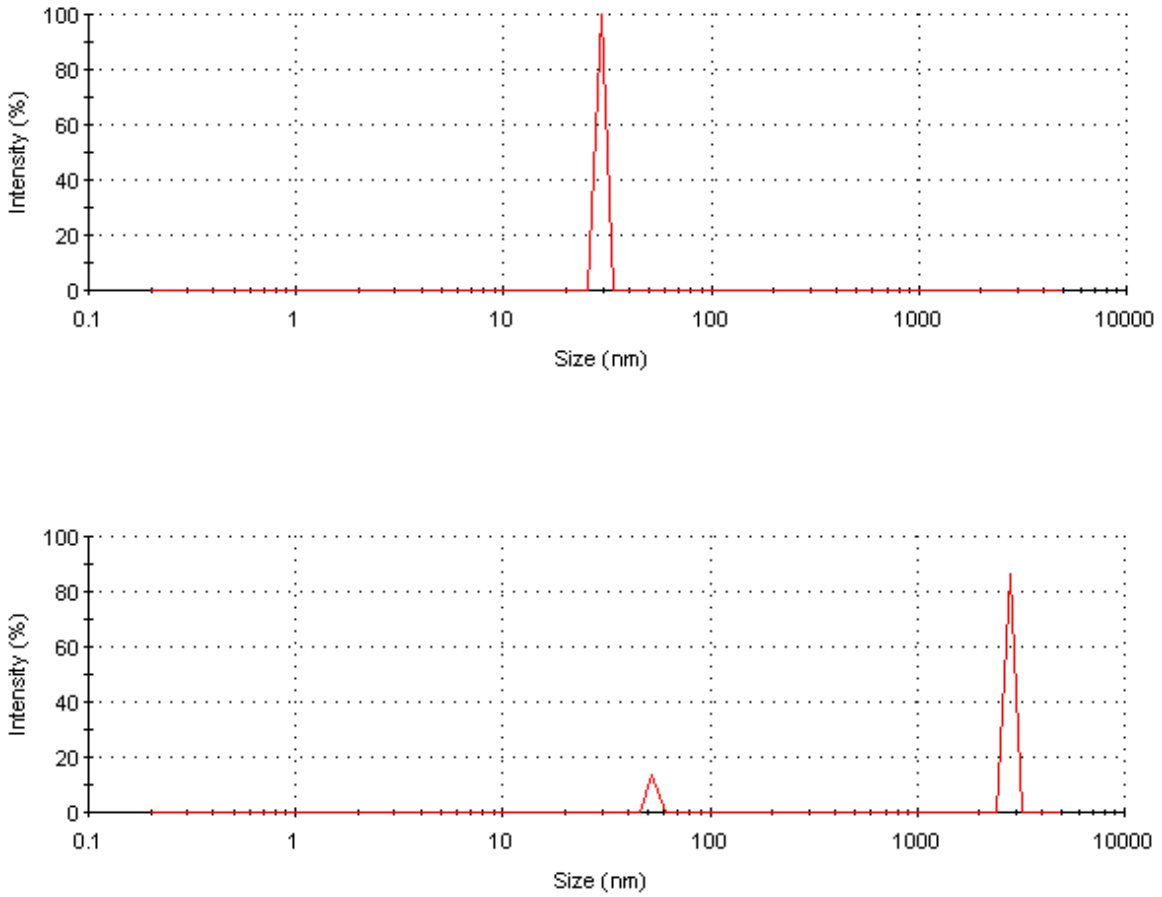

Figure 7. Oil droplet size distributions by intensity. The sample was taken after 10 minutes (Above), The sample was taken after 15 minutes (Below).

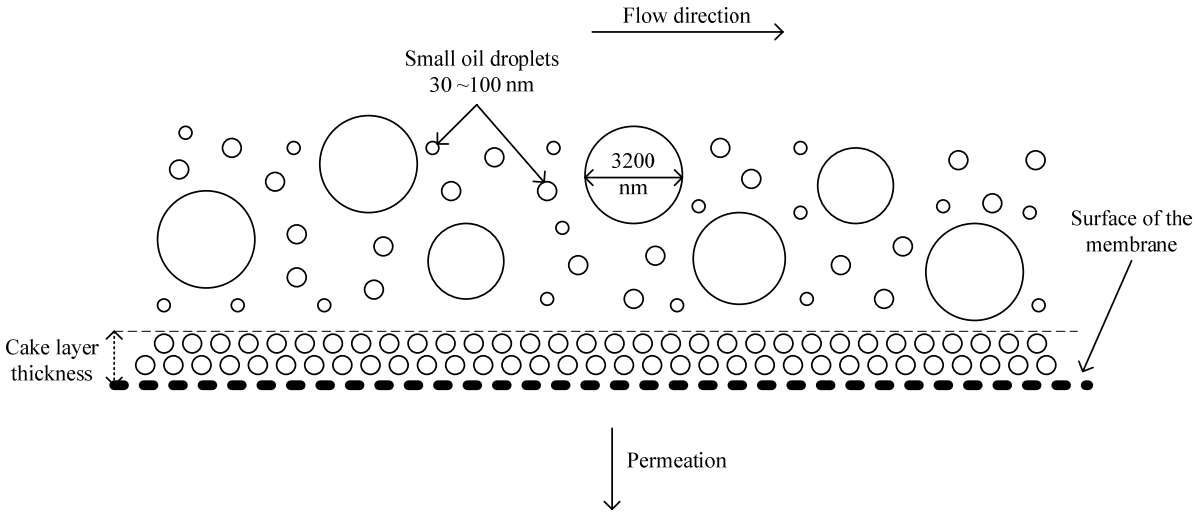

Figure 8. Cake distribution of oil droplets in the emulsion on the surface of the membrane and cake layer formation.

To find the concentration of small oil particles (30~100 nm), another set of runs was performed as shown in Table 4. Oil and water was mixed at oil ratios of 10, 20, 30 and 40 vol.% and circulated for 2 hours to make a homogenous O/W emulsion. The emulsion settled in a separatory funnel for 10 minutes, a sample of 500 mls was collected and extracted with Hexane. The quantity of small particles at two different temperatures were obtained as shown in Fig.9. It has been observed that the small oil droplet population was higher at higher temperature due to the fact that oil droplets can easily break and deform at higher temperatures.

Table 4. Design of experiment for small droplet population measurement.

Run ID	Oil content (% oil (v/v))	Water content (% distilled water (v/v))	Temperature (°C)
	4 (Levels)	4 (Levels)	2 (Levels)
1	10	90	30
2	20	80	30
3	30	70	30
4	40	60	30
5	10	90	70
6	20	80	70
7	30	70	70

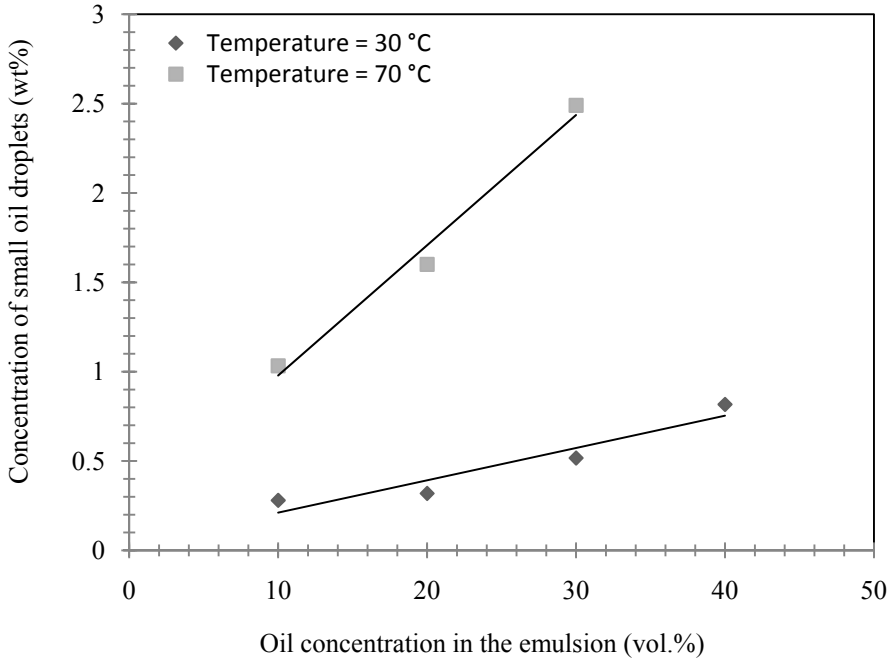

Figure 9. Concentration of small particles (wt%) versus total concentration of oil in the emulsion (vol.%).

The cake layer thickness was re-calculated, for the 10 to 30 % oil volume runs, using 75 nm as an average diameter for the smaller particles. The concentration of the smaller particles was determined experimentally and used as reported in Fig.9. The new cake layer resistances are shown in Fig.10. The values for cake thickness are more reasonable and were in the expected range for ultrafiltration.

As shown in Fig.4, cake layer resistance increases with flux. This increase is also reflected in the relation of cake layer thickness with flux shown in Fig.10. The amount of material being brought to the surface of the membrane over time is proportional to the membrane flux. This direct relation is easily seen by the linear relation between cake layer thickness and flux shown in Fig.10.

As stated before, the strong form of critical flux was observed for the oil concentration of 10 vol.% as shown in Fig.2. This explains why the cake layer resistance is low and does not increase significantly by increasing the flux as shown in Fig.4. For a given particle size and porosity, cake layer resistance is proportional to cake layer thickness. As seen in Fig.10, at 10 vol.% oil, the cake layer is thin and the membrane hydraulic resistance is the greater contribution to the total resistance towards permeation.

Temperature had less of an effect on cake layer formation. As a general trend, the cake layer thickness decreases as the temperature increases. One possibility for this is that the small droplets can more easily coalesce at higher temperatures. This coalescence increases their size and consequently their shear diffusion [28, 29]. This increased shear diffusion will move the particles away from the surface of the membrane, reducing the thickness of the cake. In addition, particle deforming tendency increases as temperature increases because the cake layer is compressible.

Although ceramic membranes are hydrophilic, the membrane surface can become oil-wet because of the existence of a concentrated oil cake. Coalescing increases as oil concentration increases. In addition to migration by shear diffusion, some larger oil

particles can also pass through the membrane when the TMP is great enough to deform the droplet and overcome surface tension effects within the membrane pores.

These results illustrate the use of membrane filtration in determining the presence of smaller particles in a complex and concentrated oil emulsion. They indicate that membrane filtration could be used to characterize and determine the finer nature of complex oil-in-water emulsions where DLS and other particle size determination techniques cannot work. They also indicate, that in concentrated oil-in-water emulsions, permeate flux cannot be merely increased to increase the flow through the membrane as oil separation is linked to flux. Operating at fluxes higher than critical flux involves a penalty above that of increased pressure requirements reflected by a reduction in the separation efficiency of the membrane.

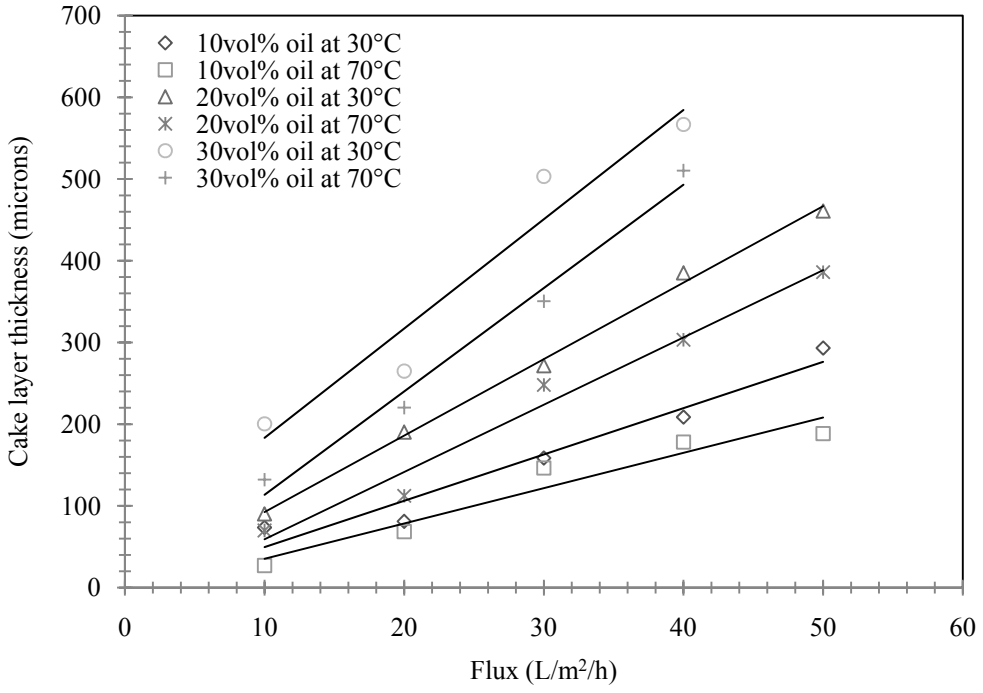

Figure 10. Cake layer thickness vs. flux.

Conclusions

The prediction of cake layer thickness based on DLS measurements led to unreasonably high cake thicknesses. Settling of the concentrated emulsion permitted the detection of a smaller particle size distribution (30-100 nm) hidden by the larger particles ranging from 1.2 to 3.2 microns. It was found that at higher temperature the concentration of small oil droplets is significantly higher than that of lower temperature. The content of the smaller particles represented 1% of the total weight of oil at 30°C and 5% at 70°C. This was too low to be detected using DLS measurements but was sufficient to affect ultrafiltration.

Cake layer thickness increases as flux increases. Oil penetration occurs because the cake diffuses gradually into the pores. Small particles can easily coalesce into the cake sub-layer resulting in oil penetration. It was also identified that the cake layer is compressible.

The critical flux based on flow and separation for this system ranged between 30 and 40 $L/m^2/h$. The results indicate that ultrafiltration was dominated a fine particle size distribution present in the concentrated emulsion and that light scattering was not sufficient to predict particle size. Membrane filtration is a useful tool to determine the presence of small oil droplet distributions in concentrated emulsions as flow through the membrane is highly affected by sub-micron sized particles present in water.

Acknowledgment

The authors gratefully acknowledge the financial support from the Natural Sciences and Engineering Research Council of Canada (NSERC).

References

[1] A.B. Koltuniewicz, R.W. Field, and T.C. Arnot, Cross-flow and dead-end microfiltration of oily-water emulsion, Part I: Experimental study and analysis of flux decline, J.Membr.Sci., 102 (1995) 193.

[2] M.C. Porter, Ultrafiltration, in: M.C. Porter (Ed.), Handbook of industrial membrane technology, Noyes publications, 1990, pp. 136-260.

[3] N.P. Tirmizi, B. Raghuraman, and J. Wiencek, Demulsification of Water/Oil/Solid Emulsions by Hollow-Fiber Membranes, AICHE J., 42 (1996) 1263.

[4] R. Ghidossi, D. Veyret, J.L. Scotto, T. Jalabert, P. Moulin, Ferry oily wastewater treatment, Sep. Purif. Technol., Volume 64, Issue 3, 12 January 2009, Pages 296-303.

[5] M. Cheryan, N. Rajagopalan, Membrane processing of oily streams. Wastewater treatment and waste reduction, J.Membr.Sci., 151 (1998) 13.

[6] A.B. Kołtuniewicz, R.W. Field, Process factors during removal of oil-in-water emulsions with cross-flow microfiltration, Desalination, 105 (1996) 79.

[7] A. Asatekin, A.M. Mayes, Oil industry wastewater treatment with fouling resistant membranes containing amphiphilic comb copolymers, J. Environ. Sci. Technol., 43 (2009) 4487.

[8] P. Lipp, C.H. Lee, A.G. Fane, and C.J.D. Fell, A fundamental study of the ultrafiltration of oil-water emulsions, J.Membr.Sci., 36 (1988) 161.

[9] M. Ebrahimi, K. Shams Ashaghi, L. Engel, D. Willershausen, P. Mund, P. Bolduan, P. Czermak, Characterization and application of different ceramic membranes for the oil-field produced water treatment, Desalination, Volume 245, Issues 1-3, 2008.

[10] R.M. Dick, Ultrafiltration for oily wastewater treatment, Lubr. Eng., 38 (1982) 219.

[11] M. Hlavacek, Break-up of oil-in-water emulsions induced by permeation through a microfiltration membrane, J.Membr.Sci., 102 (1995) 1.

[12] P. Bacchin, P. Aimar, and R.W. Field, Critical and sustainable fluxes: Theory, experiments and applications, J.Membr.Sci., 281 (2006) 42.

[13] S. Lee, Y. Aurelle, and H. Roques, Concentration polarization, membrane fouling and cleaning in ultrafiltration of soluble oil, J.Membr.Sci., 19 (1984) 23.

[14] S. Sethi, M.R. Wiesner, Performance and cost modeling of ultrafiltration, J.Environ.Eng., 121 (1995) 874.

[15] F.F. Nazzal, M.R. Wiesner, Microfiltration of oil-in-water emulsions, Water Environ.Res., 68 (1996) 1187.

[16] P. Cao, A.Y. Tremblay, M. A. Dubé, K. Morse, Effect of membrane pore size on the performance of a membrane reactor for biodiesel production, Ind. Eng. Chem. Res., 46 (2007) 1, 52-58.

[17] D.C. Montgomery, G.C. Runger, Applied Statistics and Probability for Engineers, fourth Ed., Wiley, Hoboken, New Jersey, 2007.

[18] D. Wu, J. A. Howell, R. W. Field, Critical flux measurement for model colloids, J.Membr.Sci., 152 (1999) 89-98.

[19] M. Hlavacek, Break-up of oil-in-water emulsions induced by permeation through a microfiltration membrane, J.Membr.Sci., 102 (1995) 1.

[20] W. S. Ho and K. Sirkar, Microfiltration: Definitions, in: R. H. Davis (Ed), Membrane Handbook, Van Nostrand Reinhold, New York, 1992, pp. 457-460.

[21] P. Kovalsky, G. Bushell, and T.D. Waite, Prediction of transmembrane pressure build-up in constant flux microfiltration of compressible materials in the absence and presence of shear, J.Membr.Sci., 344 (2009) 204.

[22] Davis, R. H., “Microfiltration: Definitions,” in Membrane Handbook, ed. W. S. Ho and K. Sirkar, Van Nostrand Reinhold, 1992, pp. 457-460.

[23] M. Nottegar, The effects of particulates on the ultrafiltration of bilge (oily) wastewater containing new or used lubricating oil, M.A.Sc. Thesis, University of Ottawa, 2000, pp. 27-29.

[24] S. Sethi, M.R. Wiesner, Performance and cost modeling of ultrafiltration, J.Environ.Eng., 121 (1995) 874.

[25] H. Peng, A.Y. Tremblay, Membrane regeneration and filtration modeling in treating oily wastewaters, J.Membr.Sci., 324 (2008) 59.

[26] J.A. Howell, T.C. Arnot, H.C. Chua, P. Godino, D. Hatziantoniou, and S. Metsäïmuuronen, Controlled flux behaviour of membrane processes, Macromolecular Symposia, 188 (2002) 23.

[27] C. E. Ioan, , T. Aberle, W. Burchard, Light scattering and viscosity behavior of dextran in semidilute solution, Macromolecules, 34 (2001) 2, 326-336.

[28] D. Leighton, A. Acrivos, Measurement of shear-induced self-diffusion in concentrated suspensions of spheres, J. Fluid Mech., 177 (1987) 109-131.

[29] D. Leighton, A. Acrivos, The shear-induced migration of particles in concentrated suspensions, J. Fluid Mech., 181 (1987) 415-430.

CHAPTER III

Critical flux determination in biodiesel production from various feedstocks in a membrane reactor.

H. Falahati, A.Y. Tremblay*

Department of Chemical and Biological Engineering, University of Ottawa
161 Louis Pasteur Street, Ottawa, ON, K1N 6N5, Canada

*Corresponding author:
André Y. Tremblay
Tel.: +1 613 562 5800x6108; Fax: +1 613 562 5172.
E-mail address: ay.tremblay@uottawa.ca

Article has been submitted for publication to the journal of Fuel.

CHAPTER III (Paper 2)

Critical flux determination in biodiesel production from various feedstocks in a membrane reactor.

H. Falahati, A.Y. Tremblay*
Department of Chemical and Biological Engineering, University of Ottawa
161 Louis Pasteur Street, Ottawa, ON, K1N 6N5, Canada

*Corresponding author. Tel.: +1 613 562 5800x6108; fax: +1 613 562 5172.
E-mail address: ay.tremblay@uottawa.ca (A.Y. Tremblay).

Abstract

Biodiesel produced from lipid sources is a clean-burning, biodegradable, nontoxic fuel that does not contain sulphur, aromatic hydrocarbons, metals or crude oil residues. Current biodiesel production processes are tedious and involve two to three reaction steps each followed by separation and purification. Process integration of reaction and separation in a membrane reactor (MR) offers several advantages over conventional reactors. Integration leads to the reduction of the environmental footprint of the process while maintaining the quality of the biodiesel produced. This investigation is aimed at studying the critical flux, based on pressure and composition, and residence time within a membrane reactor and their influence on fuel quality when treating a variety of raw and used feedstocks. The objective was to minimize membrane area in the MR. Low FFA oils (FFA<1%), i.e. canola, corn, sunflower and unrefined soy oils, and high FFA waste cooking oil (FFA = 9%) were used to study the quality of the biodiesel produced in terms of glycerine, mono-glyceride, di-glyceride and tri-glyceride concentrations. The present study verified that the critical flux, based on composition was greater than 70 $L/m^2/h$ for all feedstocks as the specification for both ASTM D6751 and EN 14214 standards in the biodiesel product was reached for all runs. However, a critical flux related to the operating pressure in the reactor was reached for waste oils and pre-treated corn oil. This flux ranged from approx. 30 to 40 $L/m^2/h$. It was identified that the residence time in the reactor was a key design parameter affecting the operating pressure in the reactor. Lower residence times increased the amount

of unreacted oil in the reactor which caused an increase in pressure within the reactor. However, the quality of the biodiesel produced was not affected.

Keywords: Biodiesel, Membrane reactor, Alkali-transesterification, Fatty acid methyl ester (FAME)

1. Introduction

Biodiesel is a clean-burning fuel that does not contain sulphur, aromatic hydrocarbons, metals or crude oil residues [1,2]. It is produced from renewable sources and is a good alternative to petroleum based diesel (petro-diesel) in terms of reducing green house gases (GHG) and volatile organic compounds (VOC) emissions. In fact, it can be used directly in diesel compression-ignition engines as B100 or can be blended with petro-diesel, e.g. B20 containing 20 vol.% biodiesel and 80 vol.% petro-diesel. Minor engine modifications might be required to prevent the dissolution of various seals when using B100 biodiesel [3]. Biodiesel combustion is more complete because it is oxygenated; consequently it increases engine life significantly [2].

Several techniques have been employed in the production of biodiesel including acid/alkali catalyzed transesterification of different oils, enzyme-catalyzed transesterification and catalyst-free technology for transesterification. Each method has various technical challenges, for instance the catalyst free method [4] requires a high pressure (20 MPa) and temperature (350°C). Transesterification is the most common process for the production of biodiesel. In this process tri-glyceride (TG) reacts with an alcohol in the presence of a base catalyst to form methyl esters and glycerine as shown in Fig.1. Intermediate products are Di-glyceride (DG) and Mono-glyceride (MG), which are converted to methyl ester and glycerine during the course of the reaction [3,5]. R_1, R_2 and R_3 shown in Fig.1, are fatty acid chains.

$$\text{Tri-glyceride (TG)} + CH_3OH \overset{\text{Base}}{\Longleftrightarrow} \text{Di-glyceride (DG)} + CH_3COOR_1$$

$$\text{Di-glyceride (DG)} + CH_3OH \overset{\text{Base}}{\Longleftrightarrow} \text{Mono-glyceride (MG)} + CH_3COOR_2$$

$$\text{Mono-glyceride (MG)} + CH_3OH \overset{\text{Base}}{\Longleftrightarrow} \text{Glycerine} + CH_3COOR_3$$

Figure 1. Reaction scheme for transesterification.

In general, increased energy demand due to industrialization, population rise and oil price fluctuations, is the primary reason leading to more interest in this area of research. However the production cost of biodiesel from various feedstocks is much higher than that of petro-diesel. Plant size, feedstock cost, purification of biodiesel and the value of by-products are still major issues [6]. Among these, feedstock cost and biodiesel purification are the main factors that must be taken into account. Therefore utilizing efficient production methods to help the economics of the process is important.

Membrane reactor (MR) technology offers several advantages over conventional reactors. Batch and continuous stirred tank reactors followed by a separation unit are currently used. The integration of reaction and separation in a MR offers a reduction in the number of equipment utilized in the production plant leading to lower capital and operational cost. Tremblay and Dubé demonstrated the use of membrane reactor for the production of biodiesel [7]. Cao et al. [8] used membranes having various pore sizes in a membrane reactor producing FAME and found that no tri-glycerides were present in the permeate.

Tremblay et al. [3] demonstrated the advantages of using a MR system is transesterification of oils using ultralow catalyst, i.e. 11 to 33 times lower than currently used in industry. This also reduces the amount of waste water produced leading to a more environmentally friendly process. Using ultralow catalyst concentrations also improves the color and quality of the methyl ester and glycerine.

Since transesterification is an equilibrium reaction, 100% reaction yield can never be achieved. This is of great interest because strict guidelines regarding the purity of commercial biodiesel are proposed by ASTM D6751 and EN 14214 standards. This allows 0.24% total glycerine in the final product, and implies that the reaction completion must be greater than 99.7% to meet the total glycerine standard for the fuel [8]. In addition, the unreacted materials, i.e. MG, DG and TG, could be retained in the FAME mixture causing quality problems.

The concept behind the membrane reactor for the production of biodiesel is to retain oil (TG) inside the reactor. High-quality biodiesel production is maintained by separating the oil phase within the MR. However because of phase inversion limitations the amount of unreacted oil in the reactor is limited to 40 to 50 vol.% [8]. According to international standards, the maximum concentration of MG in biodiesel should not exceed 0.8 wt% and the maximum concentration of DG and TG in the biodiesel product should not exceed 0.2 wt%. FAME is a good solvent so it increases the solubility of DG and TG in the permeate stream, while lowering the interfacial tension between the methanol and TGs at the reaction temperature. In addition, high pressure inside the reactor can force the penetration of oil through the membrane. Recently Falahati and Tremblay [9] have reported that the critical flux for both pressure and composition for a highly concentrated unstable oil-in-water emulsion ultrafiltration (UF) using a multilumen ceramic membrane is in the range of 30 to 40 $L/m^2/h$ for a pore size of 30 nm.

In membrane systems, a design objective to reduce capital cost is to minimize membrane area. Operating at the highest feasible flux will minimize membrane area in the system. To this date, the value of this feasible flux is not known. It is also speculated that this flux could be depend on the type of feedstock used in the reactor. Various feedstocks will create emulsions of a different nature that will present different levels of difficulty in their separation. In previous work performed on MR systems the reactor loop volume was fixed which implied that membrane flux and residence time in the reactor were coupled. In this work three loop volumes were used to decouple the effects of residence time and membrane flux on the performance of the MR system.

The current work is aimed at gaining knowledge on the behaviour of MR systems in separating glycerine, MG, DG and TG from products in multi-feedstock biodiesel production. In this study, biodiesel was produced from various feedstocks including refined canola, corn and sunflower oils as well as unrefined soy and waste cooking oils. The residence time, critical flux based on pressure and critical flux based on composition were determined in relation to the operating pressure of the reactor and the composition of the biodiesel produced.

2. Experimental

2.1 Basic principle

In the present MR, oil droplets are suspended in the oil and methanol emulsion since oils are immiscible in methanol, i.e. continuous/mobile phase, under various conditions. The idea of using a MR is to retain unreacted components inside the reactor, i.e. retentate side, while FAME, methanol, glycerine and catalyst penetrate through the membrane pores as shown in Fig.2. Note that contrary to dead-end filtration, the MR is operated in a cross flow filtration mode.

The transesterification reaction takes place at the interface between the TG droplet and methanol [10]. The products of this reaction, FAME and glycerine, are miscible in methanol. FAME, methanol, glycerine and catalyst permeate through the membrane pores while the emulsified TG droplets are retained inside the reactor due to the fact that their size exceeds that of the membrane pores [8].

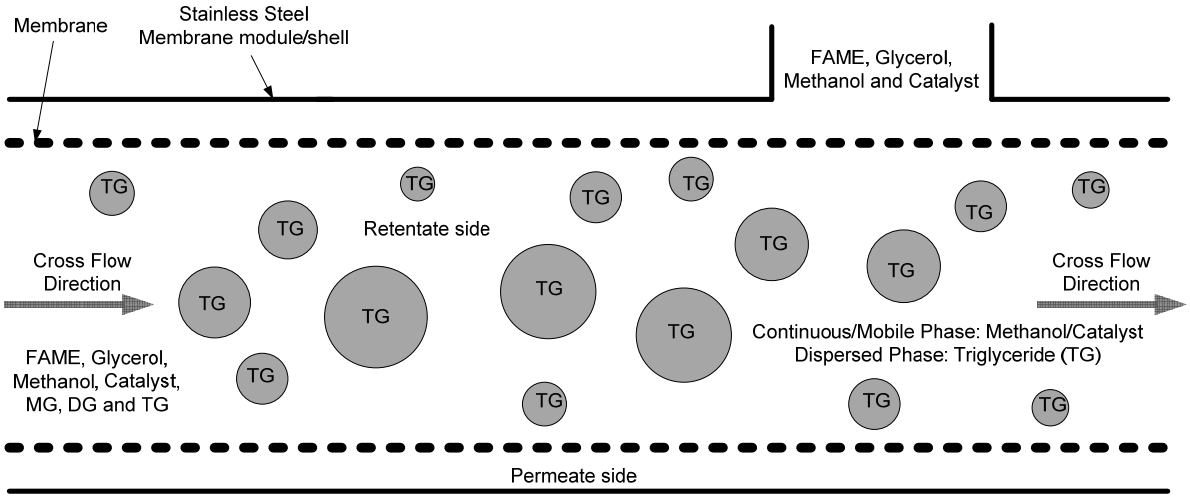

Figure 2. Schematic of membrane module for the production of biodiesel.

2.2 Materials

High-purity FAME production from refined canola, un-refined soy, pre-treated and refined corn, refined sunflower oil and waste cooking oil were processed using a MR. The canola oil was refined, bleached and degummed (RBD) (Spectra Canola, Canada); crude soy and pre-treated corn oils were obtained commercially. The refined sunflower and corn oils were "no name" brands (Purchased locally from a store, Ottawa, Canada). Waste cooking oil (WCO) containing 9.0% FFA was collected from a fast food restaurant. Sodium methoxide (25 wt% in methanol solution, Sigma Aldrich, Canada), Methanol (Assay: 99.3-99.9 %, Optima® grade, Fisher scientific, Trinidad), hydrochloric acid (36.5–38%, reagent grade, Fisher scientific, Nepean, ON, Canada) and sulphuric acid (Assay: 95-98%, reagent grade, Fisher scientific, Canada) were used. Gas chromatography standards including 1,2-4 Butanetriol (Chromatography specialties Inc., Brockville, Canada), Caperin (Sigma Aldrich, Canada) and Tricaprin (Sigma Aldrich, Canada), all in pyridine, were used for gas chromatography (GC) analysis. Phenolphthalein (0.5% w/v in iso-propanol, VWR, Canada) was used as an indicator. Filter paper (Porosity: fine, flow rate: slow, Fisher scientific, UK) was employed to filter the biodiesel in the post treatment stage of the process.

2.3 Experimental prototype set-up and biodiesel production process

In the present study, a lab scale MR apparatus was employed to investigate the use of various oil feedstocks in a continuous biodiesel production process as shown in Fig.3. Three loop volumes were utilized to maintain a constant residence time while changing the membrane permeation flux. The loop volumes used in this study were 480, 630 and 740 mL. A water bath heater was utilized to control the temperature. A platinum resistance temperature detector (RTD) was used in the membrane loop to measure the temperature of the emulsion. Three pumps were employed in the loop: two gear pumps were used to pump methanol, containing catalyst, and oil separately to the loop and a canned motor pump (Laing, Model No. SM-1212-STW-26) was used to circulate the emulsion in the loop. The cross flow velocity of the flow inside the membrane loop was estimated at 1.8 m/s.

The methanol feed pump was also used to backflush the membrane with pure methanol between two subsequent runs to ensure that no fouling or oil deposition remained on the membrane surface and inside the pores. A valve in the system was utilized to change the direction of pure methanol flow from retentate side to the permeate side in order to backflush the membrane. For safety reasons, a relief valve was used to release the pressure in the reactor should it exceed 700 kPa. A back pressure valve was also installed to adjust the differential pressure (TMP) between the pressurized reaction loop and the permeate side of the membrane. A process control software named Labview® (National Instruments) was employed to control the methanol/catalyst feed pump and record the flux stepping, temperature, operational cycle and TMPs in all runs. Balances placed under the methanol/catalyst, and oil tanks were used to control and record flow rates. The measurement of TMPs during each run was achieved by a differential pressure gauge.

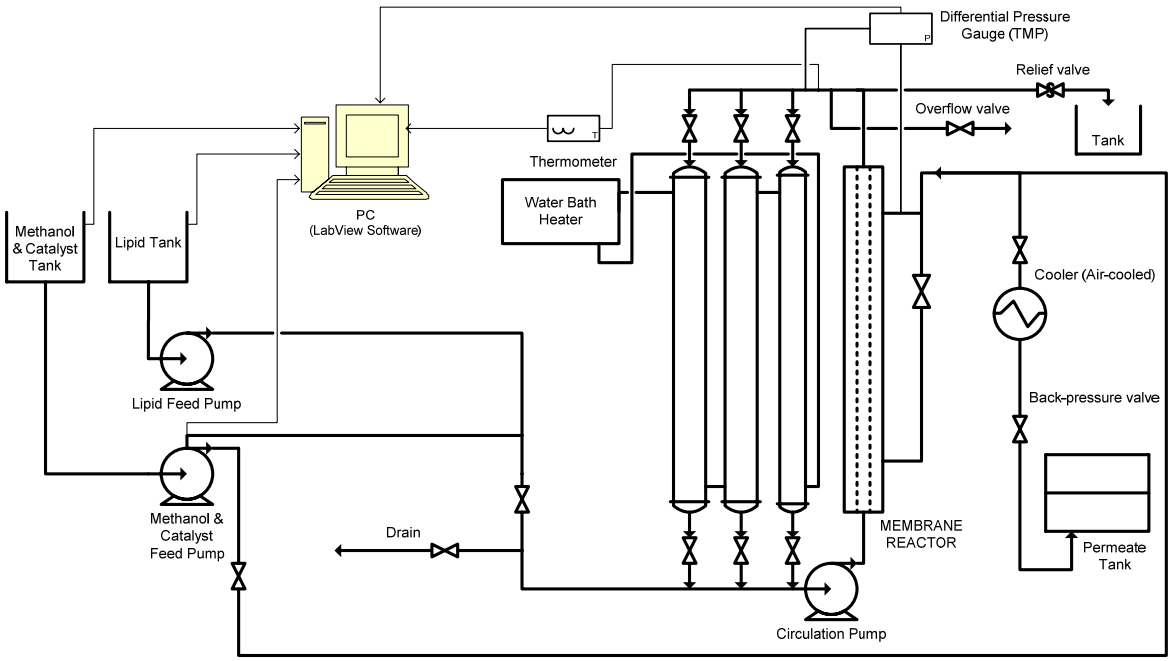

Figure 3. Schematic of the prototype biodiesel membrane reactor system.

2.4 Membrane

A tubular ceramic membrane manufactured by Inopore® having a pore size of 30 nm was employed in all experiments. The membrane characteristics are summarized in Table 1.

Table 1. Membrane characteristics.

Brand name	Ultrafiltration Inopore® Ultra
Materials	Titanium oxide
Mean Pore Size	30 nm
Open porosity	30% - 55%
Length	500 mm
Number of channels	1
External diameter	10 mm
Channel diameter	7 mm
Filtration area	0.011m^2
Inflow area per tube	39 mm^2

2.5 Experimental production procedure

All runs were performed at a reaction temperature of 65 °C. The residence time of 60 minutes was used for all oils except waste cooking oil. A residence time of 80 minutes was used for waste cooking oil.

A number of runs were performed and analyzed as shown in Table 2. The overall process consists of two steps. The first step was a batch mode in which the system was initially loaded with the oil and methanol, methanol containing sodium methoxide, at the volume ratio of 1:1. The total catalyst concentrations for all runs are shown in Table 2.

The permeate valve was closed when filling the loop with oil and methanol. The circulation pump was turned on once the loop was full. After circulating the emulsion for the desired residence time, i.e. 60 or 80 min, the permeate valve was opened and oil and methanol/catalyst were continuously pumped into the loop for the rest of the run at a volume ratio of 1:1. Continuous feeding of feedstock at a given volume ratio ensures sufficient TMP to ease the permeation of FAME/methanol/glycerine/catalyst through the membrane while retaining the oil inside the membrane reactor loop [11].

The loop was fed oil and methanol/catalyst for the duration of the run. Most runs lasted 6 hours. The permeate side of the membrane module was drained between each run. The permeate was brought to atmospheric conditions using a back-pressure valve and an air cooled shell and tube heat exchanger. This reduced volatilization of methanol on release to atmospheric conditions and accelerated phase separation. The permeate was a single phase at the reaction temperature of 65 °C, and dephased into a FAME-rich phase and a methanol/glycerine-rich phase upon cooling to room temperature.

The membrane was backflushed with pure methanol for 20 min between two subsequent runs at a pressure greater than the operating pressure of the previous run. The content of the loop was replaced before each run. The pressure across the membrane, defined as the transmembrane pressure (TMP) was recorded at 10 second intervals during the run.

Table 2. Experimental conditions used in this study.

Run ID	Lipid Type	Flux ($L/m^2/h$)	Catalyst Concentration wt.% (Based on oil mass)	Residence Time (min)
1	RBD canola oil	44	0.5	60
2	RBD canola oil	60	0.5	60
3	RBD canola oil	70	0.5	60
4	Crude soy oil	41	0.5	60
5	Crude soy oil	56	0.5	60
6	Crude soy oil	70	0.5	60
7	RBD sunflower oil	41	0.5	60
8	RBD sunflower oil	59	0.5	60
9	RBD sunflower oil	70	0.5	60
10	RBD corn oil	41	0.5	60
11	RBD corn oil	60	0.5	60
12	RBD corn oil	74	0.5	60
13	Waste cooking oil	30	1.4	80
14	Waste cooking oil	44	1.4	80
15	Waste cooking oil	56	1.4	80
16	Pre-treated corn oil	40	0.5	60
17	Pre-treated corn oil	51	0.5	68
18	Pre-treated corn oil	54	0.5	65
19	RBD canola oil	60	0.5	35
20	RBD canola oil	60	0.5	82
21	Waste cooking oil	44	1.4	55
22	Waste cooking oil	44	1.4	105
23	Waste cooking oil	30	0.5	80
24	Waste cooking oil	30	1.0	80

2.6 Biodiesel preparation

Two litres of permeate was collected for each run and settled at room temperature in a separatory funnel for 5 hours. The top and bottom layers were collected and kept in two separate 1 L bottles. Three (3) mL of each layer was added to 27 mL of pure methanol to test TG penetration through membrane qualitatively. No TG was observed in the mixture. Water washing tests were performed to verify the FAME layer. It was identified that the bottom layer was FAME since the top phase, i.e. glycerine in methanol, dissolved in water to some extent. This was expected due to the 1:1 oil to methanol volumetric feed ratio to the reactor.

The bottom layer was evaporated under vacuum (20 mbar absolute) using a rotary evaporator at a temperature of 40°C for 1.5 hours to remove the methanol. Before analysis, the resulting FAME was water washed once, to remove catalyst. This was done using 1 part pure water to 4 parts FAME on a volume basis. The pH of the FAME was tested after water washing and was always 7 indicating that the FAME did not contain residual catalyst. The FAME was then filtered twice under vacuum (200 to 400 mbar absolute) using filter paper and was ready for analysis.

2.7 Characterizations

The concentrations of glycerine, MG, DG and TG present in the biodiesel produced from various feedstocks were obtained using gas chromatography (GC) (Varian® Inc.; CP-3800 gas chromatograph, equipped with a 1079 injector, 8410 auto-sampler and FID) in accordance with ASTM D6584 method. A calibration curve was obtained from six standards: triolein (TG), diolein (DG), monoolein (MG), methyl oleate (FAME), glycerine, and methanol. The regression factors for the calibration curves exceeded the ASTM requirements. A high-temperature WCOT fused silica column having a VF-5HT stationary phase was used in the GC. Sample preparations were followed in accordance to ASTM D6584. The concentrations of MG, DG and TG were determined by comparison with monoolein, diolein, and triolein standards, respectively as defined in ASTM D6584.

3. Results and discussion

3.1 Critical Flux Determination

In the case of an oil-in-water emulsion the critical flux based on composition can be defined as a flux above which a significant amount of oil can easily pass through the membrane pores [9,12] or the flux beyond which a significant amount of oil accumulates on the membrane. The equivalent definition can be applied to an oil-in-methanol emulsion. Since the MG, DG and TG contents of final biodiesel must be in conformity with ASTM D6751/EN 14214 standards, determining this critical flux is very important for the operation of the reactor. In the present study, membrane flux was held constant for the duration of a run. Several runs were performed at various fluxes. This is similar to the flux-stepping method to determine the critical flux [13]. This method provides much better control of permeate flow and material deposition on the membrane surface throughout the run. This is due to the fact that the convective flow is constant during the run [13,14].

Since the MR is a reactive separator, a variation of this technique was used where separate runs were performed at various fluxes. Fig.4 illustrates the permeate flux versus TMP (Flux-TMP relationship) for these runs. As a general trend, there is no significant increase in TMP for the reactions involving RBD feedstocks such as; canola, sunflower, corn and soy oils operated at various operating fluxes. However there is a significant TMP rise for the reactions involving waste cooking and pre-treated corn oils. In the case of pre-treated corn oil, since waxes might still be present in the feedstock, the oil-in-methanol (O/M) emulsion in the MR was thicker than those obtained from refined oils, i.e. canola, sunflower and corn (RBD). This thick emulsion imposes a higher pressure inside the MR resulting in a TMP rise at a given flux as shown in Fig.4.

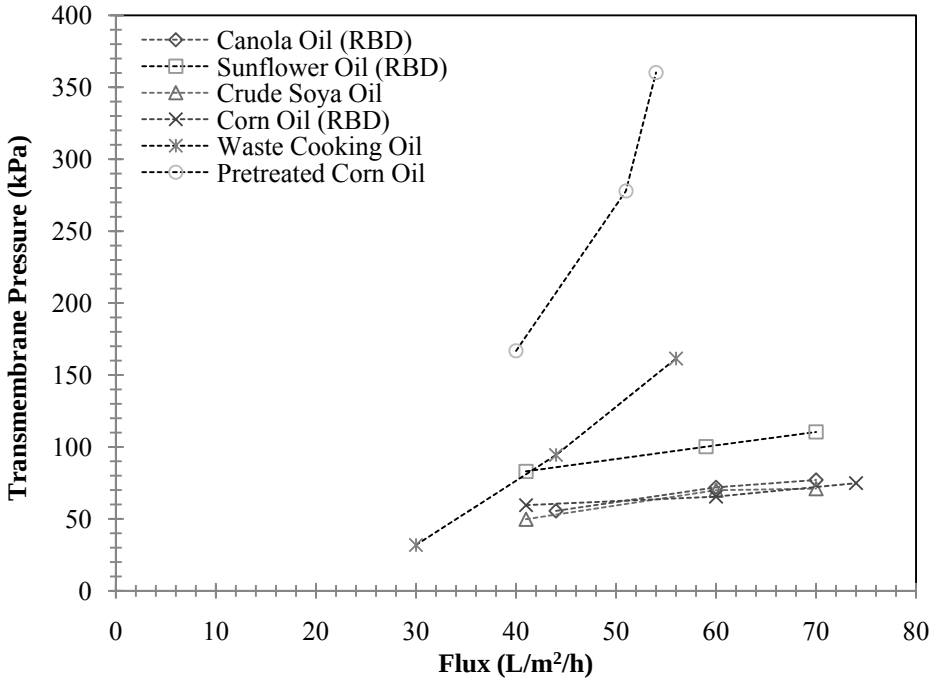

Figure 4. Flux-TMP relationships for various oil feedstocks at a residence time of 60 min for all oils except waste cooking oil (80 min residence time).

Tremblay et al. [3] have reported that 100% conversion is obtained using a membrane reactor at very low catalyst concentration at 0.05 wt% catalyst concentration and 1 hour residence time for the conversion of canola oil. The membrane itself and material on its surface imposes a resistance towards permeation of products in the MR. The TMP is a function of the concentration of unreacted oil in the emulsion within the reactor. The residence time affects the concentration of unreacted oil in the reactor. It was hypothesized that the TMP is dominated by the residence time of the reaction not the membrane resistance. Therefore when the residence time of the reaction is not sufficient, a higher amount of unreacted oil is present in the reactor during the run. In order to investigate this phenomenon, another set of runs (Run ID# 19-22 shown in Table 2) were performed. In these runs, flux through the membrane was kept constant while residence time was changed in order to study the effect of residence time on TMP. This was done by maintaining the feed flow rates to the membrane loop constant and changing the volume of the MR. Fig. 5 depicts the TMP versus residence time for canola and waste cooking oils at a flux of 60 and 44 L/m^2/h respectively.

As shown in Fig. 6, in the case of canola oil for the residence time of 35 minutes a considerable amount of unreacted oil was present in the reactor and a steady state TMP was not obtained at this residence time. A steady state TMP was obtained at the 60 and 82 min residence times. The residence times for the waste cooking oil were all sufficient to give constant TMPs at steady state. The lower residence time of 55 min caused a higher TMP across the membrane due to the thicker emulsion present in the reactor.

A residence time of 60 min for canola oil and 80 min for waste cooking oils offered easily manageable TMPs in the reactor. It is interesting to note that at these residence times, the TMPs for canola (80 kPa) and waste oil (90 kPa) were almost the same. This indicates that particulates in the waste cooking oil did not significantly increase the TMP but the amount of unreacted oil in the emulsion within the reactor affected the TMP. Thus the transmembrane pressure is strongly a function of residence time of the transesterification reaction.

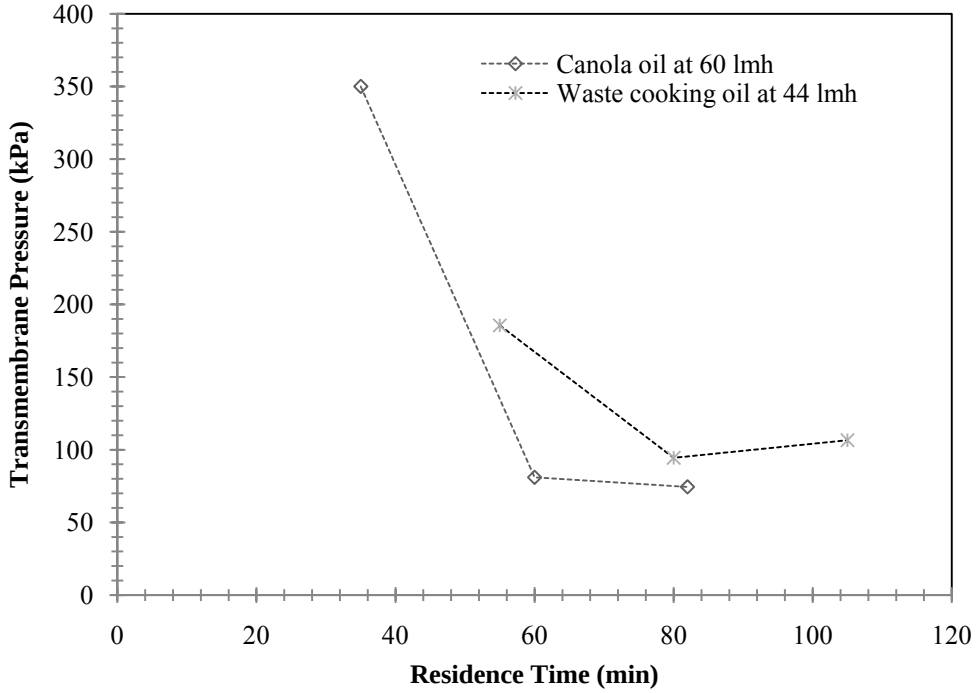

Figure 5. TMP versus different residence time for canola and waste cooking oil feedstocks.

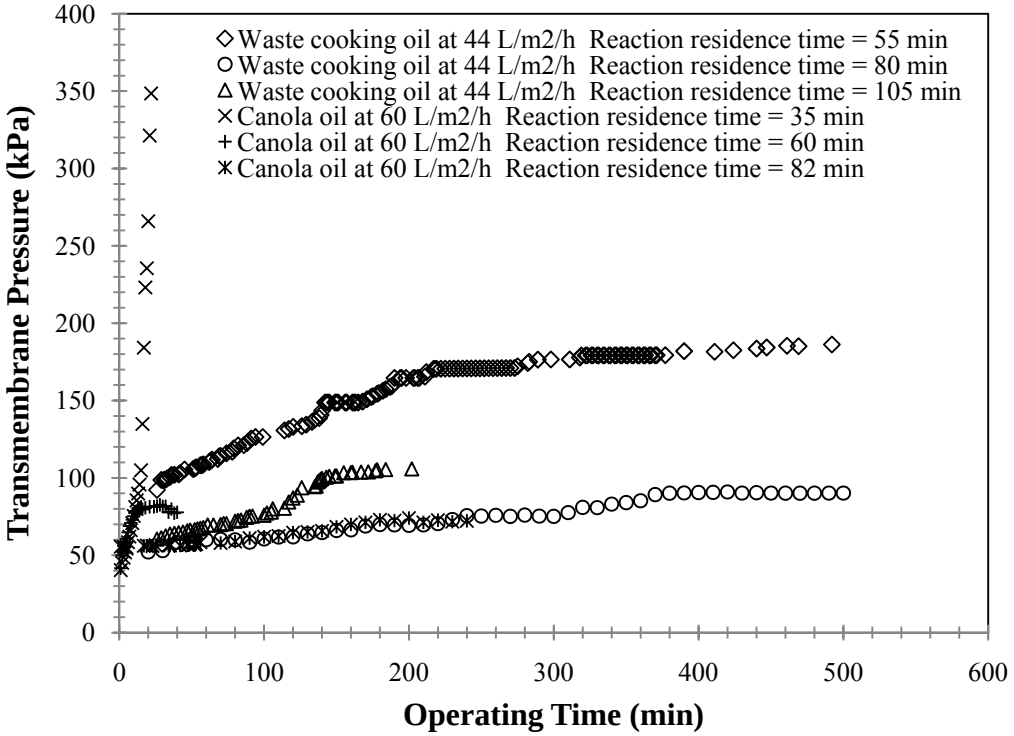

Figure 6. TMP versus operating time for canola and waste cooking oil feedstocks at various reaction residence times.

3.1.1 Particle size analysis

The oil in methanol emulsion in the reactor was characterized by dynamic light scattering (DLS). A Malvern® Zetasizer™ particle size analyzer was employed in this study. The results of this analysis shown in Fig. 7 depict that the majority of the particles have larger diameter than that of membrane pores. As a result, this pore size could be considered a good candidate to retain the oil inside the MR.

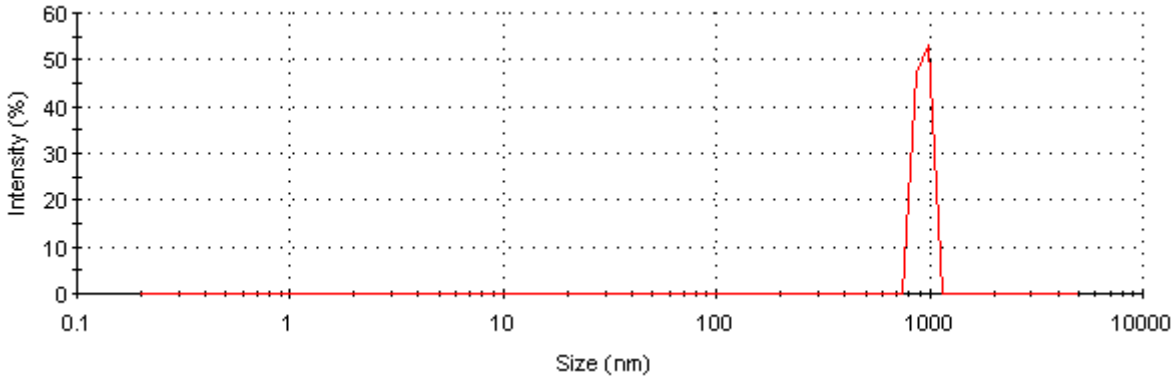

Figure 7. Canola oil droplet size distribution by intensity (Malvern® Zetasizer™ particle size analyzer).

In order to investigate the existence of a bimodal droplet size distribution, an emulsion containing 50 vol.% canola oil-in-methanol was prepared and circulated for one hour in the reactor to produce a homogenous emulsion. The MR was then emptied quickly and the emulsion allowed to dephase in a separatory funnel. Two samples containing 10 mL of the upper phase (methanol rich phase) were taken after 15 minutes of settling. Their droplet size distributions were measured using DLS. The same procedure was performed for waste cooking oil-in-methanol as well. The droplet size distributions are shown in Fig.8. It can be observed from Fig.8 that the oil has a bimodal droplet size distribution. Falahati and Tremblay [9] have recently studied the bimodal droplet size distributions of highly concentrated and unstable oil-in-water (O/W) emulsions using an ultrafiltration membrane. The O/W emulsion in their work was evaluated as a non-reactive model system to study the hydrodynamic and separation aspects of transesterification in the MR.

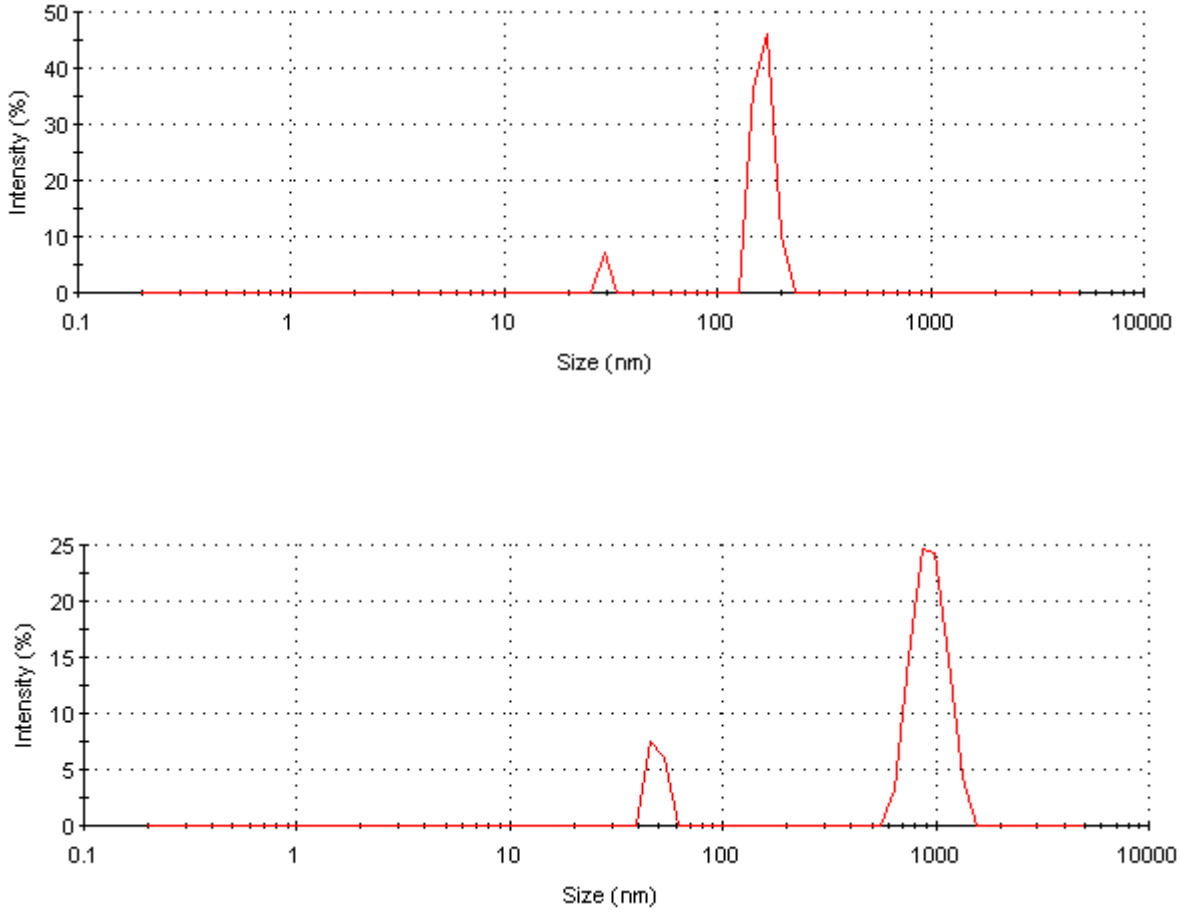

Figure 8. Canola oil droplet size distribution by intensity, the sample was taken from the methanol phase after 15 minutes of settling (Above); Waste cooking oil droplet size distribution by intensity, the sample was taken from the methanol phase after 15 minutes of settling (Below).

Dimensionless numbers can be employed to compare different model systems specifically in case of fluid flow. The Weber (We) number is a dimensionless group representing a ratio between inertial forces and the force that is due to interfacial tension [15]. The Weber number of the flow system can be calculated using Eq.1 [16].

$$We = r_p \rho v^2 / \gamma \quad (1)$$

where r_p is the radius of the particle, ρ is the density, v is the velocity and γ is the interfacial tension. Interfacial tension can be estimated by using a model proposed by Kim et al. [17] as given in Eq.2.

$$\gamma_{Oil/MeOH} = (\gamma_{MeOH} - \gamma_{Oil}) \exp(\alpha' V^{0.7}) + \gamma_{Oil} \quad (2)$$

In which γ_{MeOH} and γ_{Oil} are the interfacial tension of methanol and oil respectively, α' is an exponential coefficient and V is the volume fraction of the oil in the emulsion. The value of the Weber number for this O/M flow system is We =0.012. The Weber number is small which implies the interfacial forces are dominant. The critical value of the dimensionless Weber number in liquid/liquid systems ranges from 1 to 2. Above this range, the droplets become unstable and break up into smaller droplets [18]. Therefore in this oil/methanol system the oil droplets are stable and will not break up. This value is close to the Weber number for a similar cross flow membrane system containing oil and water studied by Falahati and Tremblay [9]. Using the data for the system in Falahati and Tremblay we obtain a value of We =0.016. Consequently, a highly concentrated and unstable O/W emulsion is a good model system to study the separation aspect of the biodiesel production through transesterification of various oils in the MR. In the O/W system described in ref. [9], both critical fluxes ranged from 30 to 40 $L/m^2/h$ for a cross flow velocity of 0.8 m/s.

3.1.2 Critical pressure for oil penetration

Critical pressure can be defined as a pressure above which a significant amount of oil can pass through the membrane pores [12]. Falahati and Tremblay [9] have recently reported that ultrafiltration is dominated by a fine particle size distribution present in the concentrated emulsion. Eq.3 [12] was used to calculate the critical pressure for the pore size of 30 nm used in this study.

$$P_{Critical}=2\gamma_{Oil/MeOH}\frac{\cos\theta}{r_{pore}}*\left[1-\left\{\frac{2+3\cos\theta-\cos^3\theta}{4\left(\frac{r_{droplet}}{r_{pore}}\right)^3\cos^3\theta-\left(2-\sin\theta+\sin^3\theta\right)}\right\}^{\frac{1}{3}}\right] \quad (3)$$

where $P_{Critical}$ is critical pressure, $\gamma_{Oil/MeOH}$ is the interfacial tension, θ is the contact angle, r_{pore} and $r_{droplet}$ is the pore and oil droplet radii respectively.

In the case of oil-in-methanol emulsions, oil and methanol are dispersed and continuous/mobile phases respectively and oil concentration should not exceed 50 vol.% [9]. For systems above this concentration, the phases revert. Critical pressures for the concentrations of 10, 20, 30, 40 and 50 vol.% were obtained for various oil droplet sizes as shown in Fig.9.

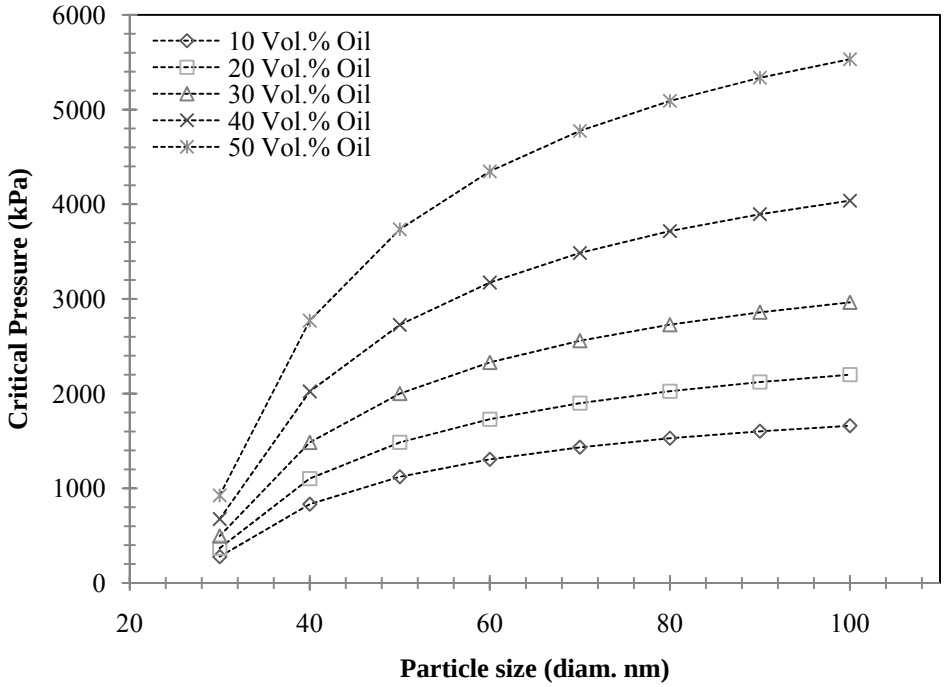

Figure 9. Critical pressure vs. oil droplet size for the pore size of 30 nm.

As a general trend, the critical pressure decreases as droplet size decreases. This is due to the fact that, larger particles require higher driving force, i.e. pressure, to overcome surface tension inside the membrane pores. All operating pressures obtained in this study are much lower than the critical pressures shown in Fig.9 except for the case of pre-treated corn at the flux of 51 $L/m^2/h$. The critical pressure associated for the smallest oil droplet size, i.e. 30 nm, calculated using Eq.3 is about 278 kPa (40 psi). In the case of pre-treated corn oil, the pressure went up to 280 kPa which is at the critical pressure. Therefore it was hypothesized that the small oil droplets might penetrate through the membrane pores and affects the quality of biodiesel produced. However for other cases there should not be a significant oil penetration through the membrane pores since the operating pressures were all lower than critical pressure. In the next section, we will investigate the GC chromatogram of the biodiesel produced to find the glycerine, MG, DG and TG contents.

3.2 MG, DG and TG concentration determination using gas chromatography

The GC analysis of MG, DG and TG contents in the biodiesel produced from various oil feedstocks at various fluxes, was performed according to method ASTM D6584. The concentrations of MG, DG and TG were calculated and summarized in Table 3.

Results showed that the concentrations of MG, DG and TG determined using ASTM D6584 are well below the acceptable range proposed by the EN 14214 standard. For all runs, at or below the critical flux, the results for DG and TG are on average half of the commercial biodiesel values.

The only results above that of the commercial biodiesel was for the case of pre-treated corn oil at the flux of 54 $L/m^2/h$, the concentration of TG is higher than that of commercial biodiesel, however it is in the acceptable EN range. This was previously discussed and is due to the fact that the TMP was high enough for small oil droplets to overcome the surface tension inside the pore and penetrate through the membrane pores. The results for MG are slightly higher than those of commercial biodiesel as the FAME used in this study was only washed once with water and not treated with adsorbents. These MG

concentrations depend on the degree of water washing or dry washing while the DG and TG removal are not affected by commercially used hydrophilic sorbents. The commercial biodiesel would need to be further reacted or distilled to reach the DG and TG levels obtained using the membrane reactor.

Commercial biodiesel was also analysed and used as a baseline for the composition of biodiesel produced in this study is shown in Table 4. The MG, DG and TG concentrations of a few biodiesel samples produced in a conventional reactor from other studies are also shown in Table 4. In most cases, these values were higher than those obtained in the present study indicating the advantages of using a membrane reactor rather than conventional reactors.

Table 3. Concentration of free glycerine, MG, DG and TG in the final biodiesel produced from different oil feedstocks using the membrane reactor.

Oil feedstock	Residence Time (min)	Flux ($L/m^2/h$)	Free glycerine (wt%)	Composition of the biodiesel MG (wt%)	DG (wt%)	TG (wt%)
EN 14214 (max)		**-**	**0.020**	**0.800**	**0.200**	**0.200**
ASTM D6751 (max)			**0.020**			
RBD canola oil (unwashed)	60	44	0.072	0.288	0.046	0.006
RBD canola oil	60	60	0.010	0.248	0.059	0.033
RBD canola oil	60	70	0.013	0.338	0.054	0.012
Crude soy oil	60	41	0.007	0.329	0.037	0.013
Crude soy oil	60	56	0.005	0.254	0.037	0.014
Crude soy oil	60	70	0.009	0.312	0.031	0.010
RBD sunflower oil	60	41	0.019	0.274	0.032	0.013
RBD sunflower oil (unwashed)	60	59	0.034	0.246	0.026	0.013
RBD sunflower oil	60	70	0.013	0.262	0.031	0.012
RBD corn oil	60	41	0.003	0.235	0.039	0.003
RBD corn oil	60	60	0.003	0.243	0.034	0.013
RBD corn oil	60	74	0.007	0.242	0.029	0.012
Waste cooking oil (unwashed)	80	30	0.022	0.263	0.048	0.012
Waste cooking oil (unwashed)	80	44	0.019	0.217	0.044	0.012
Waste cooking oil (unwashed)	80	56	0.087	0.347	0.054	0.013
Pre-treated corn oil	60	40	0.005	0.299	0.044	0.013
Pre-treated corn oil	68	51	0.002	0.271	0.045	0.135
Pre-treated corn oil*	65	54	-	-	-	-
RBD canola oil	82	60	0.003	0.288	0.038	0.013
RBD canola oil*	35	60	-	-	-	-
Waste cooking oil (unwashed)	55	44	0.030	0.252	0.038	0.013
Waste cooking oil (unwashed)	105	44	0.005	0.273	0.040	0.012

* Steady state operation was not achieved as the TMP kept on rising. No sample was collected.

Table 4. Concentration of free glycerine, MG, DG and TG in biodiesel produced from different oil feedstocks.

Oil feedstock	Residence Time (min)	Flux ($L/m^2/h$)	Free glycerine (wt%)	Composition of the biodiesel		
				MG wt%	DG wt%	TG wt%
EN 14214 (max)	**-**	**-**	**0.020**	**0.800**	**0.200**	**0.200**
ASTM D6751 (max)			**0.020**			
Commercial Biodiesel (tested in this study)	-	-	0.007	0.123	0.078	0.027
Sunflower oil† [19]	-	-	0.020	0.050	0.030	0.030
Sunflower oil‡[20]	240	-	0.004	0.285	N/A	N/A
Tallow [21]	480	-	N/A	0.100	3.500	1.500
Soy oil [21]	-	-	N/A	0.600	1.200	0.800
Waste oily pulp [22]	-	-	N/A	0.590	0.180	0.350
Waste oily pulp [22]	-	-	N/A	0.420	0.350	0.390
Canola & waste oils mixture [23]	120	-	N/A	1.100	2.500	0.300
Canola (Commercial Biodiesel) [24]	-	-	0.006	0.301	0.078	0.020
Soy (Commercial Biodiesel) [24]	-	-	0.012	0.473	0.088	0.019
Yellow grease [24]	-	-	0.012	0.300	0.130	0.019
Rapeseed oil [25]	-	-	N/A	0.500	0.100	0.100
Brassica carinata [26]	-	-	0.038	0.530	0.130	0.070
Brassica carinata [27]	-	-	0.010	N/A	N/A	N/A
Vegetable oil [28]	-	-	0.020	N/A	N/A	N/A

† This is the composition of the best sample obtained after washing twice with phosphoric acid and pure water. This biodiesel was produced in a batch stirred tank reactor using sunflower oil.
‡ This biodiesel was produced using a batch reactor at the catalyst concentration of 1 wt%.
N/A = Not available.

3.3 Free glycerine concentration determination using gas chromatography

The GC analysis of free glycerine content in the biodiesel produced from various oil feedstocks at various fluxes was performed according to method ASTM D6584. The concentrations of free glycerine were calculated and summarized in Table 3. All washed biodiesel samples were water washed only once at the volume ratio of 1:4 water to FAME and filtered; others were not washed but filtered. It was observed that free glycerine concentrations determined using ASTM D6584 in all water washed biodiesel samples were lower than the ASTM D6751 and EN 14214 levels. Biodiesel samples obtained through the transesterification of waste cooking oil were not water washed; this is the reason for the existence of higher glycerine concentration in these samples.

Unwashed biodiesel samples from RBD canola and sunflower oils were also shown in Table 3 for comparison. For the case of RBD canola oil, the free glycerine was reduced from 0.07 to 0.01 wt% by performing water washing once only. In the case of biodiesel samples obtained from sunflower oil, the free glycerine concentration was reduced from 0.034 to 0.013 wt%. The permeate from the membrane reactor has been ultrafiltered and is free of hydrophilic colloidal matter such as cell debris. Filtering the mixture readily removes glycerine bound to these suspended colloids and reduces the glycerine content of the FAME. This is not the case in conventional reactors where more washes are required to remove all finely suspended hydrophilic materials from the FAME and reduce the glycerine content to below 200 ppm as required by ASTM and EN standards.

The glycerine concentrations of biodiesel produced in other studies using conventional reactors are shown in Table 4. In most cases, these values were higher than those obtained in the present study. The biodiesel samples were water washed once only. Using less water washing stages in the process reduces the waste water production leading to a more environmentally friendly process.

Conclusions

The retention of lipids within the membrane reactor was verified for various feedstocks including low and high FFA content. The critical flux, based on pressure and composition, and residence time within a membrane reactor was determined and their influence on fuel quality when treating a variety of raw and used feedstocks was studied.

The present work verified that the critical flux, based on composition was greater than 70 $L/m^2/h$ for RBD oils and crude soy oil as the specification for both ASTM D6751 and EN 14214 standards in the biodiesel product was reached for all runs. However, a critical flux related to the operating pressure in the reactor was reached for waste cooking and pre-treated corn oils. This flux ranged from approx. 30 to 40 $L/m^2/h$. It was identified that the residence time in the reactor was a key parameter affecting the operating pressure in the reactor. Very low residence times increased the amount of unreacted oil in the reactor which caused an increase in pressure within the reactor. However, the quality of the biodiesel produced was not affected.

The residence time in the reactor was investigated for biodiesel production from canola and waste cooking oils. It was identified that the operating pressure and product purity were dominated by the residence time of the reaction not the membrane resistances towards permeation.

Particle size distributions for canola and waste cooking oils obtained using dynamic light scattering of the methanol phase after 15 minutes of settling revealed a very small particle size distribution. The results showed a bimodal droplet size distribution for the oil-in-methanol (O/M) emulsion. The Weber number value of the non-reactive model system containing oil-in-water emulsion (O/W), studied previously, was close to that of the reactive separation of O/M emulsion system used to produce biodiesel. It was also found that the interfacial forces are dominant because the value of the Weber number was small. As a result, the droplets are stable and do not break up into smaller droplets. Therefore the

non-reactive O/W system was found to be representative of the reactive O/M system in a membrane reactor to study the separation aspect of the process.

A pressure of 278 kPa (approx. 40 psi) was obtained as the lowest critical pressure for the small oil droplet size distribution using a theoretical model. In addition, free glycerine concentrations of all water washed biodiesel samples produced from various feedstocks were below the levels specified by the ASTM D6751/EN 14214. These concentrations were obtained by washing the biodiesel samples once only with water. Using less water washing stages in the process reduces the waste water production leading to a more environmentally friendly process.

Acknowledgment

The authors gratefully acknowledge the financial support from the Natural Sciences and Engineering Research Council of Canada (NSERC and BDR Technologies through the NSERC Strategic Grant program).

References

[1] Knothe G, Krahl J, Van Gerpen J. The Biodiesel Handbook. Illinois: AOCS Press; 2005.

[2] Dubé MA, Tremblay AY, Liu J. Biodiesel production using a membrane reactor. Bioresour Technol 2007;98:639-47.

[3] Tremblay AY, Cao P, Dubé MA. Biodiesel production using ultralow catalyst concentrations. Energy and Fuels 2008;22:2748-55.

[4] Dasari MA, Goff MJ, Suppes GJ. Noncatalytic alcoholysis kinetics of soybean oil. JAOCS 2003;80:189-92.

[5] Freedman B, Pryde EH, Mounts TL. Variables affecting the yields of fatty esters from transesterified vegetable oils. JAOCS 1984;61:1638-43.

[6] Nelson, RG, Hower, SA. Potential feedstock supply and costs for biodiesel production. In Bioenergy ’94, proceedings of the sixth national bioenergy conference, Reno/Sparks, NV, 1994.

[7] Tremblay AY, Dubé MA. Biodiesel production using membrane reactors, PCT Patent filed February 27, 2006. PCT/CA2006/000286.

[8] Cao P, Tremblay AY, Dubé MA, Morse K. Effect of membrane pore size on the performance of a membrane reactor for biodiesel production. Industrial and Engineering Chemistry Research 2007;46:52-8.

[9] Falahati H, Tremblay AY. The identification and effect of bimodal droplet size distributions in the ultrafiltration of highly concentrated and unstable oil-in-water emulsions. Submitted for publication 2010.

[10] Ataya F, Dubé MA, Ternan M. Single-phase and two-phase base-catalyzed transesterification of canola oil to fatty acid methyl esters at ambient conditions. Industrial and Engineering Chemistry Research 2006;45:5411-7.

[11] Cao P, Dubé MA, Tremblay AY. High-purity fatty acid methyl ester production from canola, soybean, palm, and yellow grease lipids by means of a membrane reactor. Biomass Bioenergy 2008;32:1028-36.

[12] Nazzal FF, Wiesner MR. Microfiltration of oil-in-water emulsions. Water Environ Res 1996;68:1187-91.

[13] Lee S, Aurelle Y, Roques H. Concentration polarization, membrane fouling and cleaning in ultrafiltration of soluble oil. J Membr Sci 1984;19:23-38.

[14] Sethi S, Wiesner MR. Performance and cost modeling of ultrafiltration. J Environ Eng 1995;121:874-83.

[15] Russell TWF, Robinson AS, Wagner NJ. Mass and heat transfer: analysis of mass contactors and heat exchangers, Vol. 10. 1st ed. New York: Cambridge university press; 2008.

[16] Kosvintsev SR, Gasparini G, Holdich RG. Membrane emulsification: Droplet size and uniformity in the absence of surface shear. J Membr Sci 2008;313:182-9.

[17] Kim H, Burgess DJ. Prediction of interfacial tension between oil mixtures and water. J Colloid Interface Sci 2001;241:509-13.

[18] Wallis GB. One-Dimensional Two-Phase Flow. New York: McGraw-Hill; 1969.

[19] Antolín G, Tinaut FV, Briceo Y, Castao V, Pérez C, Ramírez AI Optimisation of biodiesel production by sunflower oil transesterification. Bioresour Technol 2002;83:111-4.

[20] Vicente G, Martínez M, Aracil J Integrated biodiesel production: A comparison of different homogeneous catalysts systems. Bioresour Technol 2004;92:297-305.

[21] Nelson LA, Foglia TA, Marmer WN. Lipase-Catalyzed Production of Biodiesel. JAOCS 1996;73-8:1191.

[22] Obibuzor JU, Abigor RD, Okiy DA. Recovery of Oil via Acid-Catalyzed Transesterification. JAOCS 2003;80-1:77.

[23] Issariyakul T, Kulkarni MG, Meher LC, Dalai AK, Bakhshi NN Biodiesel production from mixtures of canola oil and used cooking oil. Chem Eng J 2008;140:77-85.

[24] Sanford SD, White JM, Shah PS, Wee C, Valverde MA, Meier GR. Feedstock and biodiesel characteristics report. 2009.

[25] Bournay L, Casanave D, Delfort B, Hillion G, Chodorge JA. New heterogeneous process for biodiesel production: A way to improve the quality and the value of the crude glycerin produced by biodiesel plants. Catalysis Today 2005;106:190-2.

[26] Cardone M, Mazzoncini M, Menini S, Rocco V, Senatore A, Seggiani M, Vitolo S. Brassica carinata as an alternative oil crop for the production of biodiesel in Italy: agronomic evaluation, fuel production by transesterification and characterization. Biomass Bioenergy 2003;25:623-36.

[27] Bouaid A, Diaz Y, Martinez M, Aracil J. Pilot plant studies of biodiesel production using Brassica carinata as raw material. Catalysis Today 2005;106:193-6.

[28] Ahn E, Koncar M, Mittelbach M, Marr R. A Low-Waste Process for the Production of Biodiesel. Separ Sci Technol 1995; 30(7-9):2021-33.

CHAPTER IV

Discussions

The objective in the determination of critical flux is to obtain descent operating fluxes and pressures in the operation of a membrane system. Operating at fluxes above the critical flux reduces the separation efficiency of the membrane and increases transmembrane pressures. In the membrane industry, operating at the highest feasible flux is desirable in order to reduce the surface area of the membrane required for filtration leading to a lower capital investment. Operating at an excessive pressure increases the chance of breaking the seals of a ceramic membrane module. Working at very high fluxes increases the frequency of membrane cleaning cycles, increases irreversible membrane fouling and reduces membrane life.

Studies to date have been focused on the concept of critical flux in non-reactive membrane separation systems. To date no work has been reported on using this concept in a reactive system. In the present study both the residence time of the reaction and separation phenomena were studied together. The present work is centered on the investigation of critical flux based on the pressure and composition of the permeate in the reactive separation of biodiesel from various feedstocks using a membrane reactor.

A model system containing a highly concentrated and unstable oil-in-water (O/W) emulsion was investigated prior to studying the reactive separation of an alkali-catalyzed transesterification reaction. The primary reason for using this model system was to facilitate data interpretation, to observe the nature of the emulsion, and the separation behaviour for a concentrated emulsion using a non toxic system. Methanol is highly toxic and is difficult to manipulate in large quantities in a laboratory setting. The model system gave us an understanding of the convective flow on the surface of the membrane and the associated separation phenomena. The critical flux based on composition and pressure could be easily investigated using this model system since the separation was dominated

by the particle size distribution present in the dispersed phase. Water was the continuous/ mobile phase that could easily pass through the membrane pores. The investigation of this model system resulted in demonstrating that good separation efficiencies of 99.5% and higher up to the critical flux could be obtained. The critical flux of this model system based on composition and pressure ranged between 30 and 40 $L/m^2/h$ for a cross flow velocity of 0.8 m/s.

Cross flow velocity is the velocity of the fluid flowing across the surface of the membrane. At this stage, the hypothesis was that the cross flow velocity may affect the separation of the emulsion in the membrane reactor. In other words, higher cross flow velocities improve separation. This was proven by our latter study on the reactive separation of biodiesel in another membrane reactor system in which a higher cross flow velocity of 1.8 m/s was reached. It was identified that the cross flow velocity does have an effect on the separation of the materials from the products of the reaction. A very high flux of 70 $L/m^2/h$ was obtained in this system for the case of biodiesel production from refined, bleached and degummed canola oil. Therefore it can be concluded that higher cross flow velocities provide more efficient convective flow and reduce the amount of material deposited on the surface of the membrane offering higher operating fluxes leading to higher separation efficiency.

It was found that the total resistance towards permeation increased as flux increased in the non-reactive model system. The cake layer thickness increased as flux increased. Therefore the resistance is linked to the cake layer thickness, in other words higher cake layer thickness imposed higher resistance towards permeation causing higher transmembrane pressure. However resistance towards permeation was less pronounced for the second system (reactive system) due to the existence of higher cross flow velocity, and the reaction of the oil droplets reacted on the surface of the membrane as well.

To study the separation of the reactive system in terms of separation and compare it to the non-reactive model system, all biodiesel samples were analysed using gas chromatography technique according to ASTM D6584 method. According to ASTM D6751 and EN 14214 standards, the concentrations of mono-glyceride (MG), di-glyceride (DG) and tri-glyceride (TG) should not exceed 0.8 wt%, 0.2 wt% and 0.2 wt% respectively. It was found that the

composition of all biodiesel samples were below the limits required by ASTM D6751 and EN 14214 standards. A commercial biodiesel sample was analyzed as a baseline to compare with the results of this work. It was observed that, at or below the critical flux, the results for DG and TG content were on average half of the commercial biodiesel values. The only results above that of the commercial biodiesel were for the case of pre-treated corn oil at the flux of 54 $L/m^2/h$, the concentration of TG is higher than that of commercial biodiesel, however it is in the acceptable ASTM range. This is due to the fact that the transmembrane pressure was high enough for small oil droplets to overcome the surface tension inside the pore and penetrate through the pores. The results for MG are slightly higher than those of commercial biodiesel as the FAME used in this study was only washed once with water and not treated with adsorbents. These MG concentrations depend on the degree of water/acid washing or dry washing while the DG and TG removal are not affected by commercially used hydrophilic sorbents. The commercial biodiesel would need to be further reacted or distilled to reach the DG and TG levels obtained using the membrane reactor.

In the non-reactive model system, above 30 to 40 $L/m^2/h$, a significant amount of oil penetrated through the membrane pores resulting in higher oil concentration i.e. >0.2 wt% in the collected permeate. This was due to the low cross flow velocity of the system leading to the deposition of materials on the surface of the membrane. This represents more oil penetration through the membrane pores.

In addition, the free glycerine content of all biodiesel samples was analysed after a single water wash. For the case of canola oil, the free glycerine was reduced from 0.07 to 0.010 wt% by performing water washing once only. In the case of biodiesel samples obtained from sunflower oil, the free glycerine concentration was reduced from 0.034 to 0.013 wt% with one water wash. These concentrations were well below the maximum glycerine content proposed by ASTM and EN standards, i.e. 0.02 wt%. This was due to the use of a membrane reactor rather than conventional reactors to produce biodiesel since the product was being ultrafiltered during its production. As shown in Table 7 of chapter IV (Paper 2), the glycerine concentration of some biodiesel samples produced in a conventional reactor from other studies indicated higher values than those obtained in the present work.

Therefore, it can be conclude that the critical flux based on composition was not reached in the reacting membrane system used in this study due to the high cross flow velocity of the emulsion on the boundary layer of the membrane. Even though, for the case of pre-treated corn and waste cooking oils, the critical flux, based on pressure, ranged between 30 to 40 $L/m^2/h$, the composition of the biodiesel was in accordance with the standard. This was in good agreement with the critical flux obtained in the non-reactive model system. In the case of pre-treated corn oil, the presence of waxes does not allow higher fluxes to be reached.

Due to the existence of free fatty acid in the waste cooking oil, soap (sodium oleate) was formed during the neutralization of the waste cooking oil. Soap could change the nature of the emulsion and it can also cause fouling on the surface of the membrane imposing a mass transfer resistance towards permeation of the products. Therefore, high operating fluxes were not achieved for waste cooking oil.

The residence times of 60 min and 80 min for canola and waste cooking oils respectively offered easily manageable transmembrane pressures (TMP) in the reactor. It is interesting to note that at these residence times, the TMP for canola (80 kPa) and waste cooking oil (90 kPa) were almost the same. This indicates that particulates in the waste cooking oil did not tremendously increase the TMP however the amount of unreacted oil in the emulsion within the reactor affected the TMP.

In the reactive system, the effect of residence time within the reactor loop was studied for the production of biodiesel from canola and waste cooking oils at constant flux. The residence times and fluxes were; in the case of canola oil, 35, 60 and 82 min at 60 $L/m^2/h$; and for waste cooking oil 55, 80 and 105 min at 44 $L/m^2/h$. For canola oil, it was found that operating at a residence time of 35 min was not possible at a flux of 60 $L/m^2/h$ since the pressure kept rising due to the accumulation of unreacted oil inside the reactor. The steady state pressure was not reached at this condition. However, operating at higher residence times, i.e. 60 and 82 min, was successful for canola oil and a steady state pressure was reached at a flux of 60 $L/m^2/h$. For waste cooking oil, all residence times allowed the steady state operation of the reactor at a flux of 44 $L/m^2/h$. Therefore the

process is dominated by the residence time in the reactor loop not the resistance towards permeation provided the cross flow velocity is high enough.

The investigation on the nature of the emulsion in terms of particle size in both oil-in-water and oil-in-methanol emulsions resulted in an unexpected bimodal droplet size distribution for both systems. Small and large particle size distributions ranged from 30 to 100 nm and 1200 to 3200 nm respectively. Since both emulsions are highly concentrated and unstable due to immiscibility of oil, in water and methanol, a settling technique was coupled with a dynamic light scattering (DLS) method to find the bimodal droplet size distributions. Aside from the objective of the research thesis, it was observed that due to high concentration of the emulsion, the DLS method by itself was not sufficient to measure the particle sizes.

In addition, the particle Weber number, i.e. dimensionless group, was calculated for both systems. The Weber numbers for the oil-in-water and oil-in-methanol emulsion systems were 0.016 and 0.012 respectively. Weber numbers smaller than a value ranging from 1 to 2 implies that the interfacial forces are dominant in the droplet system, thus the oil droplets are stable and do not break up easily. Therefore these emulsions contain spherical oil droplets dispersed in the mobile phase i.e. water or methanol.

One of the very important design factors in membrane systems is to minimize the surface area of the membrane by increasing the flux. Ceramic membranes are well-known for their stability at a very high pressure (90 bars) and temperature (150°C). They are not sensitive to pH changes and can be easily backwashed at a very high pressure and autoclaved. Therefore using a ceramic membrane rather than organic membranes is of great interest specifically in the presence of a reaction. However the capital cost of the ceramic membrane is much higher than other type of membranes used in separation industry. Therefore minimizing the surface area of the membrane by operating at the maximum flux can significantly reduce the capital investment. Operating at the flux range of 30 to 40 $L/m^2/h$ with a cross flow velocity of 0.8 m/s can double the capital investment of the membrane compared to operating at a flux of 70 $L/m^2/h$ with a cross flow velocity of 1.8 m/s for a given production capacity.

Both the cross flow velocity on the surface of the membrane and the reaction residence time are linked in the design of a membrane reactor to transesterify lipids. The process is dominated by the reaction residence time and not the total membrane resistances towards permeation providing that the cross flow velocity of the flow on the surface of the membrane is high enough.

CHAPTER V

Conclusions

In a non-reactive model system containing highly concentrated and unstable oil-in-water emulsions, cake layer thickness based on dynamic light scattering (DLS) measurements resulted in unreasonably thick cake layers. Settling of the concentrated emulsion permitted the detection of a smaller particle size distribution ranged between 30 and 100 nm hidden by the larger particles ranging from 1200 to 3200 nm. It was found that at higher temperature the concentration of small oil droplets is significantly higher than that of lower temperature. The content of the smaller particles represented 1% of the total weight of oil at 30°C and 5% at 70°C. This was too low to be detected using DLS measurements but was sufficient to affect ultrafiltration.

Cake layer thickness increases as flux increases. Small particles can easily coalesce into the cake sub-layer resulting in oil penetration. It was also identified that the cake layer is compressible.

The critical flux based on pressure and separation/composition for the model system ranged between 30 and 40 $L/m^2/h$. The results indicate that ultrafiltration was dominated by fine particle size distribution present in the concentrated emulsion and DLS method was not sufficient to predict the particle size distribution. Therefore, membrane filtration is a useful tool to determine the presence of small oil droplet distributions in concentrated and unstable emulsions as flow through the membrane is highly affected by sub-micron sized particles present in water.

Particle size distributions of canola and waste oils were obtained using dynamic light scattering of the methanol phase after 15 minutes of settling revealed a very small particle size distribution. The results showed a bimodal droplet size distribution for oil in methanol emulsion which is in pretty good agreement with the model system studied beforehand.

Therefore a non-reactive oil-in-water system could be sufficient to study the separation aspect of the reactive oil in methanol system in a membrane reactor since the separation is linked to the oil droplet sizes.

The retention of the oil within the membrane reactor was verified for various feedstocks including low and high FFA content. The critical flux, based on pressure and composition, and residence time within a membrane reactor was determined and their influence on fuel quality when treating a variety of raw and used feedstocks was studied.

The present study verified that the critical flux, based on composition was greater than 70 $L/m^2/h$ for all feedstocks as the specification for both ASTM D6751 and EN 14214 standards in the biodiesel product was reached for all runs. However, a critical flux related to the operating pressure in the reactor was reached for waste cooking and pre-treated corn oils. This flux ranged from approx. 30 to 40 $L/m^2/h$. This is in agreement with the model system. It was identified that the residence time in the reactor was a very important parameter affecting the operating pressure in the reactor. Lower residence times increased the amount of unreacted oil in the reactor which caused an increase in pressure within the reactor. However, the quality of the biodiesel produced was not affected.

The residence time in the reactor was investigated for biodiesel production from canola and waste oils. It was identified that the operating pressure and product purity were dominated by the residence time of the reaction not the membrane resistances towards permeation.

The particle Weber number value of the non-reactive model system containing oil-in-water emulsion, was close to that of the reactive separation of oil in methanol emulsion system. It was also found that the interfacial forces are dominant because the value of particle Weber number is small. As a result, the droplets are stable and do not break up into smaller droplets.

A pressure of 278 kPa (approx. 40 psi) was obtained as the lowest critical pressure for the small oil droplet size distribution using a theoretical model. In addition, free glycerine concentrations of all water washed biodiesel samples produced from various feedstocks were in the range required by ASTM D6751 and EN 14214 specifications. These

concentrations were obtained by water washing the biodiesel samples once only. Using less water washing stages in the process reduces the waste water production leading to a more environmentally friendly process.

CHAPTER VI

Further works

According to the results of this research thesis, the following recommendations could be provided for future research.

1. The critical flux based on composition was not reached for a cross flow velocity of 1.8 m/s. Increasing the flux implies an increase in the feed rate to the membrane loop. A proportional decrease in the residence time follows. The loop volume of the membrane reactor should be increased to examine higher fluxes for RBD feedstocks. Another experiment should be conducted to investigate higher fluxes than 70 $L/m^2/h$ in order to find the critical flux based on pressure and composition.
2. The influence of water present in the waste cooking oil on catalytic activity of sodium methoxide and soap formation, and their effects on separation in the membrane reactor should be investigated.
3. The possibility of recycling the glycerine phase after soap removal should be studied. This will help the economics of the biodiesel production from waste cooking oil by reducing the pure methanol consumption in the membrane reactor.

APPENDIX A

Lab scale membrane reactor system operational guide

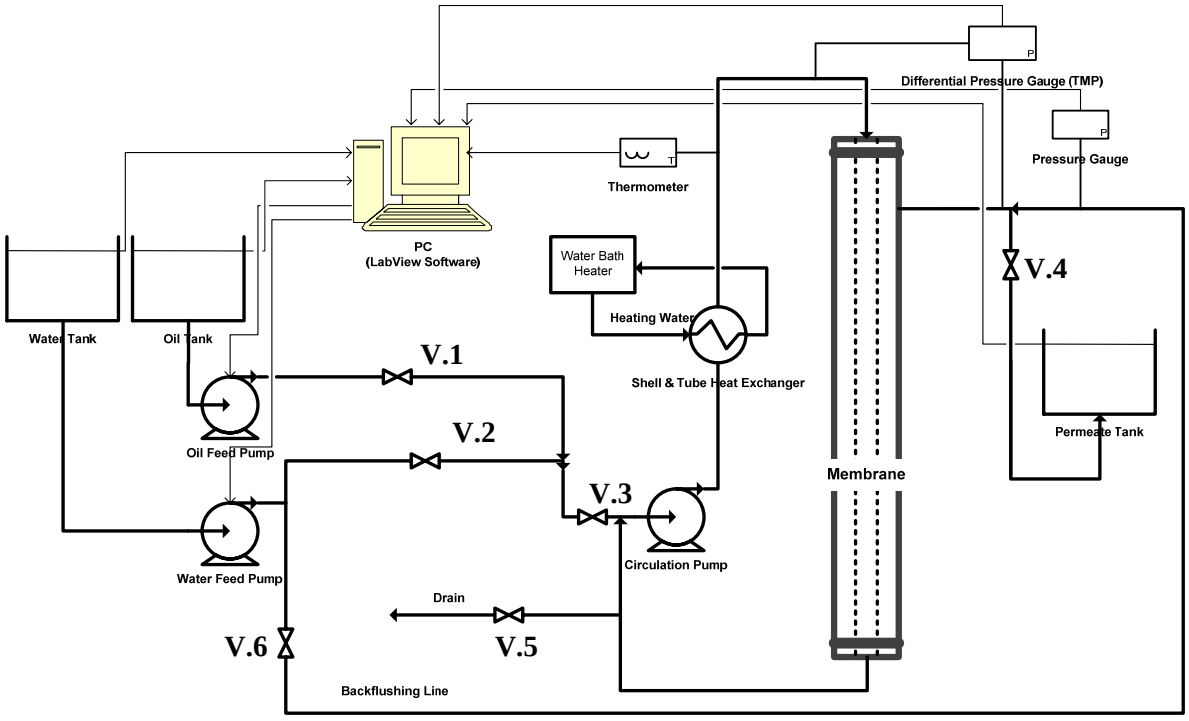

Figure A-1. Schematic diagram of the lab scale apparatus.

In the first study, a non-reactive model system was used to investigate the separation aspect of the biodiesel production. The lab scale apparatus employed in this study is shown in Fig.A-1.

1. Components of the membrane loop/reactor system.

- An oil feed pump was used to pump oil from the oil tank into the membrane loop.
- A water feed pump was used to pump water from water tank into the membrane loop. This pump was also employed to backflush the membrane.
- A drain line was used to drain the content of the loop after each run. The content of the loop should be replaced with fresh materials for each run.
- A backflushing line was utilized to backflush the membrane with pure water at a high pressure between two subsequent runs to remove fouling. In order to backflush the membrane after a run, valve#6 should be opened to change the

direction of the water flow from the retentate side to the permeate side of the membrane. Valve#2 & 4 should be closed during backflushing operation.

- A circulation pump was employed to circulate the emulsion in the loop to make a homogenous emulsion and maintain the cross flow velocity on the surface of the membrane.
- A water bath heater was employed to maintain a given temperature of the emulsion in the loop.
- A platinum resistance temperature detector (RTD) was used to measure and record the temperature of an emulsion in the membrane loop.
- A differential pressure gauge was employed to record the transmembrane pressure (TMP).
- The process control software named Labview® (National Instruments), was employed to control the water feed pump and record the flux stepping, temperature, operational cycle and TMPs in all runs. Balances placed under the water, oil and permeate tanks were used to control and record flow rates. Recording TMPs during each run was achieved by a differential pressure gauge.
- A permeate tank was used to collect all permeate samples.

2. Start up procedure

- Valve# 1, 2 & 3 should be opened to fill the membrane loop/reactor at a given oil concentration, other valves should be closed.
- Turn on the water bath heather. Check the water level in the water bath. There should be enough water in the bath to maintain the temperature inside the membrane loop. Since there is a significant heat dissipation in the system, the temperature of the bath should be always 2 to 3 degrees above the desired temperature. The emulsion temperature is recorded and monitored by the RTD.
- Since the flows are controlled by balances, all balances should be tared beforehand.
- Turn on the water and oil pumps.
- Inject a given amount of oil into the membrane loop.
- Inject a given amount of water into the membrane loop.

- Close all valves.
- Turn on the circulation pump.
- Let the emulsion circulated for a given holding/residence time.
- Open all valves except valve#1, 5 & 6.
- Start feeding the membrane loop with pure water only. This technique ensures that the concentration of the oil in the membrane loop remains the same for the rest of the run (Continuous part).
- Temperature and transmembrane pressures are recorded in a comma separated value (.csv) file on the personal computer (PC).

3. Shut down procedure

- Turn off all pumps and water bath heather.
- Turn off the circulation pump immediately to avoid cavitations.
- Open valve#5 to drain the membrane loop content.
- Back up the data file and turn off the PC and balances.

4. Backflushing procedure

- Close all valves except valve# 5 & 6.
- Turn on the water feed pump.
- Backflush the membrane for 20 min at 40 psi.

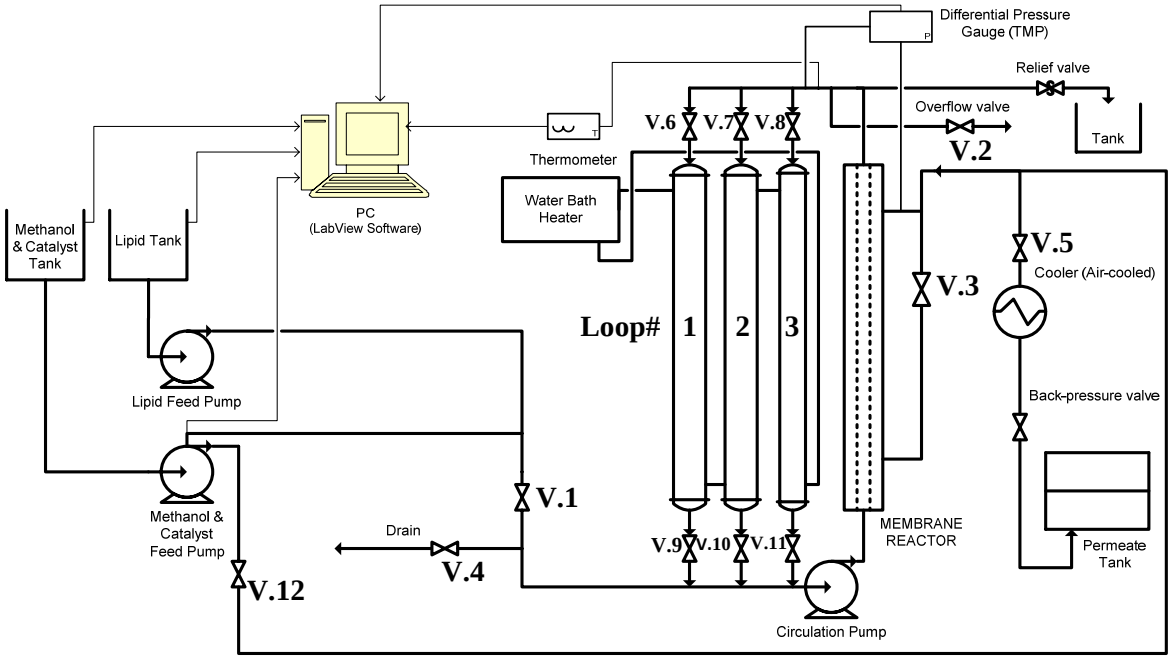

Figure A-2. Schematic of the prototype biodiesel membrane reactor system.

A membrane reactor system consisting of three reactor loops was employed to investigate the critical flux based on pressure and composition for the biodiesel production through alkali-transesterification of various lipids as shown in Fig.A-2.

1. Components of the membrane reactor system.

- Three membrane reactor loops were utilized to change the reactor volume in order to study the effect of reaction residence time at a constant flux.
- For safety reason, a relief valve was utilized. This valve releases the pressure when a pressure of 100 psi reached.
- An oil feed pump was used to pump oil from the oil tank into the membrane loop.
- A methanol/catalyst feed pump was employed to pump methanol/catalyst from the methanol/catalyst tank into the membrane loop. This pump was also used to backflush the membrane with pure methanol.
- A drain line was used to drain the loop content between runs. The content of the loop was replaced with fresh materials for each run.

- A backflushing line was utilized to backflush the membrane with pure methanol at a high pressure between two subsequent runs to remove fouling.
- A circulation pump was employed to circulate the emulsion (oil in methanol emulsion) in the loop to make a homogenous emulsion and maintain the cross flow velocity on the boundary layer of the membrane.
- A water bath heater was employed to maintain the temperature of the emulsion in the membrane reactor.
- A platinum resistance temperature detector (RTD) was used to monitor and record the temperature of the emulsion inside the reactor.
- A differential pressure gauge was employed to monitor and record the transmembrane pressure (TMP).
- The process control software named Labview® (National Instruments) was employed to control the methanol/catalyst feed pump and record the flux stepping, temperature, operational cycle and TMPs in all runs. Balances placed under the methanol/catalyst and oil tanks were used to control and record flow rates.
- A permeate tank was used to collect all reaction products.

2. Start up procedure

- All valves should be closed at the beginning of the operation.
- Turn on the water bath heater and check the water content of the bath. Tare the balances.
- Open valves#1 & 2 and adjust the volume of the reactor by opening the related valves. For instance to use loop# 1, valve# 6 and 9 should be opened. Valves# 7,8,10 and 11 should be remained closed.
- Turn on oil and methanol/catalyst pumps. Oil pump is controlled manually (set on INT) and methanol/catalyst pump is controlled automatically by the software (set on voltage).
- Inject a given amount of oil and methanol to the membrane loop. For instance in this study, oil to methanol 1:1 volume ratio was selected. Therefore half of the

reactor volume should be filled with methanol/catalyst and the other half should be filled with oil. This is a batch part of the process.

- Once the reactor gets full, close valve# 1 & 2. Turn on the circulation pump and let the emulsion circulated for a given reaction residence time at the temperature of 65°C.
- Open valve#1, 3 & 5. The backpressure valve should be adjusted to increase pressure on the permeate side. It is best to leave it fully open for this study.
- Turn on oil and methanol/catalyst pumps. Set a voltage on the oil pump for a given flow rate. Just adjust the oil flow rate and let the Labview® software on the PC set the methanol/catalyst flow rate.
- The products are collected in the permeate tank

3. Shut down procedure

- Turn off all pumps and water bath heater.
- Cool down the reactor to avoid polymerization on the surface of the membrane. You can replace the water in the water bath with cold water to cool the reactor faster.
- Once the reactor gets cooled, close valve#1 and open valve#4. Collect the retentate from the drain line. Do not collect the retentate when the reactor is not cold enough. This causes methanol vaporization.

3.1 Backflushing the membrane

- All valves should be closed except valve#2, 4 & 12.
- The membrane should be backflushed after each run to make sure that the hydraulic resistance of the membrane is the only resistance towards permeation. The backflushing should be maintained for 20 min. Backflushing the membrane can also reduce the cake layer formation on the surface of the membrane during the operation. Backflushing should be performed at a pressure higher than the operating pressure of the system to remove fouling.

- Do not flush the reactor with compressed air. This can dry the surface of the membrane and accelerate polymerization.
- Close all the valves.
- Take all samples including permeate and retentate for analysis. All samples should be neutralized with a strong acid (e.g. Hydrochloric acid) prior to analysis.

Safety guidelines

- All Lab workers should take the WHMIS exam and Lab training prior to working in the Lab.
- All safety equipment i.e. lab coat, safety goggle and gloves should be used during these experiments.
- Both methanol and sodium methoixde (The homogenous catalyst) are extremely toxic. The MSDS of methanol and sodium methoxide should be carefully read beforehand.
- The reactor temperature should not exceed 67°C to avoid the methanol evaporation.
- Always lower the fume hood sash when working with methanol and sodium methoxide.
- Locate spill kit and pads.
- Reactor pressure should not exceed 50 psi. If it reaches this pressure, turn off all pumps and consult your supervisor.

APPENDIX B

Sample calculations

Sample calculations for separation factor

$$\text{Separation factor} = 1 - \frac{\text{oil concentration in permeate}}{\text{oil concentration in feed}} \quad (1)$$

For the case of 10 vol.% oil at a flux of 10 L/m^2/h at the temperature of 30 °C:

Oil concentration in the permeate : 0.0052 vol.%

Oil concentration in the feed : 10 vol.%

Separation factor: 1 - (0.0052 vol.%/ 10 vol.%) = 0.99948

The rest of the separation factors are summarized in Table B-1.

Table B-1. Separation factors.

Oil content	**10%**	**20%**	**30%**	**40%**	
Flux					
10	0.999481	0.999719	0.999908	0.99715	
20	0.999373	0.997191	0.999625	0.988166	
30	0.99588	0.988754	0.997637	0.971095	T = 30 °C
40	0.989188	0.984736	0.980468		
50	0.987142	0.975214			
60	0.973874				
10	0.999438	0.99971	0.998544		
20	0.999438	0.999698	0.997687		
30	0.996957	0.997731	0.990189		T = 70 °C
40	0.983106	0.99446	0.969204		
50	0.959899	0.960106			
60	0.992123	0.947237			

Sample calculations for cake layer resistance

$$J = \frac{\Delta P_L}{\mu \, . R_{Total}} \quad (2)$$

where: $R_{Total} = R_m + R_{f\,(reversible)} + R_{f\,(irreversible)} + R_c$ (2.a)

where J is the flux (which is held constant during a run), ΔP_L is the transmembrane pressure (TMP), μ is the viscosity of the mobile phase (distilled water in this study), R_m is the membrane hydraulic resistance, $R_{f\,(reversible)}$ is the resistance due to reversible fouling, $R_{f\,(irreversible)}$ is the resistance due to irreversible fouling and R_c is the cake layer resistance.

$R_{f\,(reversible)} = 0$

$R_{f\,(irreversible)} = 0$

$$J = \frac{\Delta P_L}{\mu \, . \, (R_m + R_c)}$$

Rearranging the above equation:

$$R_c = \frac{\Delta P_L}{\mu \, . \, J} - R_m$$

For the case of 30 vol.% oil at 40 L/m^2/h (Actual flux = 38.79 L/m^2/h) at the temperature of 30°C:

$R_m = 1.02099 * 10^{13}$ m^{-1}

$\Delta P_L = 276479.75570$ Pa

$\mu = 0.000798$ (Pa.s) at 30°C

$J = 1.07770 * 10^{-5}$ m^3/m^2.s (m/s)

$$R_c = \frac{276479.75570}{0.000798 * 1.07770 * 10^{-5}} - 1.02099 * 10^{13} = 2.19387 * 10^{13} \text{ m}^{-1}$$

Sample calculations for cake layer thickness

$$\delta_{ss}=\frac{\sqrt{\left(R_m^2+2C\alpha t_{ss}\right)}-R_m}{\alpha} \quad (3)$$

where:

$$C=\frac{\Delta P_L\ \phi_b}{\mu(\phi_{max}-\phi_b)} \quad (3.a)$$

$$\alpha=\frac{37.5\ \phi_{max}^2}{a_p^2\ (1-\phi_{max})^3} \quad (3.b)$$

where ΔP_L is the transmembrane pressure (TMP), ϕ_b is the solute volume fraction in the emulsion, ϕ_{max} is the maximum solute volume fraction in the cake layer, μ is the viscosity, α is the specific cake layer resistance, R_m is membrane hydraulic resistance, a_p is particle size and t_{ss} is the time required to reach steady state transmembrane pressure.

For the case of 10 vo.% oil at 10 L/m^2/h at the temperature of 30 °C:

$$C=\frac{137859.2549*0.0028}{0.000798\ (0.58-0.0028)}=838038.4433$$

$$\alpha=\frac{37.5*(0.58)^2}{(75*10^{-9})^2\ (1-0.58)^3}=3.02703*10^{16}\ m^{-2}$$

$$\delta_{ss}=\frac{\sqrt{\left(\left(1.05754*10^{13}\right)^2+2*838038.4433*3.02703*10^{16}*7080\right)}-1.05754*10^{13}}{3.02703*10^{16}}=367\ \text{microns}$$

Sample calculations for Weber number

The Weber number of the flow system can be calculated using Eq.1 [16].

$$We = r_p \rho v^2 / \gamma \quad (4)$$

where r_p is the radius of the particle, ρ is the density, v is the velocity and γ is the interfacial tension.

For the case of oil-in-water emulsion in the first study, the Weber number can be estimated as below.

v =	0.8	m/s	
ρ =	1000	kg/m^3	
r_p =	0.000001	m	We = 0.012308
γ =	0.052	N/m	

Sample calculations for critical pressure

The critical pressure of the system can be calculated using Eq.5.

$$P_{Critical} = 2\,\gamma_{Oil/MeOH}\,\frac{\cos\theta}{r_{pore}} * \left[1 - \left\{\frac{2 + 3\cos\theta - \cos^3\theta}{4\left(\frac{r_{droplet}}{r_{pore}}\right)^3 \cos^3\theta - \left(2 - \sin\theta + \sin^3\theta\right)}\right\}^{\frac{1}{3}}\right] \quad (5)$$

where $P_{Critical}$ is critical pressure, $\gamma_{Oil/MeOH}$ is the interfacial tension, θ is the contact angle, r_{pore} and $r_{droplet}$ is the pore and oil droplet radii respectively.

$\gamma_{Oil/MeOH}$ can be estimated using Eq.6 for various oil concentration.

$$\gamma_{Oil/MeOH}=(\gamma_{MeOH}-\gamma_{Oil})\exp(\alpha' V^{0.7})+\gamma_{Oil} \quad (6)$$

$\alpha = 4.4$ (For oil in methanol emulsion)

$V=0.1$ (For the case of 10 vol.% oil)

$\gamma_{Oil/MeOH} = 0.027029$ N/m

$r_{pore}=15*10^{-9}$ m

$r_{droplet}=30*10^{-9}$ m for the smallest oil droplet

$\theta = 52.712°$

Therefore:

$$P_{Critical}=2*0.027029*\frac{\cos(52.712°)}{15*10^{-9}}*\left[1-\left\{\frac{2+3\cos(52.712°)-\cos^3(52.712°)}{4\left(\frac{30*10^{-9}}{15*10^{-9}}\right)^3\cos^3(52.712°)-(2-\sin(52.712°)+\sin^3(52.712°))}\right\}^{\frac{1}{3}}\right]$$

$P_{Critical} = 277.7$ kPa

APPENDIX C

ASTM D6584 test method for determination of free glycerine, mono-glyceride, di-glyceride and tri-glyceride in B100 biodiesel using gas chromatography

Characterizations

The concentrations of free glycerine, mono-glyceride, di-glyceride and tri-glyceride present in the biodiesel produced from various feedstocks were obtained using gas chromatography (GC) (Varian® Inc.; CP-3800 gas chromatograph, equipped with a 1079 injector, 8410 auto-sampler and FID) in accordance with ASTM D6584 method. Calibration equations were obtained from standards: triolein, diolein, monoolein, and glycerine as shown in Table C-1. The injection masses were plotted against the peak area. The regression factors for the calibration curves exceeded the ASTM requirements. A high-temperature WCOT fused silica column having a VF-5HT stationary phase was used in the GC. Sample preparations were followed in accordance to ASTM D6584. The concentrations of MG, DG and TG were determined by comparison with monoolein, diolein and triolein standards, respectively as defined in ASTM D6584.

100 mg of sample was weighed into a 10 mL septa vial. Exactly 100 µL of each N-methyl-N-(trimethylsilyl) trifluoracetamide (MSTFA), Tricaprin (Internal standard #2 in 8000 µg/mL pyridine) and 1,2,4-butanetriol (Internal standard #1 in 1000 µg/mL pyridine) were added to this vial. 8 mL of n-Heptane was added to the sample. Then the vial was shaken well and sat for 10 min. 2 mL of the reactant mixture was filtered through a 0.2 mm polytetrafluoroethylene syringe filter into a clean small vial for injecting into the GC.

FAME sample was injected into a capillary column for separation and a flame ionization detector (FID) was utilized for detection. The typical retention times for free glycerine, mono-glyceride, di-glyceride, tri-glyceride and standards are shown in Fig.C-1 for unwashed biodiesel and Fig.C-2 for washed biodiesel.

Table C-1. Calibration equations.

Component	Calibration equation	Regression factor (R^2)
Glycerine	(area of glycerine/area of standard 1) = 1.0972*(Mass of glycerine/mass of standard 1) + 0.0185	0.9993
MG	(area of MG/area of standard 2) = 1.3491*(Mass of MG/mass of standard 2) - 0.0039	0.9994
DG	(area of DG/area of standard 2) = 1.0283*(Mass of DG/mass of standard 2) -0.0005	0.9976
TG	(area of TG/area of standard 2)= 0.705*(Mass of TG/mass of standard 2) +0.0177	0.9968

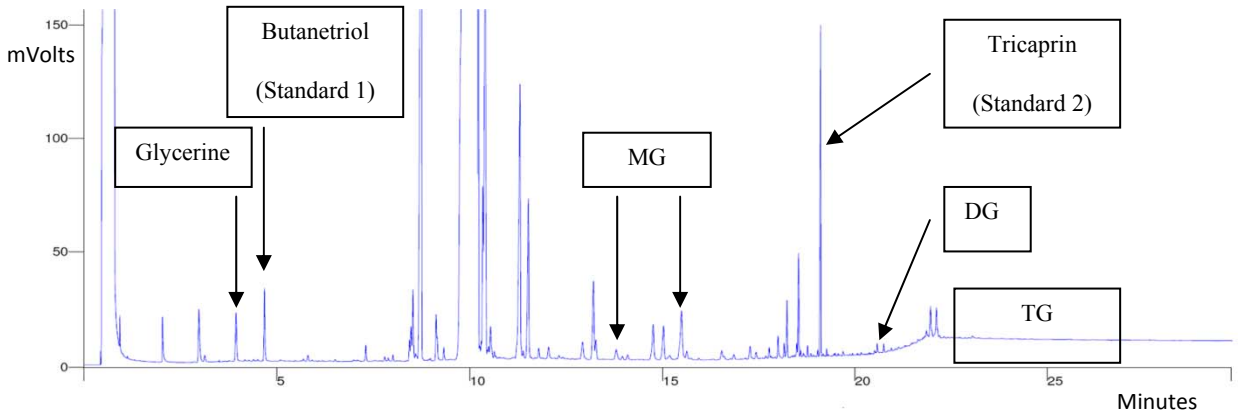

Figure C-1. Typical chromatogram for biodiesel according to ASTM D6584 (This chromatogram was obtained in the Lab for the unwashed biodiesel from canola oil).

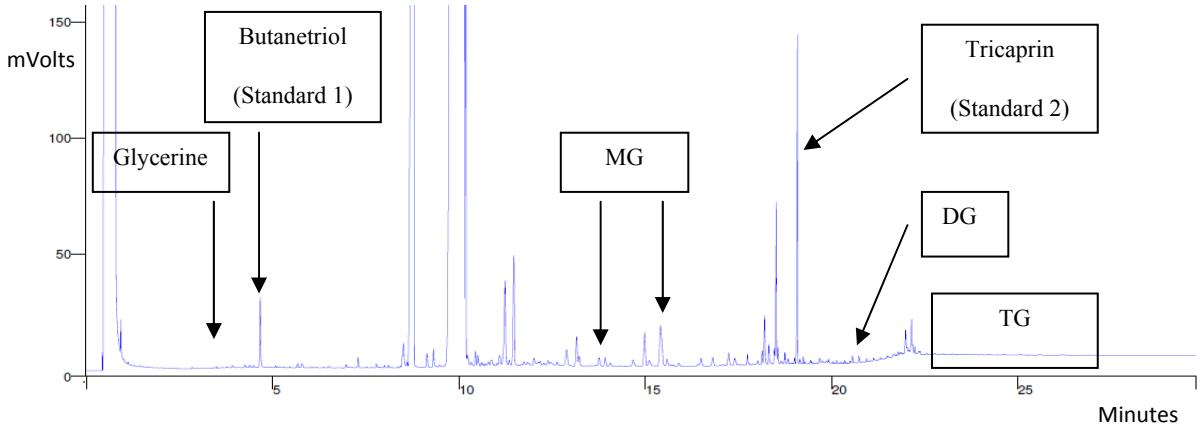

Figure C-2. Typical chromatogram for biodiesel according to ASTM D6584 (This chromatogram was obtained in the Lab for the washed biodiesel from corn oil).

Sample calculations for the commercial biodiesel tested in the Lab.

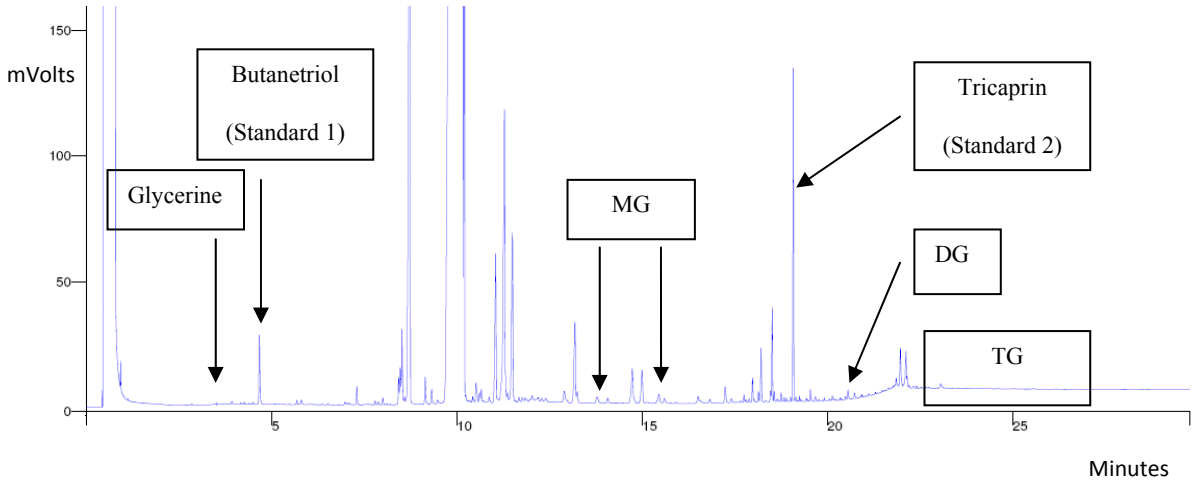

Figure C-3. Gas chromatogram for the commercial biodiesel tested in this study.

Peak areas (mV×sec)	
Area of standard 1 peak:	51.2
Area of standard 2 peak:	169
Area of glycerine peak:	4.89
Area of MG peak:	34.55
Area of DG peak:	16.98
Area of TG peak:	6.94

Area of components ratios	
Area of glycerine/area of standard 1 =	0.095508
Area of MG/area of standard 2 =	0.204438
Area of DG/area of standard 2 =	0.100473
Area of TG/area of standard 2 =	0.041065

Mass of glycerine/mass of standard 1 = (0.095508-0.0185)/1.0972 = 0.070186

Mass of MG/mass of standard 2 = (0.204438+0.0039)/1.3491 = 0.154427

Mass of DG/mass of standard 2 = (0.100473+0.0005)/1.0283 = 0.098194

Mass of TG/mass of standard 2 = (0.041065-0.0177)/0.705 = 0.0331418

Mass of standard 1 = 0.1 g

Mass of standard 2 = 0.8 g

Mass% of glycerine = (0.070186*0.1*100/100) = 0.0070186

Mass% of MG = (0.154427*0.8*100/100) = 0.1235416

Mass% of DG = (0.098194*0.8*100/100) = 0.0785552

Mass% of TG = (0.0331418*0.8*100/100) = 0.0265134

All GC peak areas are summarized in Table C-2.

Table C-2. GC peak areas (mV*sec) obtained for glycerine, MG, DG, TG and standards.

Lipid feedstock	MG	DG	TG	Free Glycerine	Std† 1	Std 2
Commercial Biodiesel	34.55	16.98	6.94	4.89	51.2	169
Canola oil	90.9	11.15	2.4	45.5	56.5	189
Canola oil	79.5	14.6	9	11.4	90	192
Canola oil	96.9	11.93	1.16	8.24	52.1	171
Soybean oil	96.1	8.23	1.01	4.63	51.2	174
Soybean oil	88.4	10.05	1.14	3.72	50.1	208
Soybean oil	88.3	6.67	1.42	5.6	49.1	169
Sunflower oil	79.9	7.25	1.08	12.1	53.2	174
Sunflower oil	72.3	5.92	1.1	19.8	51.2	176
Sunflower oil	71	6.31	1.14	9.05	54.9	162
Refined corn oil	70.2	9.01	3.7	4.71	82.9	179
Refined corn oil	79.5	8.42	1.09	3.23	58.2	196
Refined corn oil	70.08	6.51	1.22	5.11	52.5	173
Waste cooking oil	77.5	10.77	1.27	19.7	74.3	176
Waste cooking oil	63.7	9.91	1.19	16.66	72	176
Waste cooking oil	100	11.88	1.07	70	71.9	172
Pre-treated corn oil	86.8	9.79	1.05	4.01	53	173
Pre-treated corn oil	83	10.54	25	3.22	76.4	183
Canola oil (RT*=82 min)	83.4	8.46	1.03	4.75	84.7	173
Waste cooking oil (RT=55 min)	69.3	8.04	1.08	18.3	53.1	164
Waste cooking oil (RT=105 min)	75	8.46	1.09	5.76	74.2	164

†Std = Standard

*RT = Reaction residence time

Ratio between free glycerine, MG, DG and TG and corresponding standard peak areas for the rest of the biodiesel samples are summarized in Table C-3.

Table C-3. Ratio between free glycerine, MG, DG, TG and standards.

Lipid feedstock	**MG/Std†2**	**DG/Std2**	**TG/Std2**	**Glycerine/Std1**
Commercial Biodiesel	0.2044	0.1005	0.0411	0.0955
Canola oil	0.4810	0.0590	0.0127	0.8053
Canola oil	0.4141	0.0760	0.0469	0.1267
Canola oil	0.5667	0.0698	0.0068	0.1582
Soybean oil	0.5523	0.0473	0.0058	0.0904
Soybean oil	0.4250	0.0483	0.0055	0.0743
Soybean oil	0.5225	0.0395	0.0084	0.1141
Sunflower oil	0.4592	0.0417	0.0062	0.2274
Sunflower oil	0.4108	0.0336	0.0063	0.3867
Sunflower oil	0.4383	0.0390	0.0070	0.1649
Refined corn oil	0.3922	0.0503	0.0207	0.0568
Refined corn oil	0.4056	0.0430	0.0056	0.0555
Refined corn oil	0.4051	0.0376	0.0071	0.0973
Waste cooking oil	0.4403	0.0612	0.0072	0.2651
Waste cooking oil	0.3619	0.0563	0.0068	0.2314
Waste cooking oil	0.5814	0.0691	0.0062	0.9736
Pre-treated corn oil	0.5017	0.0566	0.0061	0.0757
Pre-treated corn oil	0.4536	0.0576	0.1366	0.0422
Canola oil (RT*=82 min)	0.4821	0.0489	0.0060	0.0561
Waste cooking oil (RT=55 min)	0.4226	0.0490	0.0066	0.3446
Waste cooking oil (RT=105 min)	0.4573	0.0516	0.0066	0.0776

†Std = Standard

*RT= Reaction residence time

Table C-4. Mass ratio of glycerine, MG, DG and TG over the corresponded standard.

Lipid feedstock	Mass of MG/mass of std† 2	Mass of DG/mass of std 2	Mass of TG/mass of std 2	Mass of glycerine/mass of std 1
Commercial Biodiesel	0.1544	0.0982	0.0331	0.0702
Canola oil	0.3594	0.0579	0.0071	0.7171
Canola oil	0.3098	0.0744	0.0414	0.0986
Canola oil	0.4229	0.0683	0.0155	0.1273
Soybean oil	0.4123	0.0465	0.0169	0.0656
Soybean oil	0.3179	0.0475	0.0173	0.0508
Soybean oil	0.3902	0.0389	0.0132	0.0871
Sunflower oil	0.3433	0.0410	0.0163	0.1904
Sunflower oil	0.3074	0.0332	0.0162	0.3356
Sunflower oil	0.3278	0.0384	0.0151	0.1334
Refined corn oil	0.2936	0.0494	0.0042	0.0349
Refined corn oil	0.3035	0.0423	0.0172	0.0337
Refined corn oil	0.3032	0.0371	0.0151	0.0718
Waste cooking oil	0.3293	0.0600	0.0149	0.2248
Waste cooking oil	0.2712	0.0552	0.0155	0.1940
Waste cooking oil	0.4338	0.0677	0.0163	0.8705
Pre-treated corn oil	0.3748	0.0555	0.0165	0.0521
Pre-treated corn oil	0.3391	0.0565	0.1687	0.0216
Canola oil*	0.3602	0.0480	0.0167	0.0343
Waste cooking oil‡	0.3161	0.0482	0.0158	0.2972
Waste cooking oil§	0.3419	0.0507	0.0157	0.0539

†Std = Standard
* Reaction residence time = 82 min
‡ Reaction residence time = 55 min
§ Reaction residence time = 105 min

Concentrations of free glycerine, MG, DG and TG for all biodiesel samples were calculated based on the calculation procedure mentioned above according to ASTM D 6584 method and shown in Table 3 of paper 2.

APPENDIX D

Raw data

The following is the data recorded from experimental runs performed with an oil-in-water emulsion system using a ceramic membrane to study the compressibility of the cake layer. The obtained plot from these data was shown in Fig.5 of paper 1.

Table D-1. TMP versus time for various oil concentrations at a flux of 20 L/m^2/h.

30 vol.% at 20 L/m^2/h T=70°C		10 vol.% at 20 L/m^2/h T=30°C		20 vol.% at 20 L/m^2/h T=70°C		10 vol.% at 20 L/m^2/h T=70°C	
Time (sec)	**TMP (kPa)**	**Time (sec)**	**TMP (kPa)**	**Time (sec)**	**TMP (kPa)**	**Time (sec)**	**TMP (kPa)**
10	20.5	10	16.2	10	13.6	10	13.0
20	20.5	20	16.7	20	14.6	20	13.0
30	21.8	30	18.2	30	14.6	30	13.1
40	21.7	40	17.7	40	15.1	40	13.6
50	21.9	50	18.3	50	15.7	50	14.8
60	22.7	60	19.2	60	15.4	60	14.6
70	23.1	70	18.7	70	15.5	70	15.4
80	22.9	80	18.7	80	17.1	80	15.5
90	23.4	90	18.9	90	16.5	90	15.7
100	23.9	100	19.0	100	16.8	100	16.4
110	23.9	110	18.7	110	17.0	110	16.9
120	24.3	120	19.8	120	18.0	120	17.0
130	25.0	130	19.6	130	17.6	130	16.9
140	24.6	140	19.4	140	18.0		
150	25.2	150	19.7	150	18.3		
160	25.6	160	19.3	160	18.1		
170	26.1	170	19.8	170	18.7		
180	26.2	180	20.0	180	18.9		
190	26.5	190	20.5	190	19.0		
200	28.2	200	20.1	200	18.9		
210	27.5	210	20.8	210	19.7		
220	28.5	220	20.9	220	19.4		
230	28.4	230	20.9	230	19.4		
240	28.8	240	20.6	240	20.4		
250	29.6	250	20.5	250	19.6		
260	30.2	260	21.2	260	20.4		
270	30.3	270	20.9	270	20.9		
280	30.6	280	21.6	280	20.8		
		290	21.5				
		300	21.7				
		310	21.4				
		320	21.6				
		330	21.8				

Table D-2. TMP versus time for oil concentrations of 40 and 45 vol.% at a flux of 20 $L/m^2/h$.

45 vol.% for 20 $L/m^2/h$ at 50°C		40 vol.% for 20 $L/m^2/h$ at 30°C			
Time (sec)	**TMP (kPa)**	**Time (sec)**	**TMP (kPa)**	**Time (sec)**	**TMP (kPa)**
10	161.1	10	30.2	310	71.0
20	168.1	20	31.7	320	71.7
30	174.4	30	33.4	330	73.3
40	179.5	40	34.3	340	74.2
50	184.5	50	35.6	350	75.5
60	190.5	60	36.8	360	76.9
70	197.3	70	37.7	370	77.9
80	203.2	80	39.3	380	79.9
90	209.2	90	40.8	390	81.0
100	215.7	100	41.9	400	82.5
110	222.8	110	43.6	410	83.6
120	229.1	120	44.5	420	84.7
130	235.6	130	46.0	430	85.5
140	242.3	140	46.9	440	86.4
150	249.3	150	48.7	450	87.6
160	256.3	160	50.0	460	89.0
170	262.6	170	51.6	470	89.9
180	270.5	180	52.5	480	90.9
190	277.8	190	53.8	490	92.4
200	285.1	200	55.4	500	94.1
210	287.3	210	56.8	510	94.8
220	291.4	220	57.7	520	96.4
230	298.1	230	59.4	530	97.5
240	304.2	240	60.7	540	98.7
250	310.8	250	61.6	550	99.8
260	317.2	260	63.4	560	101.5
270	323.6	270	64.5	570	102.4
280	329.8	280	66.0		
290	335.9	290	67.9		
300	342.1	300	68.9		

Table D-3. TMP versus time for oil concentrations of 20 and 30 vol.% at a flux of 20 $L/m^2/h$.

30 vol.% at 20 $L/m^2/h$ at 30°C				20 vol.% at 20 $L/m^2/h$ at 30°C			
Time (sec)	**TMP (kPa)**	**Time (sec)**	**TMP (kPa)**	**Time (sec)**	**TMP (kPa)**	**Time (sec)**	**TMP (kPa)**
10	30.2	310	61.9	10	27.4	310	50.3
20	31.7	320	63.5	20	24.3	320	50.7
30	32.9	330	63.9	30	22.0	330	51.9
40	34.0	340	64.8	40	24.3	340	52.3
50	35.4	350	65.6	50	25.8	350	53.4
60	36.4	360	66.5	60	26.9	360	53.7
70	37.8	370	67.0	70	28.2	370	54.6
80	38.7	380	67.6	80	29.1	380	55.8
90	39.9	390	68.4	90	30.2	390	55.9
100	40.3	400	69.0	100	31.3	400	56.9
110	41.4	410	70.2	110	32.6	410	57.3
120	42.9	420	71.0	120	33.2	420	57.7
130	44.5	430	71.5	130	35.0	430	58.8
140	46.1	440	72.6	140	35.5	440	59.5
150	46.5			150	36.3	450	60.3
160	47.5			160	37.2	460	60.3
170	48.4			170	38.3	470	61.5
180	49.7			180	38.6		
190	51.0			190	39.6		
200	51.7			200	40.7		
210	52.7			210	41.5		
220	53.8			220	42.5		
230	54.7			230	43.4		
240	55.5			240	44.5		
250	56.6			250	45.9		
260	57.5			260	46.2		
270	58.4			270	46.7		
280	59.2			280	47.8		
290	60.3			290	48.8		
300	60.9			300	49.4		

The following is the data recorded for all experimental runs performed in biodiesel production through transesterification of various lipids using a membrane reactor. These data are transmembrane pressure (TMP) versus time for the various experimental runs.

The reaction residence time was investigated for biodiesel production through alkali-transesterification of canola and waste cooking oils. The raw data is as follows:

Table D-4. Data from waste cooking oil run at 44 L/m^2/h at the residence time of 55 min.

Time (min)	TMP (kPa)	Time (min)	TMP (kPa)	Time (min)	TMP (kPa)	Time (min)	TMP (kPa)	Time (min)	TMP (kPa)
26	92.2	89	123.5	171	150.9	240	170.8	338	179.2
29	98.7	91	125.5	174	152.4	243	170.8	339	179.2
31	98.9	94	126.5	175	152.9	246	170.8	342	179.3
32	99.0	99	126.5	178	154.4	249	170.9	343	179.3
33	99.7	114	130.7	179	154.9	252	170.9	346	179.3
35	100.6	117	131.7	182	156.4	255	170.9	347	179.3
36	101.9	120	133.0	184	157.4	258	171.0	350	179.3
38	102.0	126	133.5	187	158.9	261	171.0	351	179.3
41	102.3	129	134.4	188	159.4	264	171.0	354	179.3
42	103.1	133	136.2	190	164.6	267	171.0	355	179.3
45	105.5	135	137.7	194	164.6	270	171.1	358	179.3
51	105.7	138	138.7	195	164.6	273	171.1	359	179.3
52	106.2	139	140.6	198	164.6	275	172.2	362	179.3
53	106.8	140	143.5	203	164.6	282	174.3	363	179.3
56	108.2	142	148.8	204	164.6	283	175.1	366	179.3
57	108.2	143	148.8	206	164.6	289	176.5	367	179.3
58	108.8	144	148.8	207	164.6	298	176.6	370	179.3
62	110.3	145	148.8	211	165.4	311	176.6	371	179.4
63	111.1	149	148.8	212	168.5	318	177.8	377	179.4
64	111.8	150	148.8	217	170.5	319	179.2	390	182.0
68	112.2	151	148.8	218	170.6	322	179.2	411	181.6
69	114.0	156	148.8	219	170.6	323	179.2	424	182.5
70	114.2	157	148.8	222	170.6	326	179.2	440	183.6
74	115.9	161	148.8	225	170.6	327	179.2	447	184.3
78	116.9	162	148.8	228	170.7	330	179.2	461	185.4
79	119.1	163	148.8	231	170.7	331	179.2	469	185.2
82	121.0	165	148.8	234	170.7	334	179.2	492	186.3
86	121.2	168	149.4	237	170.7	335	179.2		

Table D-5. Data from waste cooking oil run at 44 L/m^2/h at the residence time of 80 min.

Time (min)	TMP (kPa)	Time (min)	TMP (kPa)
20	52.1	290	75.3
30	52.9	300	75.1
40	58.3	310	77.6
50	60.2	320	80.9
60	60.0	330	80.8
70	60.2	340	83.0
80	60.0	350	84.0
90	58.5	360	85.2
100	60.5	370	89.2
110	61.8	380	90.2
120	61.9	390	90.3
130	63.8	400	90.6
140	64.7	410	90.6
150	66.0	420	90.9
160	66.5	430	90.2
170	68.9	440	90.5
180	69.9	450	90.2
190	69.6	460	90.1
200	69.3	470	90.1
210	69.6	480	90.2
220	70.5	490	90.2
230	73.1	500	90.2
240	75.6		
250	75.3		
260	75.8		
270	75.1		
280	76.0		

Table D-6. Data from waste cooking oil run at 44 L/m^2/h at the residence time of 105 min.

Time (min)	TMP (kPa)	Time (min)	TMP (kPa)
26	60.4	106	80.0
29	61.2	114	80.4
32	62.5	117	84.4
35	63.7	120	87.0
38	64.1	123	88.8
41	64.5	126	93.6
44	64.9	135	94.3
47	65.8	136	94.7
49	66.2	137	97.3
52	66.5	138	98.0
54	67.0	139	99.0
56	67.4	140	99.5
58	67.8	143	100.4
61	69.5	145	100.9
65	69.5	149	101.2
70	69.8	150	101.2
72	70.5	155	103.3
74	70.5	160	103.4
80	72.0	161	103.5
82	72.4	167	103.7
84	72.7	172	103.8
88	74.4	177	104.5
90	75.1	178	105.2
92	75.3	184	105.3
100	75.8	202	105.7
102	77.2		
105	77.9		

Table D-7. Data from canola oil runs at 60 L/m^2/h at various reaction residence times.

60 L/m^2/h at 35 min		**60 L/m^2/h at 60 min**		**60 L/m^2/h at 82 min**	
Time (min)	**TMP (kPa)**	**Time (min)**	**TMP (kPa)**	**Time (min)**	**TMP (kPa)**
1	40.4	1	41.6	1	55.6
2	45.1	2	49.9	3	55.6
3	48.4	3	56.1	5	55.1
4	51.8	4	58.5	17	56.1
5	54.3	5	60.7	19	56.3
6	58.5	6	64.8	23	56.0
7	62.0	7	68.8	25	56.5
8	66.2	8	70.9	34	56.3
9	70.7	9	72.9	35	56.3
10	75.4	10	75.3	42	56.3
11	81.2	11	78.3	47	56.7
12	85.5	12	78.3	48	56.7
13	89.9	13	80.4	52	56.7
14	95.7	14	80.1	53	57.2
15	104.9	15	80.4	56	58.3
16	134.8	16	79.7	70	57.9
17	184.2	18	80.7	80	58.9
18	223.1	21	81.3	90	61.1
19	235.5	24	81.3	100	61.9
20	265.9	26	81.8	110	62.5
21	321.3	28	82.6	120	64.7
22	348.5	30	81.6	130	65.1
		32	81.6	140	65.8
		34	77.8	150	68.4
		36	79.8	160	69.9
		38	77.2	170	71.3
		40	77.8	180	72.9
				190	72.4
				200	74.0
				210	71.3
				220	72.7
				230	71.7
				240	72.2